Efficient Extraction of Phenolic Compounds from Wheat Distiller's Dried Grain; Ultrasonic Pretreatment and Dielectric Studies

A Thesis Submitted to the College of Graduate Studies and Research

In Partial Fulfillment of the Requirements

for the Degree of Master of Science

in the Division of Biomedical Engineering

University of Saskatchewan,

Saskatoon, Saskatchewan, Canada

By

Zahra Izadifar

PERMISSION TO USE

In presenting this thesis in partial fulfillment of the requirements for a postgraduate degree from the University of Saskatchewan, I agree that the libraries of this University may make it freely available for inspection. I further agree that permission for copying of this thesis in any manner, in whole or in part, for scholarly purposes may be granted by the professor or professors who supervised my thesis work or, in their absence, by the department Head of the Department or the Dean of the College in which my thesis work was done. It is understood that any copy or publication or use of this thesis or parts thereof for financial gain shall not be allowed without my written permission. It is also understood that due recognition shall be given to me and to the University of Saskatchewan in any use which may be made of any material in my thesis.

Requests for permission to copy or to make any other use of material in this thesis in whole or part should be addresses to:

Head of the Division of Biomedical Engineering,

University of Saskatchewan,

57 Campus Drive,

Saskatoon, Saskatchewan,

Canada, S7N 5A9

ACKNOWLEDGMENTS

I would like to express my deepest gratitude and appreciation to God for giving me this opportunity to study and do research, and having made everything possible to do this work.

My special thanks go to my beloved father and mother for their endless and unconditional love and support through out my life. I am grateful to my lovely sister, Zohreh, for her help, guidance, warm encouragement, and unflinching support during my study in Canada. My many thanks go to my dear brother, Mohammad, for his valuable advice, guidance and support during my study. I would also like to thank my kind sister, Maryam, for her help and calm words to support me in hard times.

I would like to thank my supervisor, Dr. Oon Doo Baik, for his comments and support during this research work. I would like to express my gratitude to my advisory committee members, Dr. Chris Zhang and Dr. Venkatesh Meda for their comments and time spent on reviewing the draft of this thesis. I am also thankful to Dr. R.T. (Bob) Tyler for serving as the external examiner, and for his valuable feedbacks on my thesis. I would also like to thank Bob Blackmore and Ramin Azargohar for their scientific and technical help with Micromeritics ASAP 2020 operation. I would also like to thank Mr. Louis Roth for his technical assistance during my research. I appreciate Dr. Lee Wilson for his valuable discussions. I acknowledge the support of Dr. Cathrin Niu in providing access to Micromeritics ASAP 2020 in her lab. I additionally acknowledge Ms. Heli Eunike, Mr. Richard Blondin and Mr. Rlee Prokopishyn for their technical support.

ABSTRACT

Phenolic compounds are useful bioactive molecules with important medicinal properties. Wheat dried distillers grain (DDG), a coproduct of the ethanol production process, is rich in potentially health-promoting phenolic compounds. As the concentration of natural medicinal compounds (e.g. phenolic compounds) in plant materials (e.g. DDG) is low, an efficient solid-solvent extraction process would improve their solubility and effective diffusivity. In the extraction of phenolic compounds from DDG, the DDG cell wall is an important barrier for mass transfer from inside to outside the cell. High-power ultrasound pretreatment of plant material (e.g. DDG) can break down the cell wall and increase the extraction rate and yield of natural medicinal compounds (e.g. phenolic compounds). Radio frequency (RF) heating can provide uniform internal heating of all particles and solvent in the packed-bed extraction unit which results in improved, uniform solubility of the solute in the solvent and diffusivity of the desired compound without overheating specific areas.

The kinetics and mechanism of the extraction were studied and the rate constant of extraction, the saturated concentration, the activation energies, and the temperature independent factors of solid-liquid extraction of phenolic compounds from DDG under different extraction conditions were determined, assuming second-order extraction kinetics. The effect of particle moisture content, ethanol fraction of solvent and extraction temperature on the kinetics, rate and yield of extraction were analyzed. The results of these calculations were compared and discussed with a view to optimizing the extraction process. The maximum extraction rate and yield were obtained with 70% ethanol concentration, 70°C extraction temperature and 59% particle moisture content (w.b.). The effective diffusivity of phenolic compounds in DDG particles was also determined for each extraction condition.

The effect of high-power ultrasound pretreatment on destruction of DDG cell walls and the extraction yield and rate was investigated. Direct sonication by an ultrasound probe horn at 24 kHz was applied and factors such as ultrasound power, treatment time and consumed energy were investigated. The effect of ultrasound on destruction of DDG cell walls was studied by characterizing the physical properties (specific surface area, pore volume and pore size) of the untreated and treated samples at different levels of ultrasound power and treatment time using

the method of nitrogen (N_2) adsorption at 77 K. The increased surface area, pore volume, pore size, and extraction yield and rate after ultrasonic treatment showed the positive effect of ultrasound pretreatment on breaking down cell walls and pore developement. Among tested ultrasound conditions, 100% ultrasound power for 30 seconds was determined to be the best pretreatment with appropriate consumed energy compared to other tested conditions. Under this extraction condition a 14.29% increase in extraction yield was observed compared to the control, and the BET (Brunauer, Emmett, and Teller) surface and extraction rate constant increased from 13.90 to 18.85 m^2/g and 0.057 to 3.933 $Lg^{-1}min^{-1}$, respectively.

The dielectric properties of the packed bed of wheat DDG particles with ethanol/water solution were measured for more than eight different frequencies using a precision LCR (inductance, capacitance and resistance) meter and a liquid test fixture. The power penetration depth of the packed bed was measured for all applied experimental conditions at 13.56 and 27.12 MHz. The effect of the ethanol fraction of the solvent, moisture content of the DDG particle and temperature on the dielectric constant, loss factor and power penetration depth were investigated. Both the dielectric constant and the loss factor of the packed decreased with frequency for all levels of ethanol fractions and temperatures. The dielectric constant and loss factor of the bed increased with temperature for all levels of particle moisture content and ethanol fraction; however, for the particle moisture content of 0.0373 d.b. with 100% and 70% ethanol, and also for the particle moisture content of 1.58 d.b. with 100% ethanol, the effect of temperature on the dielectric constant was insignificant. The dielectric constant and loss factor of the packed bed were significantly decreased with ethanol volumetric fraction of solvent for all levels of temperature and particle moisture content. The dielectric constant and loss factor increased with moisture content for 40%, 70% and 100% ethanol; however, for 0% ethanol, the effect of moisture content was not significant. Power penetration depth decreased with temperature, and particle moisture content increased with ethanol fraction. Multiple regression equations for the dielectric constant and dielectric loss factor of the packed bed were developed for frequencies of 13.56 and 27.12 MHz. The dielectric properties of the packed beds with solvent in this study assure the possibility of applying RF-assisted extraction for extraction of phenolic compounds from DDG.

TABLE OF CONTENTS

LIST OF FIGURES

LIST OF TABLES

CHAPTER 1
Background

Natural pharmaceutical and nutraceutical products have been spotlighted by researchers and industries. Extraction of bioactive compounds from biological resources is economically more feasible compared to chemical synthesis of the products. Synthetic products might possess some side effects to human health. The World Health Organization (WHO) released that about 80% of the population of the world relies on natural medicine and 41% of the confirmed drugs between 1983 and 1994 contained natural products as their sources (Farnsworth et al., 1985).

Phenolic compounds are useful bioactive molecules with important medicinal properties such as decreasing the risk of Parkinson disease, multiple sclerosis, dementia, several types of cancer and liver diseases, etc. (McBain, 2008). Phenolic compounds have been found in various fruits and vegetables. Studies have been conducted for detection and extraction of phenolic compounds from different main and by-products such as extraction from *Amaranthus* species (Amin et al., 2006), pistachio hull (Goli et al., 2005), wheat bran (Wang et al., 2008), grape seeds (Ghafoor et al., 2009), fresh and dry hazelnuts, walnuts, and pistachios (Arcan and Yemenicioglu, 2009). Cereal grains are rich sources of phenolic compounds, which are found in both free and bound forms, and concentrated in the bran portion of cereal kernels (Lempereur et al., 1997). Besides the distinctive medicinal activities of phenolic compounds, wheat distillers dried grain (DDG), a natural source of phenolic compounds, is available in both Canada and the USA. DDG is the co-product of bioethanol production processes where ethanol is produced from wheat grains during a fermentation process. As DDG is easily available from ethanol production industries, it can be considered as an alternative source of phenolic compounds.

Based on observations by Gibreel et al. (2009), the concentration of phenolic compounds can vary from 6.3 to 10.4 mg Gallic acid/gram of the DDGS obtained from VHG jet cooking fermentation and VHG modified STARGEN-based fermentation. So, there is a considerable concentration of phenolic compounds in fermented wheat DDGS to be extracted.

The vast majority of byproducts and wastes are produced from agricultural processing industries. These by-products or waste materials can be converted to value-added products. For example, wheat straw can be used to produce ethanol. In western Canada, because of the productivity and availability of wheat on the prairies, wheat is used for ethanol production. One tonne of ethanol can be produced from 3.3 tonnes of wheat. Many co-products originate from the raw wheat used in ethanol production, such as wet distillers grain (WDG), distiller's dried grains (DDG), distiller's dried solubles, and distiller's dried grains with solubles (DDGS). The major co-product of fermentation of wheat during ethanol production is distiller's dried grain with solubles (DDGS) (Ziggers, 2007).

In North America, most (~98%) of the DDGS comes from plants where ethanol for oxygenated fuels is produced. The remaining 1 to 2% of DDGS is produced by the beverage alcohol industry. Approximately 3.2 to 3.5 million tonnes of DDGS are produced annually in North America. In recent years, to reduce air pollution from automobile emissions in some regions of the U.S, it is required to use oxygenated fuels (e.g. ethanol-gasoline blends). Considering growing demand for ethanol, the production of DDGS is expected to double within the next few years (U of M Distillers Grains By-products, 2010).

About 700,00 tonnes of the 3.2 million tonnes of DDGS produced annually in North America, are exported to Europe for livestock feeding. A very small amount of DDGS is exported to Mexico, leaving approximately 2.65 million tonnes available for domestic use in the U.S. and Canada. In North America, more than 80% of DDGS is used for ruminant diets (U of M Distillers Grain By-products, 2010).

In the procedure for producing ethanol, grain such as corn, wheat or milo is ground into coarse flour. In order for the flour starch to be fermented the milled grain is mixed first with acidic water (pH about 5.8) and alpha-amylase. The slurry is heated to 82-88ºC for 30-45 minutes to decrease viscosity. After that, the slurry is pumped through a pressurized jet cooker at 105ºC and held at this temperature for 5 minutes. The mixture is then cooled. Then the cooled mixture is held at 82-88ºC for 1-2 hours to give the alpha-amylase enzyme time to break down the starch into short- chain dextrins. After pH and temperature are adjusted, glucoamylase is added. The glucoamylase breaks down the dextrins to simple sugars. Then, yeast is added to change the sugar to ethanol and carbon dioxide. Then the mixture stays for 50-60 hours to be

fermented, which results in a mixture that contains about 15% ethanol, the solids from the grain and added yeast. As the fermented mash is pumped into a multi-column distillation system, additional heat is added to it. In order to boil off and separate the ethanol, the columns apply the various boiling points of ethanol and water. Now the product steam which contains about 95% (190-proof) ethanol is ready to leave the distillation columns. For further purification of ethanol, the obtained 190-proof ethanol passes through a molecular sieve resulting in 200-proof anhydrous ethanol. The stillage from the bottom of the distillation tanks contains solids from the grain, added yeast and liquid from the water added during the process. To separate thin stillage (a liquid with 5-10% solids) from wet distillers grain, the stillage is sent to centrifuges. Some of the thin stillage is routed back to the cook/slurry tanks as makeup water and the rest is sent to a multiple-effect evaporation system where it is concentrated into syrup containing 25-50% solids. This syrup, which is high in protein and fat, is then mixed back with the wet distiller's grain (WDG). The mixture is dried to extend its shelf life. This dried distiller's grain (DDG) is commonly used as a high-protein ingredient in cattle, swine, poultry and fish diets. Distiller's dried grains with solubles (DDGS) is the dried residue remaining after the starch fraction of grain is fermented with selected yeasts and enzymes to produce ethanol and carbon dioxide (ICM, 2009).

Extraction is one of the most important processes in the pharmaceutical industry. Solvent extraction of phenolic compounds from DDG particles involves mass transfer of the solute from small pores inside each DDG particle to the surface of the particle, followed by convective mass transfer from each particle surface to the moving solvent. The effective diffusivity, interfacial equilibrium concentration between particle surface and solvent, and convective mass transfer coefficient have strong influences on the mass flux of the solute. When all the free solute is dissolved in the solvent, diffusional mass transfer dominates and consequently interfacial mass transfer is influenced considerably by the interfacial equilibrium concentration that is determined by the partition coefficient. Furthermore, the size and geometry of particles as well as the mass fraction of each particle geometry in a solid mixture of DDG have meaningful influences on mass flux during the solvent extraction of phenolic compounds. To study the solid-solvent extraction process of phenolic compounds from DDG, it is required to determine key factors of the extraction process such as effective diffusivity of phenolic compounds in DDG.

Temperature strongly affects the diffusivity and solubility of bioactive compounds (e.g. phenolic compounds). In traditional extraction method (e.g. stirred reactor), the solute must diffuse through the cell wall which is the main mass transfer resistance controlling the extraction speed. Also, heat from the warm solvent must be transferred from the warm solvent to the inside of the particle by conduction and convection. Convection/conduction of heat and mass diffusion through the cell wall can be enhanced significantly if the cell wall is broken (Izadifar, 2009).

Traditional solvent extraction methods for plant materials are normally time and energy consuming and require relatively large amounts of solvent. Recently, a number of new extraction techniques have been developed and applied to the extraction of biological compounds. Pressurized solvent extraction, supercritical fluid extraction, pulsed electric field (PEF) assisted extraction, and electromagnetic irradiation assisted extraction including microwave (MW) and radio frequency (RF) assisted extraction, are examples (Izadifar, 2009).

Because of the small amount of phenolic compounds in wheat DDGS, an innovative extraction method, which demands not only a small amount of solvent and extraction time but also a low production cost, is required.

To exploit plant material resources, various extraction techniques have been developed. These techniques focused on acquiring technological solutions to decrease solvent consumption or even prevent the use of solvent in extraction processes and to obtain more highly purified products with higher yield.

Currently, solid-liquid extraction techniques are used commercially for the extraction of natural medicinal products. These techniques need a long extraction time as well as a high volume of polluting solvent (Jianyong et al., 2001). Considering the increasing demand for medicinal natural products, like phenolic compounds, the development of a more efficient extraction process is an urgent commercial need. Among the new extraction methods listed above, Super Critical Fluid Extraction (SCFE) is a fast and non-thermal extraction technology; however it is still an expensive technology that needs high pressure and significant initial capital investment. In MW assisted extraction, shallow penetration of MW causes non-uniform heating within a large extraction unit, resulting in thermal degradation of thermolabile bioactive compounds in some locations during the extraction process (Izadifar and Baik, 2008). The penetration depth of RF is much larger than that of MW (Piyasena et al., 2003), and uniform

electric fields are formed between the two electrodes of an RF application chamber, which allows RF to be used in industrial and mass scale.

RF heating of a packed-bed solvent extraction unit would improve the diffusivity/solubility of the desired compounds as temperature closely influences their properties. RF heating has been used in food processing, pasteurization and sterilization (Moyer and Stotz, 1947; Kinn, 1947; Houben et al., 1991, 1990; Zhong et al., 2003), thawing frozen products (Jason and Sanders, 1962a, 1962b), post-back drying of cookies and snack foods (Anon, 1987, 1989), drying processes (Mermelstein, 1997; Poulin et al., 1997; Balakrishran et al., 2004), thermal therapy (Maurizion et al., 2004) and RF assisted extraction (Izadifar and Baik, 2008). However, use of RF heating in extraction is very recent and has not been fully investigated. The amount of heat generated inside the material depends on the frequency, dielectric loss factor of the material (sample) and the strength of the electric field. Dielectric properties including dielectric loss factor and dielectric constant, play an important role in RF heating. Dielectric properties of the material and the solvent depend on RF frequency and the moisture content and temperature of the matter.

Pre-treating fermented wheat wastes using ultrasonic (US) waves potentially can damage cell walls, which results in improved extraction yield/speed of bioactive compounds (i.e. phenolic compounds). Ultrasound has been used recently to improve the extraction of polysaccharides and essential oils from plant material (Mason, 1997; Vinatoru M et al., 1999). It is believed that the mechanical effect of ultrasound is disruption of cell walls which accelerates the release of organic compounds within the plant body. Thus, the mass transfer rate increases due to easier access of the solvent to the cell contents. Sound waves are mechanical vibrations in a liquid, solid or gas. Ultrasound has a frequency higher than the range audible to humans (1-16 kHz). The lowest frequency of ultrasound is normally 20 kHz and the top end is limited only by the ability to generate the signals (Mason, 1997). Unlike electromagnetic waves (radio waves; infrared, visible or ultraviolet light; X-ray; gamma rays) sound waves must travel in matter as they involve expansion and compression cycles traveling through a medium. Expansion pulls molecules apart and compression pushes them together. In a liquid, the expansion cycle of sound waves creats negative pressure, which can produce bubbles or cavities in the liquid if the ultrasound is strong enough. After the vapor bubbles form and grow, they undergo implosive collapse which generates the energy for chemical and mechanical effects; this process is called

cavitation. In ultrasound-assisted extraction, the cavitation process takes place within about 400 μs. When cavitation occurs in a liquid close to the solid boundary, cavity collapse is asymmetric and produces high-speed jets of liquid. It has been observed that the liquid jets drive into the surface at a speed close to 400 km/h (Luque-Garcia and Castro, 2003). The strong impact of the jets on the solid surface results in serious damage to impact zones and can create newly exposed, highly reactive surfaces (damaged surfaces). In addition, rapid adiabatic compression of gases and vapour within the bubbles (cavities) causes extremely high temperatures and pressures (Suslick, 1994, 1998).The temperature of these hot spots has been estimated to be about 5,000ºC, similar to the surface of the sun, and the pressure is estimated to be roughly 1,000 atm, the same value as that at the Marian Trench the deepest point in the ocean. Very high effective temperatures (which increase solubility and diffusivity) and pressure (which help penetration and transport) at the interface between the solution subjected to ultrasonic energy and a solid matrix, combined with the oxidative energy of radicals (hydroxyl and hydrogen peroxide for water) created during sonolysis, result in high and efficient extraction power (Luque-Garcia and Castro, 2003). Therefore, ultrasound is a module of worth in the pre-treatment of solid samples for the extraction of organic and inorganic compounds (Go'mez-Ariza et al., 1995; Mierzwa et al., 1997).

Piezoelectricity is defined as the ability of materials to generate an electric field or electric potential difference in response to applied mechanical stress. If the material is not short-circuited, the applied mechanical stress produces a voltage across the material. The effect is closely related to a change of polarization density inside the material volume. The piezoelectric effect is reversible. A material exhibiting the direct piezoelectric effect, which means an electric potential is induced in the material volume when stress is applied, also exhibits the reverse piezoelectric effect, in which a stress or strain is produced when an electric field is applied. This effect is the basis of the production of sound waves in ultrasound. In ultrasound, the longitudinal mechanical vibrations are generated by the reversed piezoelectric effect (Wikipedia, 2011).

A combinational approach of US-RF is expected to improve considerably the solvent extraction of natural medicinal compounds, including phenolic compounds. As a prerequisite for developing US-RF assisted extraction of phenolic compounds from DDG, theoretical and experimental investigations on the characterization of the process are needed. To understand, develop, commercialize and optimize US-RF assisted extraction for extracting a biomedicinal

product (e.g. phenolic compounds), it is required to conduct related fundamental studies, including characterization of RF dielectric properties of the solvent and the biomaterial (DDG).

The main objective of this research was to develop an innovative extraction technology to extract phenolic compounds from DDG with ultrasound and radio frequency (RF) application. The specific objectives were: 1) to conduct experimental studies on the extraction kinetics, mechanism and optimum extraction conditions (temperature, volumetric concentration of ethanol and particle moisture content) for the extraction of phenolic compounds; 2) to investigate the effects of ultrasound pre-treatment on the cell wall of DDG particles, the extraction rate and yield, and mass transfer properties of phenolic compounds from DDG at different ultrasound conditions and determine the optimum ultrasound pretreatment condition; and 3) to measure and analyze the dielectric properties of a packed bed of DDG and solvent at different levels of temperature, moisture content and frequency. The dielectric properties are important for assessment of the possibility of RF-assisted extraction.

Chapter 2 presents theoretical and experimental studies of the extraction kinetics of phenolic compounds from DDG related to the optimum conditions for solid-liquid extraction of phenolic compounds. This chapter also relates the effects of extraction temperature, particle moisture content and ethanol fraction of the solvent on the yield, rate and kinetics of extraction. The effects of high intensity focused ultrasound on destruction of the cell walls of DDG particles and the extraction rate and yield of phenolic compounds are dealt with in Chapter 3. In Chapter 4, power penetration depth and dielectric properties, including dielectric loss factor and dielectric constant of the packed bed of DDG particles and a solution of ethanol-water, are measured. Also, in Chapter 4, the influence of particle moisture content, temperature and ethanol fraction of the ethanol/water solution on dielectric properties and power penetration depth are discussed in detail. Chapter 5 integrates the major findings of this study.

References

Amera Gibreel, James r. Sandercock, Jingui Lan, Laksiri A. Goonewardene, Ruurd T. Zijlstra, Jonathan M. Curtis, David C. Bressler, Fermentation of Barely by Using Saccharomyces cervisia: Examination of Barely as a Feedstock for Bioethanol Production and Value-Added Products, Appl. Environ. Microbiol. 75 (5) (2009) 1363-1372.

Amin I., Y. Norazaidah, K.I. Emmy Hainida, Antioxidant activity and phenolic content of raw and blanched Amaranthus species, J.Food Chem. 94 (2006) 47-52.

Anon, An array of ne applications are evolving for radio frequency drying. Food Engineering, 59(5) (1987), 180.

Anon, RF improves industrial drying and baking processes. Process Engineering. 70 (1989), 33.

Arcan I., A. Yemenicioglu, Antioxidant activity and phenolic content of fresh and dry nuts with or without the seed coat, J. Food Compos. Anal. 22 (2009) 184-188.

Balakrishnan P A; Vedaraman N; Sunder V J; Muralidharan C; Swaminathan G. Radiofrequency heating-a prospective leather drying system for future. Drying Technology, 22 (2004), 1969-1982.

Farnsworth, NR, Akerele, O., and Bingel, A. S., Medical plants in therapy. Bulletin Worid Health Organization, 63 (1985), 965-981.

Ghafoor K., Y.H. Chi, J.Y.Jeon, I.H. Jo, Optimization of ultrasound-assisted extraction of phenolic compounds, antioxidants, and anthocyanins from grape (vitis vinifera) sedds, J. Agric. Food Chem. 57 (2009) 4988-4994.

Goli A.H., M. Barzegar, M.A. Sahari, Antioxidant activity and total phenolic compounds of pistachio (pistachio vara) hull extracts, J. Food Chem. 92 (2005) 521-525.

Gomez-Ariza J.L., E. Morales, R. Beltran, I. Giraldez, M. Ruiz Benitez, Ultrasonic treatment of molluscan tissue for organotin speciation. Analyst (cambrige, UK), 120 (1995), 1171-1174.

Houben J, Schoenmakers L, Putten E, Roon P, Krol B, Radio frequency pasteurization of sausage emulsion as a continuous process. Journal of Microwave Power and Electromagnetic Energy, 26 (1991), 202-205.

Houben, J. H., Van Roon, P. S. and Krol, B., Radio frequency pasteurization of moving sausage emulsion. Processing and Quality of Foods, (1990.) 1.171-1.177.

ICM. 2009, Ethanol Production Process, ICM the energy of innovation, ICM, Available at http://www.icminc.com/ethanol/production_process/, Accessed 24 December 2011.

Izadifar M., O.D. Baik, Dielectric properties of a packed bed of the rhizome of P. Peltatum with an ethanol/water solution for radio frequency-assisted extraction of podophyllotoxin. Biosystems Engineering, 100 (2008), 376-388.

Izadifar M., O.D.Baik, An optimum ethanol-water solvent system for extraction of podophyllotoxin: Experimental study, diffusivity determination and modeling, Separation and Purification Technology 63 (2008), 53-60.

Izadifar M., Radio Frequency Enhanced Extraction Of An Anti-Cancer Compound From Porous Media, PhD Thesis, University of Saskatchewan, Saskatoon, SK, Canada (2009).

Jason, A. C. and Sanders, H. R., 1962a. Dielectric thawing of fish. L. Experiments with frozen herrings. Food Technologies, 16 (6), 101-106.

Jason, A. C. and Sanders, H. R., 1962b. Dielectric thawing of fish. L. Experiments with frozen herrings. Food Technologies, 16 (6), 107-112.

Jianyong W, Lidong L and Foo-tim C, Ultrasound assisted extraction of ginseng saponins from ginseng roots and cultured ginseng cells. Ultrasonics Sonochemistry, (2001) 347-352.

Lempereur I., X. Rouau and J. Abecassis, Genetic and agronomic variation in arabinoxylan and ferulic acid content of durum wheat (Triticum durum L.) grain and its milling fractions., J. Agric. *Food* Chem. **25** (1997) 103–110

Luque-Garcia J.L., M.D. Luque de Castro, Ultrasound: a powerful tool for leaching, Trends in Analytical Chemistry 22 (2003) 41-47.

Mason TJ. Ultrasound in synthetic organic chemistr. Chem. Soc. Rev. 26 (1997) 443-451.

Maurizion B; Giovanni C; Mirko G; Giancarlo P; Giuseppe L; Riccardo O, Radio frequency (RF) ablation of renal tumours does not produce complete tumour destruction: results of a phase II study. European Urology Supplement, 3 (2004), 14-17.

McBain, D.. Finding value in fractions. BBOP, 4 (2008), 1-12.

Mermelstein N H., Interest in radiofrequency heating heats up. Food Technology, 51 (1997), 94-95.

Mierzwa J., S.B. Adaaoju, H.S. Dhindsa, Anal. Sci. 13 (1997) 189.

Mierzwa J., Sun J.Y.C. and Yang M.H., Determination of Co and Ni in soils and river sediments by electrothermal atomic absorption spectrometry with slurry sampling, Anal. Chim. Acta, Vol. 355 (1997), 277–285.

Moyer J C; Stotz E., The blanching of vegetables by electronics. Food Technology, 1 (1947), 252-257.

Moyer J C; Stotz E., The blanching of vegetables by electronics. Food Technology, 1 (1947), 252-257.

Piezoelectricity, Wikipedia, The Free Encyclopedia, http://en.wikipedia.org/wiki/Piezoelectricity, Accessed 30 December, 2011.

Piyasena P; Dussault C; Koutchma T; Ramaswamy H S; Awuah G, Radio Frequency heating of foods; principles, applications and related properties-A review. Critical Review in Food Science and Nutrition, 43 (2003), 1-20.

Poulin A; Dostin M; Proulx P; Kendalla J, Convective heat and mass transfer and evolution of moisture distribution combined convection and radio frequency drying. Drying Technology, 15 (1997), 1893-1907.

Suslick K.S., 1994. The Year Book of Science and Future, Encyclopedia Britannica: Chicago 138.

Suslick, K. S., Sonochemistry, in Kirk-Othmer Encyclopedia of Chemical Technology, 4th Ed. J.Wiley & Sons, New York, vol. 26 (1998) 517-541.

U of M Distillers Grains By-products website, 2010, Anonymous, overview (Distillers Dried Grains with soluble), the University of Minnesota Distillers Grains By-products in Livestock and Poultry Feeds, Available at http://www.ddgs.umn.edu/overview.htm. Accessed 24 December 2011.

Vinatoru M, Toma M, Mason TJ., Ultrasound-assisted extraction of bioactive principles from plants and their constituents, Adv. Sonochem. 5 (1999) 209-247.

Wang J., B. Sun, Y. Cao, Y. Tian, X. Li, Optimisation of ultrasound-assisted extraction of phenolic compound from wheat bran, J. Food chem. 106 (2008) 804-810.

Zhong Q; Sandeep K P; Swartzel K R, Continuous flow radio frequency heating of water and carboxymethylcellulose solution. Journal of Food Science, 68 (2003) 217-223.

Ziggers D. Wheat dictates DDGS supply in Europe. Feed Tech 11.8 (2007)18-20.

CHAPTER 2
Determination of optimum solvent condition and diffusion kinetics for extraction of phenolic compounds from wheat dried distiller's grain (DDG)

Abstract

Dried distiller's grain (DDG), a co-product of the ethanol production process, is potentially rich in phenolic compounds. In this study, phenolic compounds were extracted from DDG with two levels of initial moisture content of DDG particles (3.75 and 59.50%, wet basis), three levels of extraction temperature (30, 50, and 70°C), and five levels of ethanol fraction of the solvent (30%, 40%, 55%, 70% and 90%). The maximum extraction rate and yield were obtained with 70% ethanol concentration, 70°C extraction temperature and 59% particle moisture content. This study also relates the effects of extraction temperature, particle moisture content and ethanol fraction of the solvent on the yield, rate and kinetics of extraction. First and second order models were investigated and compared to describe the kinetics and mechanism of the phenolic compounds extraction process, and the experimental data agreed better with the second order model. The extraction rate constant, the frequency factor, and the activation energy were determined for 18 extraction conditions. The effective diffusivity of phenolic compounds in DDG particles was also determined for each extraction condition.

Keywords: Dried distiller's grain; Phenolic compounds; Solid-liquid extraction; Kinetics; Effective diffusivity;

Notation

C_{sat}	*concentration of phenolic compounds in the solution at saturation, mg* L^{-1}
C_t	*concentration of phenolic compounds in the solution at any time, mg* L^{-1}
K	*second-order extraction rate constant, L* mg^{-1} min^{-1}
t	*time, min*
A	*temperature independent factor, L* mg^{-1} min^{-1}
E	*activation energy, J* mol^{-1}
R	*gas constant, 8.314 J* mol^{-1} K^{-1}
T	*absolute temperature, K*
RMSE	*root mean squared error*
MARE	*mean absolute relative error*
Q_i	*experimentally measured value*
$\hat{Q}_i$	*computed value from models*
$\overline{Q}$	*mean of the measured data*
$\tilde{Q}$	*mean of the computed values*
C	*phenolic compounds concentration inside of particles, mg* mg^{-1}
x	*spatial variation, m*
D	*mass diffusivity,* m^2 min^{-1}
C_0	*initial concentration of phenolic compounds in the particle, mg* mg^{-1}
C_s	*concentration of phenolic compounds at the surface in the solid, mg* mg^{-1}
L	*characteristic length, m*
C_{av}	*average concentration of phenolic compounds, mg* L^{-1}
$C(t)$	*phenolic compounds concentration at each time in the solvent, mg* L^{-1}
C_i	*initial concentration of phenolic compounds in the solvent, mg* L^{-1}
SD	*standard deviation*

2.1. Introduction

One member of the important group of biologically active molecules present as metabolites in plants is phenolic compounds (Herrea and Luque, 2005). Numerous studies have found phenolic compounds have an important influence on human health. Phenolic compounds decrease the risk of chronic diseases related to oxidative stress diseases such as Parkinson disease, multiple sclerosis, dementia, diabetes, several types of cancer and liver diseases, asthma, cystic fibroses, chronic obstructive pulmonary diseases (COPD), cardiovascular and digestive disease, kidney failure, and even the common cold (BBOP, 2008). Plants containing phenolic compounds have been of interest to many researchers for their potential antioxidant properties and significant influence in prevention of the oxidative stress associated diseases such as cancer. Recently, extracts of phenolic compounds from various plants have become a major area of health- and medical-related research (Dai and Mumper, 2010).

Phenolic compounds have been found in various fruits and vegetables. Studies have been conducted on detection and extraction of phenolic compounds from different main- and by-products such as extraction from *Amaranthus* species (Amin et al., 2006), pistachio hull (Goli et al., 2005), wheat bran (Wang et al., 2008), grape seeds (Ghafoor et al., 2009), and fresh and dry hazelnuts, walnuts and pistachios (Arcan and Yemenicioglu, 2009). Cereal grains are rich sources of phenolic compounds, which are found in both free and bound forms, and concentrated in the bran portion of cereal kernels (Lempereur et al., 1997).

In western Canada, because of the productivity and availability of wheat on the prairies, wheat is used for ethanol production. Several co-products originate from the raw wheat used in ethanol production, such as wet distiller’s grain (WDG), distiller's dried grain (DDG), distiller's dried solubles, and distiller's dried grain with solubles (DDGS). The major co- product of fermentation of wheat during ethanol production is distiller’s dried grain with solubles (DDGS) (Ziggers, 2007). Approximately 3.2 to 3.5 million tonnes of DDGS are produced annually in North America.

Based on observations by Gibreel et al. (2009), the concentration of phenolic compounds can vary from 6.3 to 10.4 mg Gallic acid/gram of the DDGS obtained from VHG jet cooking

fermentation and VHG modified STARGEN-based fermentation. So, there is a considerable concentration of phenolic compounds in wheat DDGS to be extracted.

In this study, it was of interest to investigate the extraction of phenolic compounds within the cells of DDGS, therefore DDG was used as raw material. The sample of distiller's grain that was collected for this study were originally wet, namely wheat wet distillers grain (WDG), which was dried in the lab to avoid impurities that might be added to the sample during the industrial drying process. As WDG is easily available from ethanol production industries, it can be considered as an alternative source of phenolic compounds. There is little information available on the optimum ethanol-water solvent system, effective diffusivity and the kinetics of extraction conditions of phenolic compounds from WDG or DDG.

Extraction is one of the most important processes in the pharmaceutical industry. Among the various types of extraction, such as liquid-liquid extraction, solid-liquid extraction and gas-liquid extraction, solid-liquid extraction is the most popular for extraction of medicinal compounds. In solid-liquid extraction, matter extraction kinetics occurs in four stages: (i) the solid is put in contact with the solvent of extraction that induces a distension of the particles (Harouna-Oumarou et al., 2007); (ii) the difference in concentration of compounds between fresh solvent and particles causes a significant dissolution of the compounds, which results in most of the extraction takes place in this stage (Rakotondramasy-Rabesiaka et al., 2007); (iii) then a much slower stage occurs with transfer of solute by molecular diffusion from small pores inside of each particle to the surface of the particle; and (iv) convective mass transfer occurs from each particle surface to the moving solvent. Solid-liquid extraction normally depends on the nature of the solvent and solid particles, temperature of the process, particle size, reaction time between solvent and particles, the fraction of solvent, and particle moisture content (Sayyar et al., 2009).

In this study, the effects of temperature, volumetric concentration of ethanol and particle moisture content on the extraction rate and yield of phenolic compounds from DDG have been investigated, and also the optimum condition of extraction of phenolic compounds from DDG has been found. The kinetics of the extraction and mechanism have been investigated and the kinetic parameters have been identified. The effective diffusivity of phenolic compounds for each extraction procedure has been also estimated.

2.2. Materials and method

2.2.1. Sample preparation

Wet distiller's grain (WDG) with an initial moisture content of 66.8% wet basis was obtained from Terra Grain Fuels, Inc., (Belle Plaine, SK, Canada). The WDG was dried using an oven drying method. The WDG was put in an aluminum tray, placed in an oven, and dried at a temperature of 70ºC for 24 hour. After drying, the DDG was packaged and preserved in a cold room at 4ºC until used. The DDG was sieved using a series of sieves with US standard sieve numbers of 6, 8, 12, 16, 20, 30, 40, 50, 60, 70 and 100 based on the ASABE standard method (ASAB, 2009).

2.2.2. Preparation of different levels of moisture content

Samples with desired moisture contents were prepared by spraying a pre-determined amount of distilled water on the DDG particles, followed by periodic tumbling of the samples in sealed containers. Then the samples were kept for 4-5 days at room temperature to equilibrate and then stored at 4ºC before testing. The moisture content of the DDG particles was determined using the oven method at 135ºC for 2 hours (AOAC, 2000a).

2.2.3. Extraction of phenolic compounds

Solid-liquid extraction was performed to extract phenolic compounds from DDG. One hundred millimetre of solvent was prepared and poured into a 250mL flask and placed in a water-bath on a hot plate stirrer at desired temperatures. When the solvent reached the desired temperature, five grams of accurately weighed DDG was added to the solvent and instantly mixed by a magnetic stirrer at 500 rpm. Sample of 0.7mL were drawn out at different times during the extraction and then transferred to vials followed by centrifugation for 5 min at 809×g relative centrifugal force. The supernatant after centrifugation was used for the determination of the total phenolic content.

2.2.4. Determination of phenolic compounds concentration

The phenolic content was determined using the method of Singleton and Rossi (1965) with Folin-Ciocalteu as reactive reagent, and results were expressed as mg gallic acid equivalents per dry weight of sample (mg GAE/g dry material). The DDG extract was diluted in a mixture of ethanol and distilled water (1:6 v/v). A 0.4mL sample was mixed with 2ml of 10-fold-diluted Folin-Ciocalteu reagent (1:9 Folin-Ciocalteu reagent: distilled water). After 3 min, 1.6mL of 7.5% sodium carbonate solution was added to the mixture. Then the mixture was allowed to stand for 2 h at room temperature. Then, total phenolic compounds were measured using a spectrophotometer at 765 nm. The experiment was carried out in duplicate. Gallic acid was used to prepare a standard curve.

2.2.5. Particle size measurement

A Wild M3Z microscope with a Pax cam (Digital microscope camera) and Pax-it software (version 7.2a, Heerbrugg Switzerland) was used for particle size measurement. Particles sieved with US sieve number 20 were used in extraction and size measurements. To measure the thickness of particles randomly, 22 particles were placed horizontally on a tape and placed vertically under the microscope lens. The image of particles was analyzed and particle geometries were statistically evaluated using Pax-it software. The average thickness of each particle was obtained and an average of 22 particles was determined. Fig. 2.1 shows the enlarged image (×16) of a DDG particle with several cross-section measurements. The average half thickness of particles was used to determine the effective diffusivity of phenolic compounds.

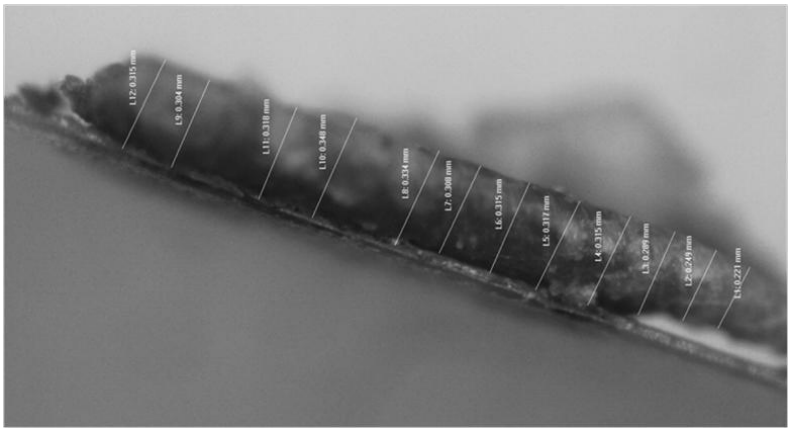

Figure 2.1. A DDG particle magnified by means of a Wild M3Z microscope with a Pax cam (×16).

2.2.6. Optimization of phenolic compound extraction from DDG

The influence of three main factors (ethanol fraction of solvent, temperature and particles moisture content) was investigated to optimize the extraction condition for maximum phenolic compound yield. Five levels of ethanol concentration (30%, 40%, 55%, 70% and 90%) were used for extraction. The extraction temperatures were 30°C, 50°C, and 70°C. The maximum temperature was 70°C to avoid boiling of the solvent (approximately 78°C). Two levels of particle moisture content (3.75% and 60.00% wet basis) were chosen as they were closer to those for DDG and WDG. Temperature, ethanol fraction of solvent and moisture content were varied one at a time to identify the optimum condition of extraction.

2.2.7. Analysis of extraction kinetics

A better understanding of the extraction process could lead to a more efficient extraction operation. Various studies have been conducted to find a suitable explanation for the kinetics and mechanism of extraction processes (Rakotondramasy-Rabesiaka et al., 2007).

The order of extraction describes the pattern of the extraction profile with time and may vary for different extraction processes. If the extraction kinetic model is found to be first-order, it can be assumed that the extraction is only a solubilization mechanism, which is a short and fast dissolution of free solute (Harouna-Oumarou et al., 2007). However, if the model is second-order it means that the mechanism of extraction proceeds in two steps: a fast dissolution of free solution followed by a slow diffusion of solute from the solid particles to the solvent. In this study, two extraction models, first- and second-order, were investigated and then kinetics parameters, rate constant, activation energy and frequency factor were determined as a function of temperature, ethanol fraction of solvent and moisture content. If the activation energy for the extraction of phenolic compounds is higher than 40 kJ/mol, the extraction is considered as solubilization reaction controlled. If less than 20 kJ/mol, the extraction is controlled by diffusion. For activation energies between 20 and 40 kJ/mol, the extraction is controlled by both reaction and diffusion (Ly and Margaritis, 2007).

In addition, it should be considered that in solid-liquid extraction, the solid structure can change the kinetics of mass transfer (Harouna-Oumarou et al., 2007). When all free solute is dissolved in the solvent, diffusional mass transfer dominates. More precisely, in this step the

solvent must penetrate the rigid cell wall. Once inside the cell, the solvent must solubilise phenolic compounds and then phenolic compounds diffuse through the cell wall, across the solid-liquid interface and across the liquid film surrounding the particle into the bulk liquid (Ly and Margaritis, 2007). If the extraction of phenolic compounds is controlled by diffusion, the effective diffusivity under different extraction conditions (e.g. extraction temperature, concentration of ethanol in the solvent and particle moisture content) is required to be determined.

- ***Kinetic model***

In solid-liquid extraction, the rate of extraction should be proportional to the driving force where the driving force is assumed to be (C_{sat} - C_t), where C_{sat} (mg L^{-1}) and C_t (mg L^{-1}) are the concentrations of phenolic compounds at saturation and at any time, respectively (Harouna-Oumarou et al., 2007).

By considering the extraction process as a first order reaction, the rate of extraction for diffusing molecules in the particle to solvent can be described as (Datta , 2001):

$$\frac{dC_t}{dt} = k(C_{sat} - C_t) \text{, or } C_{sat}\text{-}C_t = C_0 e^{-kt} \quad (1)$$

By assuming that C_0 is the concentration of phenolic compounds at saturation in mg L^{-1} (at 1 hour), the linear form of above equation would be:

$$Ln\,(C_{sat}\text{-}C_t) = LnC_{sat}\text{-}kt \quad (2)$$

The linearity of the extraction process by a first-order model was investigated by plotting $Ln\,(C_{sat}\text{-}C_t)$ vs. t. In the second step, by considering the reaction to be second-order, the rate of reaction can be described by the following equation (Sayyar et al., 2009):

$$\frac{dC_t}{dt} = k(C_{sat} - C_t)^2 \quad (3)$$

where k is the second-order extraction rate constant (L mg^{-1} min^{-1}), C_{sat} is the concentration of phenolic compounds at saturation (mg L^{-1}), C_t is the concentration of phenolic compounds in the solution at any time (mg L^{-1}), and t is time (min).

The integration of Eq. (3) is given as:

$$C_t = \frac{C_{sat}^2 kt}{1 + C_{sat} kt} \tag{4}$$

The linearized form of the Eq. (4) is:

$$\frac{t}{C_t} = \frac{1}{kC_{sat}^2} + \frac{t}{C_{sat}} \tag{5}$$

The rate constant, *k*, was calculated by plotting t/C_t vs. t/C_{sat}. It was assumed that after 1 h maximum extraction phenolic compounds were achieved, so the concentration of phenolic compounds in the solution at 1 hour was considered the saturated concentration.

Arrhenius law was used to model the temperature dependency of the reaction rate constant (Sayyar et al., 2009):

$$k = A \exp\left(\frac{-E}{RT}\right) \tag{6}$$

where *k* is the second-order extraction rate constant (L mg^{-1} min^{-1}), *A* is the temperature independent factor (L mg^{-1} min^{-1}), *E* is the activation energy (J mol^{-1}), *R* is the gas constant (8.314 J mol^{-1} K^{-1}) and *T* is the absolute temperature (K). The linear form of Eq. (6) would be:

$$\ln(k) = \ln(A) + \left(\frac{-E}{R}\right)\frac{1}{T} \tag{7}$$

Activation energy (*E*) and frequency factor (*A*) were obtained from *ln(k)* against *1/T* plot.

The performance of the models; first-order and second-order was evaluated based on three statistical criteria: root mean squared error (RMSE), mean absolute relative error (MARE), and R square (R^2) between experimental and computed data (Dawson et al., 2007):

$$RMSE = \sqrt{\frac{\sum_{i=1}^{n} (Q_i - \hat{Q}_i)^2}{n}} \tag{8}$$

$$MARE = \frac{1}{n}\sum_{i=1}^{n}\frac{\left|Q_i - \hat{Q}_i\right|}{Q_i} \tag{9}$$

$$R^2 = \left[\frac{\sum (Q_i - \overline{Q})(\hat{Q}_i - \tilde{Q})}{\sqrt{\sum_{i=1}^{n}(Q_i - \overline{Q})^2 \sum_{i=1}^{n}(\hat{Q}_i - \tilde{Q})^2}}\right]^2 \tag{10}$$

where Q_i is the experimentally measured value, $\hat{Q}_i$ is the computed value from the models, $\overline{Q}$ is the mean of the measured data, and $\tilde{Q}$ is the mean of the computed values.

- ***Diffusion model***

Considering that the main mechanism in solid-liquid extraction is diffusion, mass diffusivity of phenolic compounds, an important engineering property, was estimated by fitting experimental results into Fick's 2nd law. According to our microscopic observation, the DDG particle geometry was slab and for simplicity, the following assumptions were made: (1) external fluid resistance to be negligible by high mixing speed (high convective mass transfer coefficient) (2) the boundary condition at the surface to be zero concentration due to phenolic compounds concentration in fresh solvent and (3) particles were considered to one-dimensional slabs. Considering these assumptions, the simplified governing equation is expressed as follows (Datta, 2001):

$$\frac{\partial C}{\partial t} = D\frac{\partial^2 C}{\partial x^2} \tag{11}$$

where C is the phenolic compounds concentration inside of particles, mg mg^{-1}, x is the spatial variation, m, t is time, min, and D is mass diffusivity, m^2 min^{-1}. Initial and boundary conditions of Eq. (11) are given as:

$$\frac{\partial C(x=0,t)}{\partial x} = 0 \tag{12}$$

$$C(x=L,t) = C_s = 0 \tag{13}$$

$$C(x, t = 0) = C_0 \quad (14)$$

where C_0 is the initial concentration (mg mg^{-1}) which was assumed equal to saturated solute concentration in the solvent (after 1 hour extraction) (mg L^{-1}), and C_s is the constant concentration at the surface in the solid (mg mg^{-1}) at time>0 which was assumed to be 0 during the extraction process of phenolic compounds from DDG. This assumption is not true in reality; however it was made to oversimplify the extraction process in order to solve the mass diffusion model analytically. The volume average concentration with time for F_0> 0.2:

$$\ln \frac{C_{av} - C_s}{C_i - C_s} = \ln \frac{8}{\pi^2} - D(\frac{\pi}{2L})^2 t \quad (15)$$

where L represents the characteristic length which was the half thickness for plate-shaped DDG particles (m). Since the concentration of phenolic compounds in the fluid (solvent) was more readily available, C_{av} was converted to C_{sat}-$C(t)$ which in C_{sat} is the concentration of phenolic compound at saturation in mg L^{-1} (at 1 h of extraction), $C(t)$ is the solute concentration at each time in the solvent (mg L^{-1}) and C_i was assumed equal to C_{sat}. The effective diffusivity of phenolic compound, D, was calculated experimentally by plotting $ln\frac{(C_{sat} - C(t))}{C_{sat}}$ vs. t.

2.3. Results and discussion

2.3.1. Particle geometry analysis

On the one hand, smaller particles have faster transfer of phenolic compounds from inside to the surrounding solvent because larger particles with smaller contact surface areas are more resistant to solvent entrance and phenolic compound diffusion (Sayyar et al., 2009). On the other hand, when the particles are too small, filtering problems will occur during the extraction process. So, from series of sieved DDG particles, the medium particle size of 0.84 mm (US sieve size number 20) was selected for the extraction of phenolic compounds from DDG in this study. The appropriate size of the particle for further study using the packed bed extraction unit in radio frequency assisted extraction, was also considered in selecting the particle size. By means of a Wild M3Z microscope and Pax-it software, DDG particles were observed in plate (slab) shape with an average thickness of 0.263 mm. The half thickness of DDG particles (0.1315 mm) was used for determination of effective diffusivity.

2.3.2. The effect of extraction temperature

Fig. 2.2a shows the effect of temperature on the extraction rate of phenolic compounds for three temperatures at the particle moisture content of 3.75% (wet basis) with 30% ethanol. The extraction rate increased with temperature from 30 to 70°C. Fig. 2.2b illustrates the variation in phenolic compounds concentration with temperature and time for 70% ethanol and particle moisture content of 59% (wet basis). The total extracted phenolic compounds increased slowly with temperature at a fixed extraction time, and reached a maximum at the highest extraction temperature tested (70˚C). It was observed that in all experiments the extraction rate was rapid at the beginning of the extraction, and kept slowing down until the end, approaching equilibrium concentration. This observation was in agreement with observations by Wongkittipong et al. (2004) on the solid-liquid extraction of andrographolide, and by Izadifar and Baik (2008) on podophyllotoxin extraction.

The reason for this extraction pattern is that when particles are exposed to fresh solvent, the free phenolic compounds on the surface of DDG particles are solubilized and phenolic compounds transfer to the surface and are convected away to the solvent rapidly. At the beginning, there is a larger concentration gradient across the particles, so the phenolic compounds diffuse more quickly through the DDG particles. As time passes, the concentration gradient in the particles becomes smaller and the concentration of phenolic compounds in the solvent increases slightly. This led to a decrease in the diffusion rate. The rate of mass transfer within initial minutes of extraction was faster for higher temperatures so that the fastest extraction rate was observed at 70˚C (Fig. 2.2a).The pattern of the temperature effect on extraction rates with other ethanol fractions was similar. This is due to the thermal kinetics of mass transfer and the thermodynamic effect on solubilization of phenolic compounds inside the solid. In addition, by increasing the temperature, the viscosity of DDG extracts and the surface tension of the solvent inside the solid matrix is decreased, which results in accelerating the whole extraction (Izadifar and Baik, 2008).

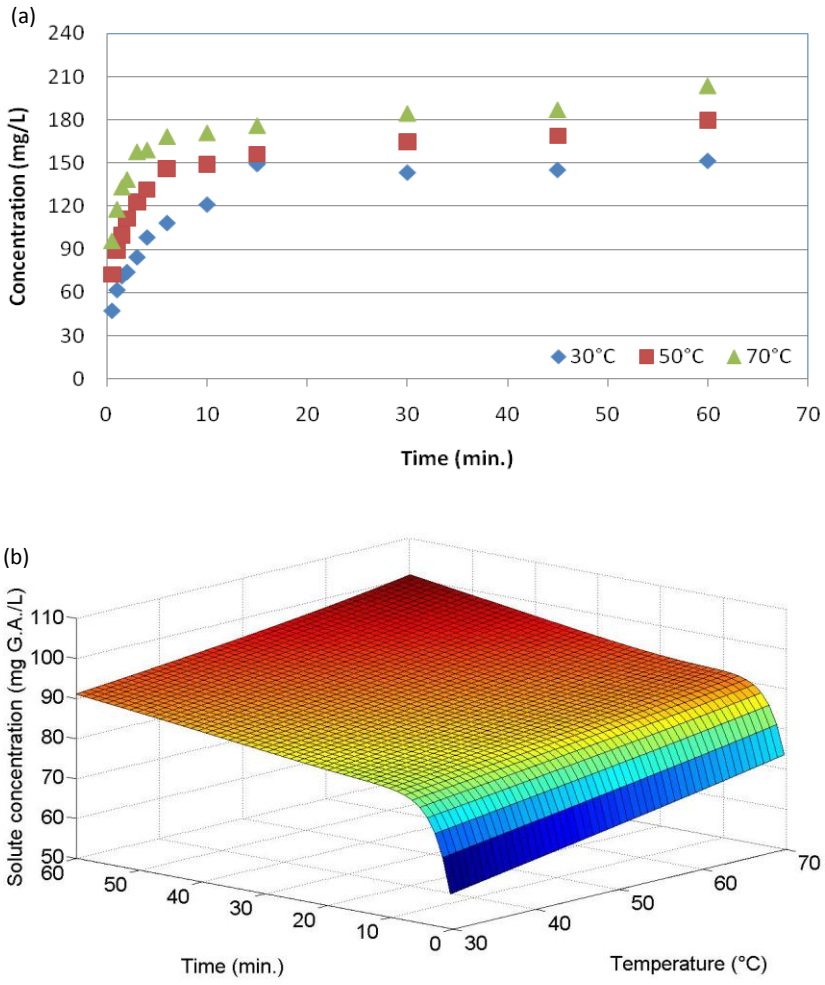

Figure 2.2. The effect of extraction temperature on the extraction rate of phenolic compounds from DDG at (a) ethanol volumetric fraction of 30%, particle moisture content of 3.75% wet basis and at (b) ethanol volumetric fraction of 70% and 59% wet basis moisture content for sieve-based particle size of 0.84 mm.

2.3.3. The effect of ethanol fraction of solvent

The effect of the volumetric fraction of ethanol in the extraction solvent on the extraction of phenolic compounds from DDG particles is shown in Fig. 2.3a and b with ethanol concentrations of 30%, 40%, 55%, 70% and 90% (v/v) at 30˚C, particle moisture content of 59% (wet basis), and sieved-based particle size of 0.84 mm. As the ethanol concentration increased from 30% to 70%, a significant improvement in yield was observed (Fig 2.3a); however, the amount of extracted phenolic compounds decreased considerably by increasing the ethanol concentration of solvent from 70% to 90%. The total extracted phenolic compounds increased

gradually with the increase of volumetric fraction of ethanol at a fixed extraction time, and nearly reached a peak at around 70% ethanol (Fig. 2.3b). However, when ethanol solution was concentrated more than 70% led to a marked decrease in total yield.

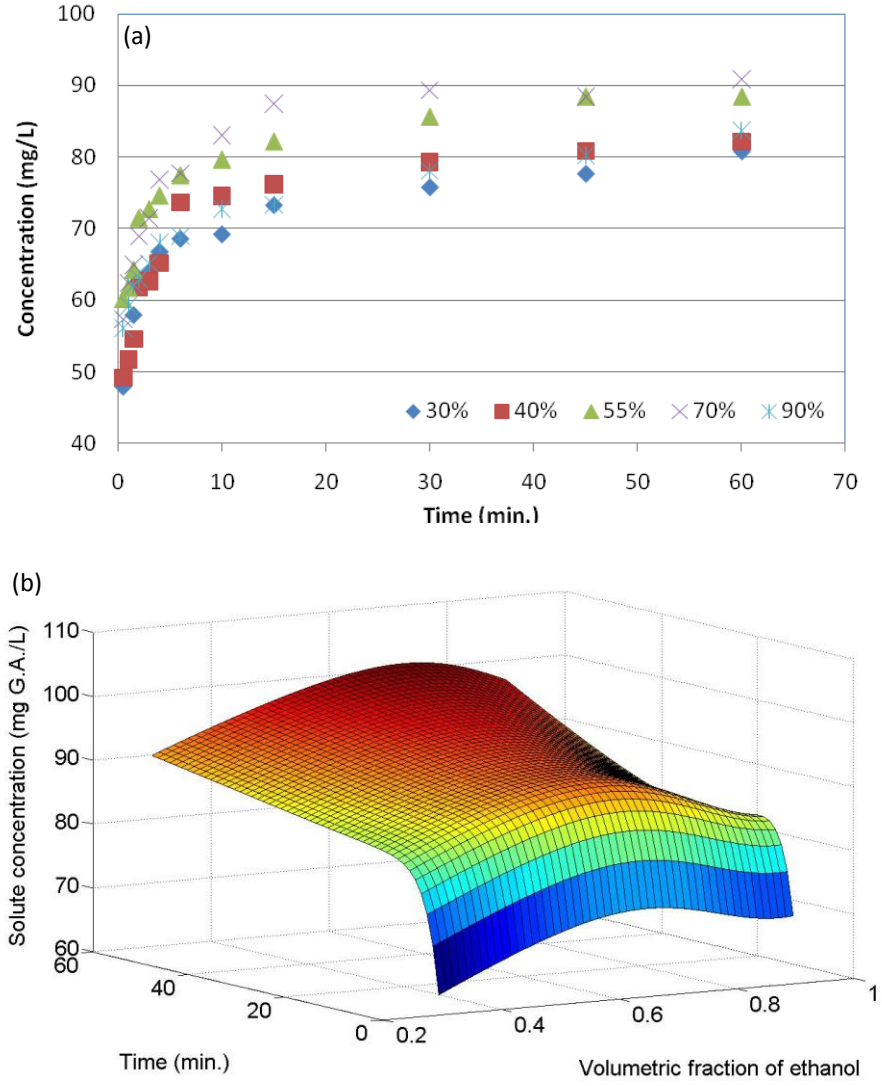

Figure 2.3. The influence of ethanol concentration on the extraction rate of phenolic compounds at the temperature of 30˚C (a) and temperature of 70°C (b) with particle moisture content of 59% wet basis and sieved-based particle size of 0.84 mm.

This is attributed to the decrease of phenolic compounds solubility and simultaneous extraction of some lipid components from DDG particles at high ethanol concentration. This observation was in agreement with Wang et al. (2008) in extraction of phenolic compounds from

wheat bran. As they reported, the extraction of phenolic compounds was improved when ethanol concentration increased from 20% to 60%. However, the extraction was decreased quickly when ethanol concentration reached and increased above 80%. At 95% ethanol, they observed some extracted lipid components.

2.3.4. The effect of moisture content

Fig. 2.4a and b show the phenolic compounds concentration in the solvent and yield of extracted phenolic compounds, respectively, at two levels of particle moisture contents (3.75% and 59%, wet basis) at 55% ethanol and operating temperature of 30°C. It can be seen clearly that the particle moisture content had significant effect on the kinetics of phenolic compounds extraction. When particle moisture content increased from 3.75% to 59% wet basis, the concentration of phenolic compounds decreased considerably (Fig. 2.4a). However, the particles with higher moisture content resulted in higher extraction yield compared to the particles with lower moisture content (Fig. 2.4b). This difference between yield and concentration was attributed to different mass of dry matter in samples with different particle moisture contents. In calculating the yield, the amount of solute in total solution was divided by the amount of dry sample (DDG in gram) to obtain a yield in mg gallic acid/g dry DDG. Thus, higher moisture content samples had lower amounts of dry mass, which resulted in higher yields compared to particles with lower moisture content and vice versa. The similar effect of moisture content on variation of concentration and yield with time was also observed for other ethanol fractions of solvent and extraction temperature tested (results are not shown here). These results suggest that it would be more efficient for industry to extract phenolic compounds from DDG with higher moisture content (i.e. WDG) rather than DDG with lower moisture content. In this case, even time and energy for drying WDG can be saved as well.

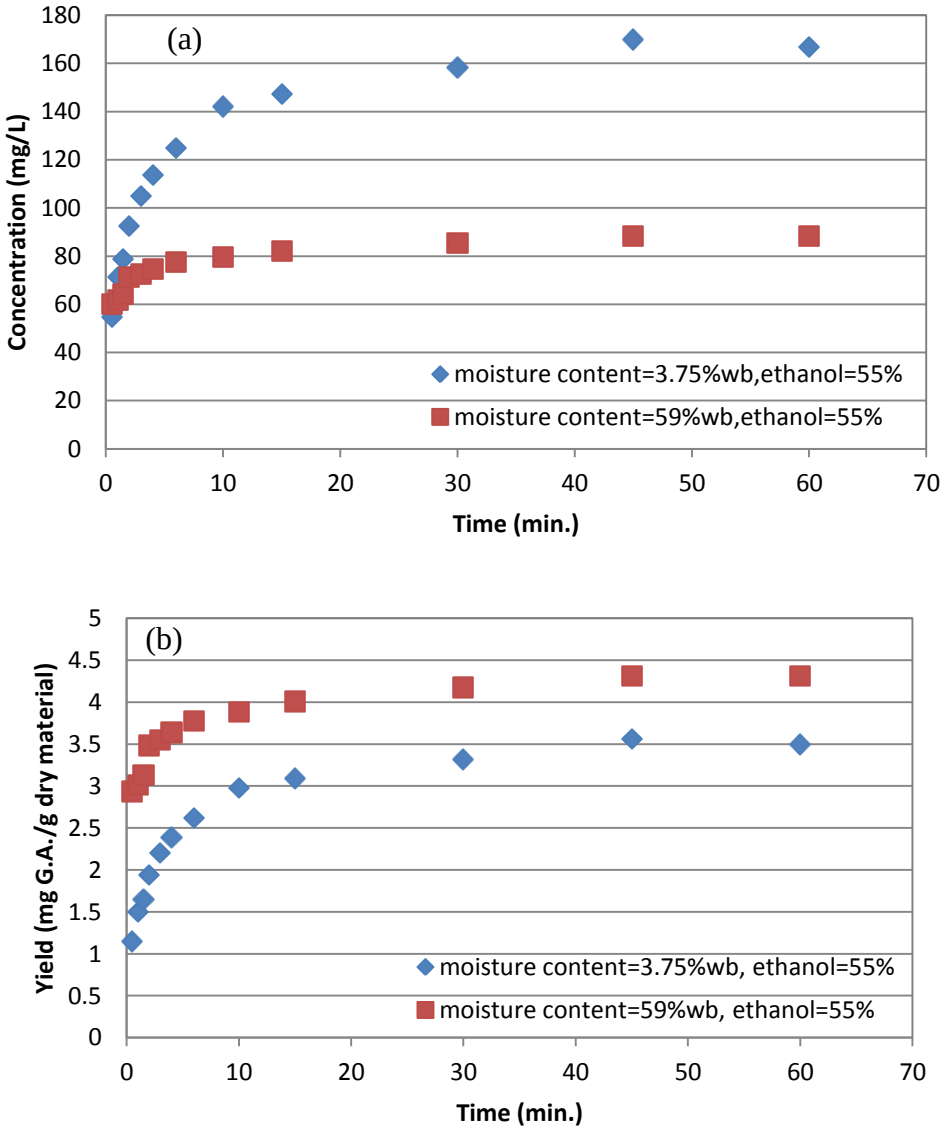

Figure 2.4. The effect of particle moisture content on the solute concentration in solvent (a) and yield (b) of extracted phenolic compounds at 30°C and ethanol volumetric fraction of 55%.

2.3.5. Modeling analysis of phenolic compounds extraction mechanism

Fig 2.5a and b show a linear representation of first- and second- order rate laws for an ethanol volumetric concentration of 40% at 30°C and a particle moisture content of 59% (wet basis). The straight line in Fig. 2.5b implies good agreement of the second-order model with the experimental results. Table 2.1 shows a comparison between the performance measures and general statistical characteristics of the errors obtained from the fitted regressions. It is apparent that the second-order model is a better fit than the first-order model with lower RMSE and

MARE and higher R square. Statistical characteristics of the errors also indicate the superiority of the second-order model with lower mean error and standard deviation (SD) values of 0.018 and 0.005, respectively, compared to those of the first-order model, -0.536 and 1.122. This result was in agreement with Sayyar et al. (2009) who reported that a solid-liquid extraction process is most appropriately fitted by a second-order model.

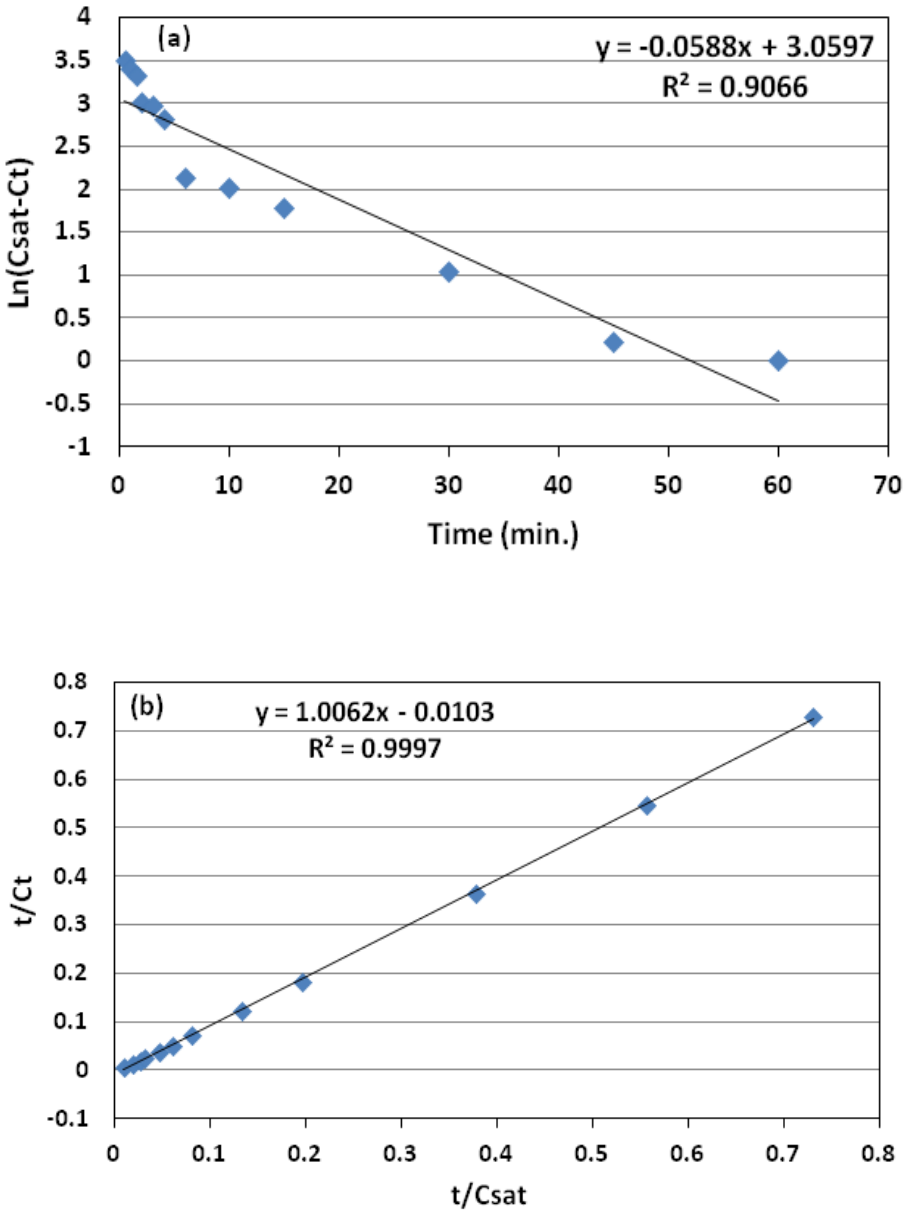

Figure 2.5. The variation of experimental data in linearized form of the first-order (a) and second-order (b) models with time at ethanol volumetric concentration of 40% , extraction temperature of 30°C, and particle moisture content of 59% wet basis.

Table 2.1. Performance measures and general statistical characteristics of the errors from the fitted regression models.

	RMSE	MARE	R^2	Mean	SD
First-order	1.2	1.5	0.908	-0.536	1.122
Second-order	0.019	0.416	1.000	0.018	0.005

2.3.6. Calculation of the kinetics parameters

By use of the linear representation of the second-order kinetics model, the extraction rate constant, *k*, was determined from the intercept of the plotted graph of t/C_t versus t/C_{sat} (Fig. 2.5b). The *k* value was obtained at an ethanol concentration of 40% at three levels of temperature and a particle moisture content of 59% (wet basis). The second-order extraction rate constant, *k*, rises with an increase of temperature for each extraction procedure (Table 2.2), and this temperature dependency of *k* followed Arhenius equation (Eq. 6).

Fig. 2.6 illustrates a linear representation of the Arrhenius equation for 40% ethanol at three levels of temperature and a particle moisture content of 59% (wet basis). The activation energy (E) and the frequency factor (A) respectively for phenolic compounds for each extraction procedure were determined from the intercept and the slope of the plotted graph between ln(k) and the inverse of absolute temperature (Table 2.2). The extraction temperature had a direct influence on saturated extraction capacity (Csat) and the extraction rate constant (k). Csat and k both increased with extraction temperature. Also, the activation energy for all extraction conditions was lower than 20 kJ/mol, which means phenolic compounds extraction from DDG was controlled by diffusion.

Table 2.2. Estimated values of activation energy, frequency factor, and extraction rate constant of extraction at different conditions.

T (°K)	Ethanol%	M.C.*	C_{sat} ** (mg L^{-1})	k (L mg^{-1} min^{-1})	A (L mg^{-1} min^{-1})	E (J mol^{-1})
303.15	30%	59%	80.867	0.022	0.652	8456.169
323.15	30%	59%	81.494	0.031	0.652	8456.169
343.15	30%	59%	93.097	0.032	0.652	8456.169
303.15	40%	59%	82.122	0.018	7.585	15143.950
323.15	40%	59%	85.884	0.029	7.585	15143.950
343.15	40%	59%	97.487	0.036	7.585	15143.950
303.15	55%	59%	88.393	0.021	17.070	16647.120
323.15	55%	59%	93.097	0.041	17.070	16647.120
343.15	55%	59%	95.605	0.046	17.070	16647.120
303.15	30%	3.75%	151.421	0.003	0.036	5975.106
323.15	30%	3.75%	179.642	0.004	0.036	5975.106
343.15	30%	3.75%	203.788	0.004	0.036	5975.106
303.15	40%	3.75%	180.583	0.003	6.554	19109.730
323.15	40%	3.75%	182.778	0.006	6.554	19109.730
343.15	40%	3.75%	192.813	0.008	6.554	19109.730
303.15	55%	3.75%	166.786	0.004	0.113	8511.873
323.15	55%	3.75%	185.287	0.005	0.113	8511.873
343.15	55%	3.75%	189.050	0.006	0.113	8511.873

* Moisture content
** Saturated extraction capacity

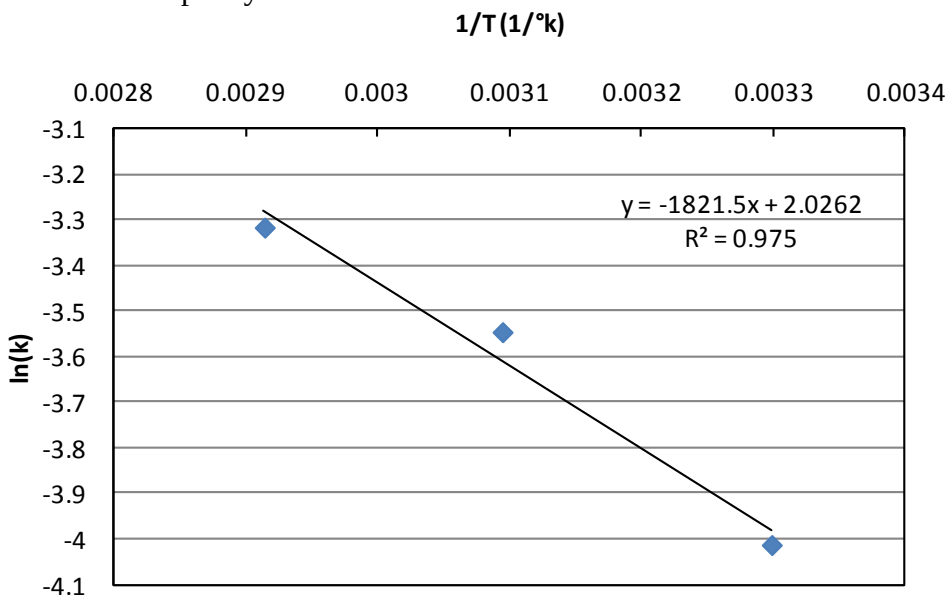

Figure 2.6. The linear relationship between *ln(k)* and inverse of absolute temperature for 40% ethanol and particle moisture content of 59% wet basis.

2.3.7. Effective diffusivity of phenolic compounds

Equation 15 was rewritten by substituting the C_{av} variable by C_{sat}-$C(t)$ and assuming C_i and C_s equal C_{sat} and zero, respectively, for determination of effective diffusivity, which is given as:

$$\ln \frac{C_{sat} - C(t)}{C_{sat}} = \ln \frac{8}{\pi^2} - D(\frac{\pi}{2L})^2 t \quad (16)$$

The identified values of effective diffusivity are given in Table 2.3 for different extraction conditions. The mass diffusivity for each extraction procedure was calculated by plotting $\ln \frac{(C_{sat} - C(t))}{C_{sat}}$ vs. time from the beginning of extraction until the time at which approximately 80% of phenolic compounds was extracted (80% of C_{sat}). The reason for considering this extraction duration is that at the beginning of the extraction (first couple of minutes), the DDG particles are exposed to the fresh solvent and also the extraction mixing rate is sufficiently high at the speed of 500 rpm, so we can assume that the concentration of phenolic compounds on the surface of particles is zero. Therefore, Eq. 16 could give more accurate results for mass diffusivity at the beginning of the extraction process, while as time passed the concentration of phenolic compounds in the solvent increases and the phenolic compounds on the surface increases slightly and the problem of concentration-dependent diffusion becomes more significant. The concentration-dependent diffusion was not considered in the present study. The mass diffusivity of phenolic compounds was determined by plotting $\ln \frac{(C_{sat} - C(t))}{C_{sat}}$ vs. time from t=0.5 to 3 min. for 70% ethanol and a particle moisture content of 59% (wet basis) at 30°C (Fig. 2.7). Table 2.3 shows the estimated values of effective diffusivity at different conditions. The effective diffusivity of phenolic compounds rose as the extraction temperature increased from 30°C to 70°C at a fixed ethanol concentration and particle moisture content. The increasing effect of temperature on mass diffusivity is attributed to the lower fluid viscosity and higher solubility and thermal kinetics of mass transfer of phenolic compounds at higher temperature (Izadifar and Baik, 2008). The effective diffusivity values of phenolic compounds varied from 6.3425×10^{-10} to 3.37099×10^{-9} $m^2\,min^{-1}$ with extraction conditions, and the highest effective diffusivity was obtained when using 55% ethanol volumetric fraction of solvent at 50°C and

particle moisture content of 59% (wet basis). The increase in particle moisture content exhibited the increase in effective diffusivity values at a fixed ethanol concentration and temperature.

Table 2.3. Estimated values of mass diffusivity of phenolic compounds at different extraction conditions for sieve-based particle size of 0.84 mm.

Moisture content (% wet basis)	Ethanol vol. Conc. (%)	Temp. (°k)	Mass diffusivity (m^2 min^{-1})	R^2
3.75%	30	303.15	8.93556E-10	0.9666
3.75%	30	323.15	1.4395E-09	0.9847
3.75%	30	343.15	1.79412E-06	0.9309
3.75%	40	303.15	6.3425E-10	0.9689
3.75%	40	323.15	1.46473E-09	0.9562
3.75%	40	343.15	1.87121E-09	0.9665
3.75%	55	303.15	1.24747E-09	0.9642
3.75%	55	323.15	1.40166E-09	0.9274
3.75%	55	343.15	1.89224E-09	0.9501
59.00%	30	303.15	2.00437E-09	0.9176
59.00%	30	323.15	2.60708E-09	0.9971
59.00%	30	343.15	1.14235E-09	0.9727
59.00%	40	303.15	1.38764E-09	0.9118
59.00%	40	323.15	1.92728E-09	0.9212
59.00%	40	343.15	2.07445E-09	0.916
59.00%	55	303.15	1.09329E-09	0.9768
59.00%	55	323.15	1.81094E-09	0.6218
59.00%	55	343.15	2.33937E-09	0.9837
59.00%	70	303.15	1.53481E-09	0.9643
59.00%	70	343.15	2.14454E-09	0.8347
59.00%	90	303.15	1.06246E-09	0.9747

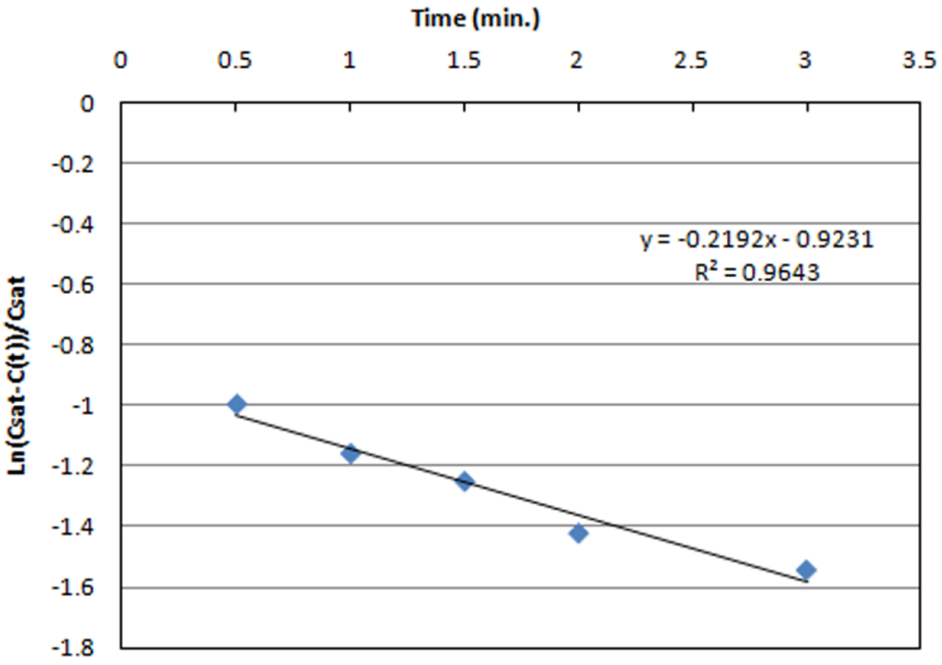

Figure 2.7. Linear relationship between $ln((C_{sat}-C(t))/C_{sat})$ and time for initial minutes of extraction of phenolic compounds at 70% ethanol, 30°C and particle moisture content of 59% wet basis.

2.4. Summary and conclusion

The kinetics of the extraction of phenolic compounds from DDG followed a second-order trend, suggesting that phenolic compounds extraction occurs in two successive stages: a fast dissolution of phenolic compounds followed by a slow molecular diffusion of phenolic compounds from DDG particles to the solvent. The kinetic parameters, namely the extraction rate constant, the frequency factor and the activation energy of extraction, along with the second-order model enable us to predict the extraction process as a function of temperature, ethanol fraction of solvent and particle moisture content. The activation energy for all the extraction conditions of phenolic compounds from DDG was lower than 20 kJ/mol, which indicates that phenolic compounds extraction from DDG was controlled by diffusion. It was also shown that the effective diffusivity of phenolic compounds for each extraction procedure can be calculated based on the assumption of an unsteady state diffusion mass transfer process in a slab. In most cases, the effective diffusivity increased with temperature. The optimum yield and extraction rate of phenolic compounds from DDG was obtained at 70°C, 70% ethanol and a particle moisture content of 59% (wet basis). When the ethanol concentration in the solvent was increased from 30

to 70%, the extraction yield and rate increased; however, both decreased when ethanol concentration was increase from 70% to 90%. The findings from this study suggest the use of WDG instead of DDG for extraction of phenolic compounds while working at a high temperature (70°C) and a 70% ethanol fraction of solvent. These results will be used for further investigations within the framework of improving phenolic compound extraction by using, for example, ultrasound, pulsed electric field and radio frequency assisted extraction.

References

Amera Gibreel, James r. Sandercock, Jingui Lan, Laksiri A. Goonewardene, Ruurd T. Zijlstra, Jonathan M. Curtis, David C. Bressler, Fermentation of Barely by Using Saccharomyces cervisia: Examination of Barely as a Feedstock for Bioethanol Production and Value-Added Products, Appl. Environ. Microbiol. 75 (5) (2009) 1363-1372.

Amin I., Y. Norazaidah, K.I. Emmy Hainida, Antioxidant activity and phenolic content of raw and blanched Amaranthus species, J.Food Chem. 94 (2006) 47-52.

Arcan I., A. Yemenicioglu, Antioxidant activity and phenolic content of fresh and dry nuts with or without the seed coat, J. Food Compos. Anal. 22 (2009) 184-188.

ASABE standards 2009, ASAE S352.2; Moisture Measurement-Unground Grain and Seeds, St. Joseph, MI, USA, APR1988 (R2008).

Association of official Agricultural Chemists (AOAC), AOAC 930.15 Loss on Drying (Moisture) for Feeds. Official Methods of Analysis of AOAC International 17th edition. Washington, D.C: AOAC (2000a).

BBOP (Barley bioproducts opportunities project), http://www.wbga.org/BBOP-April- 08.pdf (2008) 1-12 , accessed on January 2011.

Dai J., R. J. Mumper, Plant Phenolics: Extraction, analysis and their antioxidant and anticancer properties, molecules 15 (2010) 7313-7352.

Datta A. K., Biological and bioenvironmental heat and mass transfer, Ithaca, NY: Cornell university, 2001.

Dawson C.W., R.J. Abrahat, L.M. See, Hydro test, A web-besed toolbox of evaluation metrics for the standardized assessment of hydrological forecasts, Environ. Modell. Softw. 22 (2007) 1034-1052.

Ghafoor K., Y.H. Chi, J.Y.Jeon, I.H. Jo, Optimization of ultrasound-assisted extraction of phenolic compounds, antioxidants, and anthocyanins from grape (vitis vinifera) sedds, J. Agric. Food Chem. 57 (2009) 4988-4994.

Goli A.H., M. Barzegar, M.A. Sahari, Antioxidant activity and total phenolic compounds of pistachio (pistachio vara) hull extracts, J. Food Chem. 92 (2005) 521-525.

Harouna-Oumarou H. A., H. Fauduet, C. Port, Y. S. Ho, Comparison of Kinetic Models for the Aqueous Solid-Liquid Extraction of Tilia Sapwood in a Continuous Stirred Tank Reactor, Chem. Eng. Comm. 194 (2007) 537–552.

Herrera M. C., M.D. Luque de Castro, Ultrasound-assisted extraction of phenolic compounds from strawberries prior to liquid chromatographic separation and photodiode array ultraviolet detection, J. Chromatogr. 1100 (2005) 1-7.

Izadifar M., O.D. Baik, An optimum ethanol-water solvent system for extraction of podophyllotoxin:Experimental study, diffusivity determination and modeling, Sep. Purif. Technol. 63 (2008) 53-60.

Lempereur I., X. Rouau and J. Abecassis, Genetic and agronomic variation in arabinoxylan and ferulic acid content of durum wheat (Triticum durum L.) grain and its milling fractions., J. Agric. *Food* Chem. **25** (1997) 103–110

Ly M., A. Margaritis, Effect of Temperature on the Extraction Kinetics and Diffusivity of Cyclosporin A in the Fungus Tolypocladium inflatum, Biotechnol. Bioeng. 96 (5) (2007) 945-955.

Rakotondramasy-Rabesiaka L., J. L. Havet, C. Porte, H. Fauduet, Solid–liquid extraction of protopine from Fumaria officinalis L. Analysis determination, kinetic reaction and model building , Sep. Purif. Technol. 54 (2007) 253–261

Sayyar S., Z.Z. Abidin, R. Yunus, A. Muhammad, Extraction of Oil from Jatropha Seeds-Optimization and Kinetics, Am. J. Applied Sci. 6 (7) (2009) 1390-1395.

Singleton V.L., J.A. Rossi, Colorimetry of total phenolics with phosphomolibdic-phosphotungstic acid reagents, Am. J. Enology and Viticulture 16 (1965) 144-158.

Wang J., B. Sun, Y. Cao, Y. Tian, X. Li, Optimisation of ultrasound-assisted extraction of phenolic compound from wheat bran, J. Food chem. 106 (2008) 804-810.

Wongkittipong R., L, Prat, S. Damronglerd, C. Gourdon, Solid-liquid extraction of andrographolid from plants-experimental study, kinetic reaction and model, Sep. Purif. Technol. 40 (2004) 147-154.

Ziggers D., Wheat dictates DDGS supply in Europe. Feed Tech. 11 (8) (2007) 18-20.

CHAPTER 3
Ultrasound pretreatment of wheat dried distiller's grain (DDG) for extraction of phenolic compounds

Synopsis

In the last chapter, the mechanism and kinetics of extraction of phenolic compounds from DDG was investigated. In this chapter, DDG particles are pretreated by ultrasound and the effect of ultrasound power and duration on destruction of the cell wall of DDG is investigated. Using findings from the previous chapter (the extraction of phenolic compounds from DDG follows second-order kinetics), the effect of ultrasound operating conditions on the extraction rate constant was analyzed with the pretreated particles of various BET surface areas. Finally, the optimum ultrasound pretreatment condition for DDG particles for extraction of phenolic compounds is suggested.

Abstract

Wheat *Dried distiller's grain (DDG),* a coproduct from the ethanol production process, is rich in potentially health-promoting phenolic compounds. In the extraction of phenolic compounds from DDG, the DDG cell wall is an important barrier for mass transfer from the inside to the outside of the cell. The effect of high-power ultrasound pretreatment on destruction of DDG cell walls and extraction yield and rate was investigated. Direct sonication by an ultrasound probe horn at 24 kHz was applied and factors such as ultrasound power and treatment time were investigated. The method of nitrogen (N_2) adsorption at 77 K was used as a mean to determine and compare the changes in physical properties (specific surface area, pore volume and pore size) of the treated samples at different levels of ultrasound power and treatment time.

The increasing surface area, pore volume and pore size after ultrasonic treatment showed the positive effect of ultrasound pretreatment on developing pores and damaging cell walls. Also, it was observed that the ultrasound pretreatment of DDG particles increased the extraction yield and rate of phenolic compounds from DDG. Among tested ultrasound conditions, 100% ultrasound power for 30 seconds was evaluated as the best pretreatment condition.

Key words: Ultrasound; Pretreatment; Phenolic compounds; DDG; Cell wall; physical property; Solid liquid extraction;

Notation

k	second-order extraction rate constant, L g^{-1} min^{-1}
C_s	concentration of phenolic compounds at saturation, g L^{-1}
C_t	concentration of phenolic compounds in the solution at any time, g L^{-1}
t	time, min

3.1. Introduction

Natural pharmaceutical and nutraceutical products have been spotlighted by researchers and industries. Extraction from biological resources is economically more feasible compared to chemical synthesis of the products. Synthetic products might possess some side effects to human health. Phenolic compounds are useful bioactive molecules with important medicinal properties such as decreasing the risk of Parkinson disease, multiple sclerosis, dementia, several types of cancer and liver diseases, etc. (BBOP, 2008). Wheat distillers dried grain (DDG), a natural source of phenolic compounds, is produced in enormous quantities in both Canada and the USA. DDG is the co-product of bioethanol production process where ethanol is produced from wheat grains during a fermentation process. As DDG is easily available from ethanol production industries, it can be considered as an alternative source of phenolic compounds.

In the extraction of phenolic compounds from DDG, the cell wall of the wheat DDG is an important barrier for mass transfer of phenolic compounds from inside to outside the cell. There is strong potential that in the extraction process, ultrasound pretreatment of the plant materials would enhance the production rate, increase the extraction yield, decrease production costs and energy consumption, ensuring clean and green processing. It is believed that the mechanical effect of ultrasound disruptes cell walls and accelerates the release of organic compounds within the plant body. Thus, mass transfer rate increases due to easier access of the solvent to the cell contents (Chemat et al., 2004). Ultrasound is classified as sound beyond the frequency detectable by the human ear. When ultrasound is applied in the liquid phase, the molecular structure of the medium (liquid) through which ulrtrasound waves passis alternately compressed and stretched. During each stretching phase, the strong enough negative pressure overcomes intermolecular binding forces, turns apart the fluid medium, and produces tiny cavities (microbubbles). In succeeding cycles the cavitation process by which vapour microbubbles form,

grow and undergo implosion takes place within about 400 μs with the release of large amounts of energy (Luque-Garcia and Castro, 2003). It has been observed that temperature and pressure approaching 5000°C and 1000 atm are produced during this collapse (Luque-Garcia and Castro, 2003). When the cavitation bubble collapses close to or on a solid surface, cavity collapse is asymetry because the surface provides resistance to liquid flow from that side. This produces high-speed jets of liquid that drive into the surface at a speed close to 400 km/h (Luque-Garcia and Castro, 2003). The strong impact of the jets on the solid surface results in serious damage to impact zones and pitting of the surface. The mechanical effect of ultrasound allows greater penetration of solvent into the sample matrix, increasing the contact surface area between solid and liquid phase and transfering more solute through the permeable cell wall. Consequently, the solute quickly diffuses from the solid to the solvent (Wang et al., 2008). Therefore, ultrasound is a module of worthy in the pre-treatment of solid samples to provide potentially higher and faster extraction yield.

Cell wall structure has a natural rigidity to protect the intracellular contents. The effectiveness of ultrasound in damaging the cell wall depends on the amount of resistance that plant cell wall shows to ultrasonic waves. The mechanical effects of ultrasound, mainly appear in the physical properties, which include the specific surface area, pore volume and pore size of treated samples. The complete description of the cell wall topography allows a mechanistic understanding of the changes in physical properties induced by ultrasound in treated samples at different levels of ultrasound power and treatment time. In the past, the study of the cell wall porosity was a subject of resaearch and various techniques such as freeze-fracture electrocn microscopy (McCann et al., 1990), mercury porosimeter, solute exclusion (Carpita et al., 1979), electron micrograph NMR, gas adsorption and some others (Rondeau-Mouro et al., 2008). Measurement accuracy and liability are subject to the method applied to detect porosity. This means each method has its own drawbacks and limitations (Chesson et al., 1997). Some methods (McCann et al., 1990; Carpita et al., 1979) provide a single mean value or range of pore size and are unable to provide quantitative information about pore size distribution and surface area (Chesson et al., 1997). In addition, a method like mercury porosimetry is not suitable for plant material (Chesson et al., 1997). The gas adsorption method is a physico-chemical technique based on movement of gas into a structure. This method provides alternative quantitative

methods for describing pore size distribution and their quantification as well as determination of total surface area of pores (Chesson et al., 1997; Papadopoulos et al., 2004; Kojiro et al., 2010).

In this paper the influence of ultrasound pretreatmnet with different conditions such as sonication time and power on the cell wall of DDG and the extraction rate and yied of phenolic compounds from DDG was investigated. We tried to provide a mechanistic understanding of structural changes of the cell wall of treated samples by describing the topography of the cell wall using a gas adsorption method. The method of nitrogen (N_2) adsorption at 77 K was used as a mean to determine and compare the changes in physical properties induced by ultrasound in treated samples at different levels of ultrasonic power and time in order to obtain the best ultrasound pretreatment condition for extraction of phenolic compounds from DDG.

3.2. Materials and method

3.2.1. Materials

Wheat wet distiller's grain (WDG) with an initial moisture content of 66.8% wet basis was obtained from Terra Grain Fuel Ethanol Plant, Inc. (Belle Plaine, SK, Canada). The WDG was oven-dried at 70°C for 1 day with frequent stirring in order to avoid aggregation. After drying, the wheat dried distiller's grain (DDG) with a moisture content of 3.6% wet basis was sieved using a series of standard sieves with the US standard sieve number of 6, 8, 12, 16, 20, 30, 40, 50, 60, 70 and 100 based on the ASABE standard method (ASABE, 2009). The particles retained on the sieve number 20 (opening 0.84 mm) were kept in a sealed plastic bag at room temperature and used in this study. The moisture content of samples was determined using an oven method (AOAC, 2000). Three aluminum dishes, each containing 2 g of particles, were covered and shake until the contents were evenly distributed. The dishes were placed in an air oven as quickly as possible, covers removed and dried for 2 hours at 135°C. Moisture content data reported were average of triplicate measurements.

3.2.2. Ultrasound treatment

Sonication of DDG particles was performed by means of an ultrasonic processor (UP400S, 24 kHz, 400 W, Hielscher Ultrasonics GmbH, Germany) connecting a sonotrode with a flat tip diameter of 7 mm and 100 mm length (H7). The pulse mode was adjusted for

continuous acoustic irradiation and the power output of the processor was adjusted at a desired level between 20% and 100% of the maximum output. A container containing distilled water was placed in an ice-water cooling bath until the temperature of distilled water decreased to 0°C. Distilled water was used as an economic and pure surrounding medium for the sample. The sample (5.00 ± 0.01 g DDG particles) and 100mL of pre cooled distilled water was placed in a 125mL Erlenmeyer flask and then the sonotrode was inserted into the mixure (Fig.3.1a). The Erlenmeyer flask was surrounded by ice and water to minimize the thermal effect of sonication during treatment (Fig.3.1b). After this, samples were sonicated at different amplitudes and time. Sixteen different combinations of time of sonication and power were tested. The sonication times were: 30 seconds, 60 seconds, 5 minutes and 20 minutes. The powers of sonication were 20, 50, 80 and 100% of the total power output (sonication powers of 25 W, 37 W, 66 W and 87 W, respectively). In all experiments, the pH of each solution and the energy supplied by the ultrasound equipment to treat the sample were measured. The procedure of ultrasonic treatment of material was repeated twice under the same conditions to provide samples for extraction and surface area measurement.

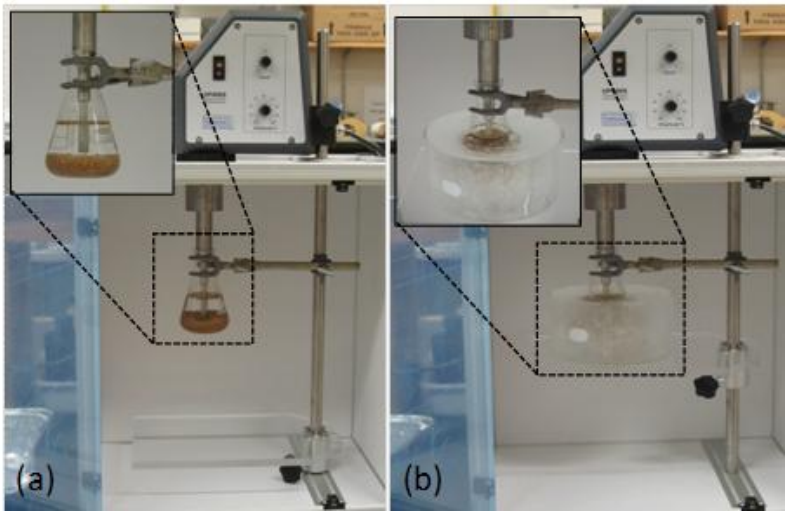

Figure 3.1. Preparation of the sample for ultrasound treatment; (a) inserting sonotrode inside and at the center of sample/water mixture (b) surrounding the Erlenmeyer flask with ice and water.

- **Measuring the pH of solution**

A probe and a precise pH meter (PHS-3C) were calibrated using two buffers (pH 7 and 10). The pH of each treated sample was measured immediately after sonication.

- ***Sample preparation for extraction***

After the sonication step, the mixtures of solution and solid particles were dried in a vacuum oven (AED146, Fisher Scientific., USA) at 60°C and stirred frequently in between using a flint glass rod to avoid aggregation until all solvent evaporated. The sample was kept in the same Erlenmeyer flask throughout all sonication, drying and extraction processes to avoid losing any extracted phenolic compounds that might be stuck to the drying container due to the drying process.

- ***Sample preparation for cell wall porosity and surface area measurement***

After the sonication step, the mixture of solution and solid particles was poured into a US standard sieve number 45 (opening 355 μm) and washed with distilled water to remove the extracted compounds from the surface of particles and avoid blocking produced pores. This sieve mesh number was used to avoid missing disintegrated particles during washing. Washed samples were transferred to flat aluminum plates and dried in a vacuum oven (AED146, Fisher Scientific., USA) at 50°C and stirred frequently in between using a flint glass rod to avoid aggregation until constant weight was achieved. Samples were kept in the vacuum oven (dry environment) until use to reduce the degas time in degassing step (see section 3.2.6).

3.2.3. Extraction method for phenolic compounds

Conventional solid-liquid extraction of phenolic compounds from DDG was performed to make an accurate comparison of extraction rate and yield between various ultrasonic pretreated samples. It consisted of mixing the solvent and the material at the selected temperature. A digital hot plate stirrer (RCT basic, Rose Scientific Ltd., USA) and an EST-D5 contact thermometer with precise temperature control (±0.5°C) was used as the heating and mixing system. 100ml of 30% ethanol solution was poured into a 100mL volumetric flask and subsequently covered with parafilm to avoid evaporation of the solution during preheating. The thermometer was placed inside and at the center of the flask through parafilm to ensure all of the solution reached the

desired temperature. A magnetic stirrer (38 mm x 8 mm) was placed inside the Erlenmeyer flask containing 5 g of dried ultrasound pretreated DDG particles. The flask containing solution and the Erlenmeyer flask containing 5 g of dried treated DDG and a magnetic stirrer were placed in a water-bath on a hot plate stirrer and preheated at 30°C to ensure the extraction process proceeded at the same temperature from beginning to the end of extraction period. The 100mL of preheated 30% ethanol solution was transferred into the preheated Erlenmeyer flask and instantly mixed at a stirring speed of 500 rpm and the extraction time was recorded. A further extraction rate investigation was conducted by taking samples during the extraction time (at 30 sec, 1, 1 min. and 30 sec., 2, 3, 4, 6, 10, 15, 30, 45, 60 min). Since particles were disintegrated during ultrasound pretreatment, a pipette with a pipette tip 101-1000 µl (standard blue tips, Rose Scientific Ltd., USA) was used as a sampler instead of a syringe to avoid blocking the needle. Each liquid sample was taken with a clean pipette tip. Sample solutions of 0.7mL were drawn out through the sampler at specified time intervals during the extraction and then transferred to vials followed by centrifugation for 5 min at 809×g relative centrifugal force. The supernatant after the centrifugation was used for the determination of the total phenolic content.

3.2.4. Determination of phenolic compounds concentration

The total phenolics content of DDG extracts was determined using the method of Singleton and Rossi (1965) with Folin-Ciocalteu as reactive reagent. Distilled water was used for the blank. After centrifugation, 0.5mL of supernatant DDG extract was diluted with 3mL of a mixture of 30% ethanol and distilled water (1:6 v/v). 0.4mL of diluted sample was mixed with 2mL of 10-fold-diluted Folin-Ciocalteu reagent (1:9, Folin-Ciocalteu reagent: distilled water). After 3 min, 1.6mL of 7.5% sodium carbonate solution was added to the mixture. The mixture was shaken and the tube was sealed with parafilm. After 2 h incubation at ambient temperature, the solution was transferred to quartz cuvettes and the absorbance was read at 765 nm on a spectrophotometer. Using gallic acid as standard, the results for total phenolics content of extracts were expressed as mg gallic acid equivalents per dry weight of sample (mg GAE/g dry material). All experiments were carried out in duplicate and data reported in averages.

3.2.5. Calculation of extraction rate constant

As shown in the previous chapter, a solid-liquid extraction process was most suitably fitted by a model based on a second-order extraction process (Adamou Harouna- Oumarou, 2006; So and Macdonald, 1986; Wiese and Snyder, 1987; Meziane et al., 2006; Meziane and Kadi 2008; Goto et al., 1990; Ho et al., 2005). According to the second-order law (Ho et al., 2005; Harouna- Oumarou, 2006), the rate of dissolution for phenolic compounds from the solid to the solution is described by Eq. (1):

$$\frac{dC_t}{dt} = k(C_s - C_t)^2 \quad (1)$$

where k is the second-order extraction rate constant (L g^{-1} min^{-1}), C_s is the concentration of phenolic compounds at saturation (g L^{-1}), C_t is the concentration of phenolic compounds in the solution at any time (g L^{-1}), and t is time (min). By considering the initial and boundary conditions as: t=0 to t and C_t=0 to C_t, the integration of Eq. (1) is given as:

$$C_t = \frac{C_s^2 kt}{1 + C_s kt} \quad (2)$$

The linearized form of the Eq. (2) is:

$$\frac{t}{C_t} = \frac{1}{kC_s^2} + \frac{t}{C_s} \quad (3)$$

The second-order extraction rate constant, k, was determined experimentally from the intercept by plotting t/C_t vs. t/C_s. It is assumed that after 1 h the concentration of the extracted phenolic reached a maximum.

3.2.6. BET surface area and pore structure analysis

BET (Brunauer, Emmett, and Teller) surface area (Brunauer et al, 1938) and pore structure of treated samples were determined by an automated gas adsorption analyzer, ASAP 2020 (Micromeritics, Instruments Inc., GA USA). The accuracy of measurements performed by this equipment was ± 5%. Analyses were carried out using N_2 at 77 K for determination of the physical properties induced by ultrasound.

A sample tube (½ inch) was used in this study. Before each test, the sample tube and a filler rode were washed well using acetone and then oven-dried. The predried sample was directly transferred from the vacuum oven to a sealed bag and then to the sample holder. Care was taken to prevent exchange of moisture content with the ambient environment through transportation. Since the sample had very low surface area, for each analysis ~2 g of sample was used (to fill the 10mL bowl and have no sample in the stem of sample holder). After this, the filler rod was put into the sample tube to fill in most of the volume in the sample tube which was not taken up by the sample (Fig. 3.2a). This gave better free space results for a biomass sample (i.e. DDG) with low gas adsorption. Then sample was degassed under the conditions given in Table 3.1.

Table 3.1. The degassing conditions used for samples in ASAP 2020.

Evacuation phase	
Temperature ramp rate	10.0 K/min
Target temperature	343 K
Evacuation rate	25.0 mm Hg/s
Unrestricted evac. From	25.0 mm Hg
Vacuum set point	5 µm Hg
Evacuation time	120 min
Heating phase	
Ramp rate	10.0 K/min
Hold temp.	343 K
Hold time	5760 min
Evacuation and Heating phase	
Hold pressure	100 mm Hg

Using heater tape, all the way up to the knurled nut of the sample tube stem was also heated at 343±1 K to avoid condensation (Fig. 3.2b). During degassing, the sample was heated at 343 K (Fig. 3.2c). The temperature of the heater tape and the surface of the sample tube stem was checked using an infrared thermometer (Fig. 3.2d).

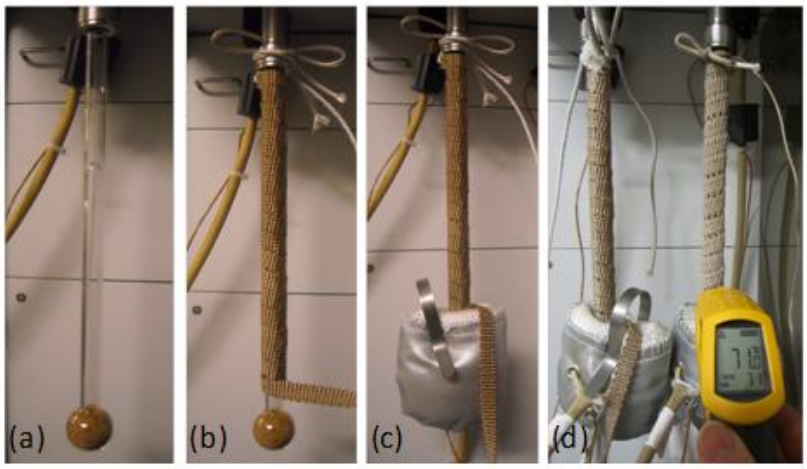

Figure 3.2. Preparation of the sample for degassing (a, b, and c) and temperature controlling during degassing (d).

To ensure the sample was fully degassed, the degassing hold time was set for 4 days and the outgas rate was frequently checked during the degas time. In each outgas test, the outgas rate value was monitored for 2 minutes. If the outgas rate value was 0.5 µm Hg/min or lower, the degassing step was manually backfilled (skipped) otherwise the degassing continued to remove any final traces of moisture. For nearly all samples, 2 days degas time was sufficient. After the degassing process, the internal surface area was characterized by the Brunauer-Emmett-Teller (BET) analysis method (Brunauer et al, 1938). Microporosity of the cell wall was detected using two methods: density functional theory (DFT) (Azargohar, 2009) and the Horvath-Kawazoe (HK) method (Horvath and Kawazoe, 1983). The mesopore size distribution and volume were calculated by applying the density functional theory (Tarazona, 1985; Seaton et al., 1989; Lastoskie et al., 1993). These analytical theories are implemented in Micromeritics ASAP 2020 software Version 3.01.

3.3. Results and discussion

3.3.1. pH

There was no significant change in the pH of samples treated at different ultrasound conditions. The pH values of the samples treated at different sonication conditions varied from 5.05 to 5.10. Therefore, measuring the pH of treated samples after sonication is not a good mean

to compare the level of cell walls damage of treated samples at different levels of sonication power and time.

3.3.2. Surface area and porous structure (characteristic) analysis

The determination of surface area and porous structure of samples was not successful in preliminary tests. The values for correlation coefficient and surface area were lower than expected. The problems were associated with either very low surface area of the sample or insufficient degassing. Since the sample was a biomass, the maximum degassing temperature used was 70°C to avoid pore collapse during the degassing process. Samples were fully degassed by decreasing the vacuum set point to 5 µm Hg, increasing the evacuation time to 120 min, using heater tape and increasing the degassing time. In the main experiments, the correlation coefficient had a value of 1.000 or at least 4 9s (0.9999) for all samples. By using a filler rod and increasing the amount of sample used for gas adsorption, a greater volume of nitrogen uptake was obtained.

Pore size and porosity are usually cited in terms of micropore (<20 Å), mesopore (20-500 Å) and macropore (>500 Å). The N_2 gas adsorption method revealed the presence of mesopores (pore width of 27.34- 503.96 Å) and macropores (pore width of 544.17-1366.77 Å) but not micropores (volume for pores<27.34 Å: 0.00000 cm^3/g) for untreated DDG. Since DDG has been subject to fermentation and enzymatic reaction, this could be speculated that during DDG production, microporosity severely decreased and finally became negligible causing an increase in the meso- and macroporosity. Studying the cumulative pore volume (cm^3/g) of untreated DDG for pore width between 27.34-1366.77 Å revealed that cell wall pores of untreated DDG was mainly composed of 2.45% of macropores and 97.55% of mesopores. The surface area and total pore volume for untreated DDG were 13.905 m^2/g and 0.012 cm^3/g respectively. The pore size distribution of untreated DDG is shown in Figure 3.3. The incremental pore volume shows the pore volume associated with a specific pore width per gram of sample.

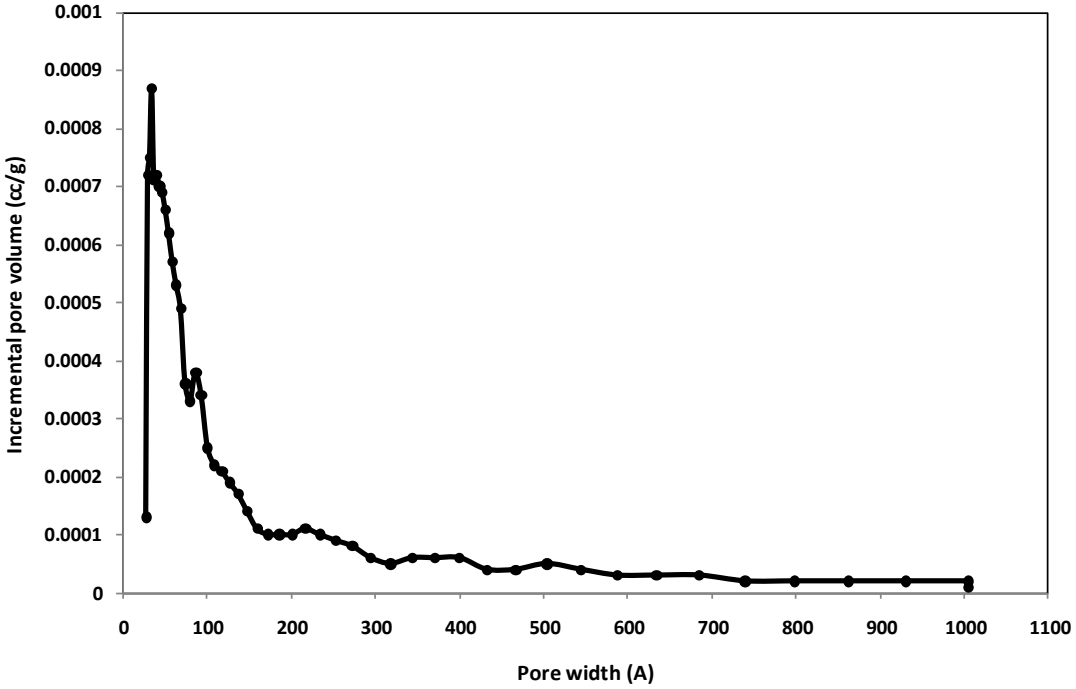

Figure 3.3. Pore size distribution for untreated DDG (measured using DFT)

It was observed that ultrasound pretreatment increased BET surface area and pore volume of sample (Table 3.2 and 3.4). As seen in Table 3.2, the BET surface area increased with sonication time and power. Interestingly the obtained BET surface areas at low powers (e.g. 20%) and long sonication times (e.g. 20 min.) were similar to those of high powers (e.g. 100%) and short sonication times (e.g. 60 sec.). In addition, consumed energy by the ultrasound processor was less at high powers and short sonication times (e.g. 100% at 30 sec.) compared to that of low powers and long sonication times (e.g. 20% at 20 min.) (Table 3.3). As a result, using higher sonication power at shorter sonication time would be more efficient in terms of resultant BET surface area as well as energy consumption.

As shown in Table 3.4, the effect of ultrasound on total pore volume of sample was not obvious at short sonication times. However it became more noticeable at longer sonication times (e.g. 20 min.). The total pore volume of the sample was increased by increasing the sonication power at 20 minutes sonication time.

Table 3.2. BET surface area (m^2/g) of the treated samples at different sonication times and powers.

Power	Duration			
	30 sec.	60 sec.	5 min.	20 min.
20%	14.604 ±0.7	16.828±0.8	16.171±0.8	18.402±0.9
50%	17.445±0.8	19.359±1	17.135±0.8	23.630±1
80%	15.571±0.8	17.051±0.8	18.305±0.9	28.537±1
100%	18.847±0.9	18.366±0.9	22.248±1	31.800±1

Table 3.3. Energy (kJ) consumption of the treated samples at different sonication times and powers.

Power	Duration			
	30 sec.	60 sec.	5 min.	20 min.
20%	0.780	1.560	7.500	30.000
50%	1.170	2.310	11.100	43.200
80%	2.070	4.140	19.500	76.800
100%	2.730	5.400	25.500	102.000

Table 3.4. Total pore volume (cm^3/g) of the treated samples at different sonication times and powers.

Power	Duration			
	30 sec.	60 sec.	5 min.	20 min.
20%	0.013± 0.00065	0.015±0.00075	0.014±0.0007	0.015±0.00075
50%	0.015±0.00075	0.016±0.0008	0.015±0.00075	0.019±0.00095
80%	0.013±0.00065	0.014±0.0007	0.015±0.00075	0.023±0.00115
100%	0.016±0.0008	0.015±0.00075	0.018±0.0009	0.026±0.0013

The nitrogen absorption method has been applied successfully in the past (Azargohar, 2009) for measuring porosity at micropore and mesopore levels using the same porosity analyzer apparatus (ASAP 2020). Both HK and DFT methods showed no micropores in the samples as the volume of micro pore (pore width<20 Å) was 0.00000 cm^3/g for all treated samples. By applying DFT method to N_2 adsorption data, porosity distributions with pore widths in the range of 20 to 500 Å (mesopores) and 500 to 1400 Å (macropores) were detected.

As an example, porosity distribution for a sample treated at 80% of total power for 20 minutes is shown in Table 3.5. From Table 3.5 it can be perceived that no pore was detected with a width smaller than 27 Å and detection of cell wall pores starts from a pore width of 27.34 Å. Various pore sizes in the range of mesopores (27.34-503.96 Å) and a number of macropores were detected. In the macropore class, the incremental volume decreased to zero and the cumulative volume became constant as the pore width was increased to 1475.96 Å. No larger pore width was detected in the macropore class. The maximum porosity detected in the macropore class was 1475.96 Å for samples treated at 100% and 80% sonication power for 20 min, and in other samples, including untreated samples, the maximum detected pore width was 1366.77 Å. Figure 3.4 shows a comparison between the pore size distribution of untreated and treated samples at 80% power and 20 minutes sonication time. It was observed that the pore size distribution in both samples was more predominant in the range of mesoporosity compared to macroporosity. In the treated sample, as the size of the measured pore width increased from 27.34 to 34.31 Å, the incremental pore volume rose sharply from 0.00004 to 0.0017 cm^3/g, which was the maximum measured pore volume. However, in untreated DDG when the pore width increased from 27.34 to 34.31 Å, the incremental pore volume sharply rose from 0.00013 to 0.00087 cm^3/g and reached the maximum value. This sharp peak in the pore volume was followed by a sudden decrease to less than 0.0002 cm^3/g, from which it decreased to zero. This shows that the pores in the cell walls of untreated and treated samples were mainly in the mesopore class and were distributed over a narrow range of pore width size. The mechanical effect of ultrasound on the sample mainly appears as a greater volume of pores in the range of mesopore size. In addition, detected macropores only form a limited fraction of measured pore volume in the sample.

Table 3.5. Porosity distribution for a sample treated at 80% of total power for 20 minutes (measured by DFT method).

Pore Width (Å)	Cumulative Volume (cm^3/g)	Incremental Volume (cm^3/g)	Pore Width (Å)	Cumulative Volume (cm^3/g)	Incremental Volume (cm^3/g)
21.62	0	0			
23.41	0	0			
25.2	0	0	185.86	0.0213	0.00021
27.34	0.00004	0.00004	200.69	0.0215	0.00019
29.49	0.0013	0.00127	216.6	0.02167	0.00017
31.81	0.00294	0.00164	233.93	0.02183	0.00016
34.31	0.00465	0.0017	252.52	0.02197	0.00014
36.99	0.00594	0.00129	272.71	0.02209	0.00012
40.03	0.00745	0.00152	294.51	0.02217	0.00008
43.25	0.00878	0.00132	317.92	0.02225	0.00009
46.64	0.01019	0.00141	343.3	0.02236	0.0001
50.4	0.01141	0.00122	370.64	0.02245	0.00009
54.33	0.01263	0.00122	400.31	0.02252	0.00008
58.8	0.01369	0.00106	432.3	0.02257	0.00005
63.44	0.01473	0.00103	466.79	0.02263	0.00005
68.45	0.01562	0.0009	503.96	0.02269	0.00006
73.99	0.01631	0.00069	544.17	0.02275	0.00006
79.88	0.01695	0.00063	587.6	0.02279	0.00004
86.32	0.01769	0.00074	634.42	0.02284	0.00005
93.11	0.01832	0.00064	684.99	0.02289	0.00005
100.61	0.01881	0.00048	739.68	0.02293	0.00004
108.66	0.01924	0.00044	798.65	0.02297	0.00004
117.23	0.01964	0.0004	862.45	0.02302	0.00005
126.53	0.01999	0.00035	931.26	0.02307	0.00005
136.71	0.0203	0.0003	1005.6	0.0231	0.00003
147.61	0.02059	0.00029	1085.66	0.02313	0.00003
159.41	0.02085	0.00027	1172.33	0.02317	0.00004
172.1	0.02109	0.00024	1265.8	0.0232	0.00003
			1366.77	0.02322	0.00002
			1475.96	0.02322	0

The results show zero volume of macropores in the samples for pore widths above 1475.96 Å (Table 3.5). This can be due to two possible reasons. Firstly, there were no pores with width larger than 1475.96 Å in the samples, and consequently the distribution of pore width is limited to a maximum of 1475.96 Å. The other reason might be the possible inability of the nitrogen gas adsorption method to detect larger pore sizes. This could be investigated by testing other porosimetry methods for macropores such as mercury porosimetry or micro computer tomography (µCT). However, the µCT scanning machine that was available in this study had limited spatial resolution and did not allow detection of pore size at levels less than 3.5 µm. It

was tested for one sample (results are not shown here). Therefore, detection of macropores with pore sizes of 500 Å and above (below 3.5 µm) was not possible via µCT scanning.

The mercury porosimetry method is not suitable for fragile compressible materials (Hoa and Hutmacher, 2006) such as plant samples. Chesson et al. (1997) examined the mercury method for studying the surface area and pore size distribution of wheat straw, whole wheat grain and grain fractions. They suggested that closed pores were distorted and some destruction of the wall did occur by the high pressure involved in the mercury method and a more realistic assessment was given by gas adsorption method (Chesson et. al., 1997). Therefore, considering the limitations associated with other methods, studying macroporosity by applying the DFT method to N_2 adsorption data seems to be the most reliable and available method and studying the porosity of larger pore size was not possible in our study.

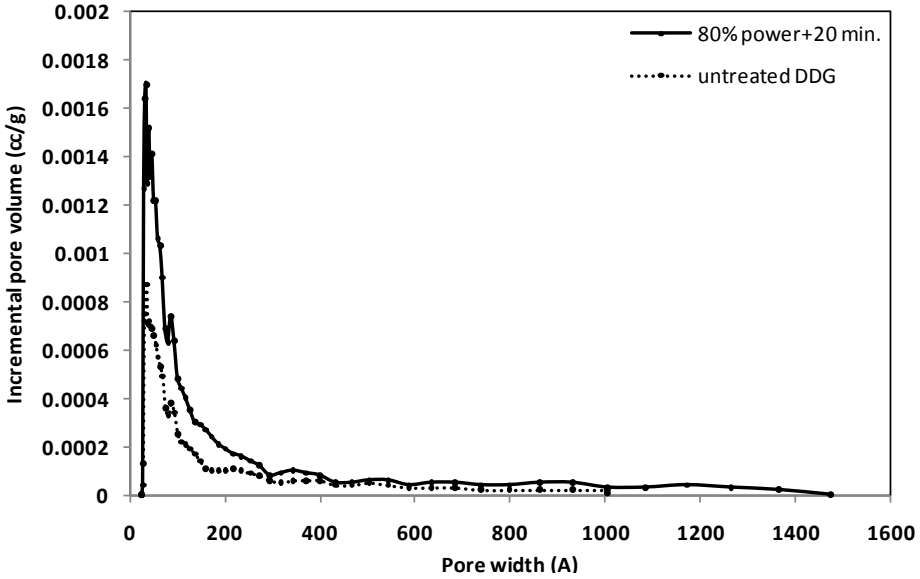

Figure 3.4. Pore size distribution of untreated DDG and the DDG sample treated at 80 % and 20 minutes sonication power and time respectively (measured by DFT).

3.3.3. Effect of ultrasound power and time

Figure 3.5 compares pore size distributions among samples treated at four different sonication powers and the same sonication times of 30 sec. (5a), 60 sec. (5b), 5 min. (5c) and 20 min. (5d). Since the accumulation of measured data was in the mesopore class, especially in the range of 20-200 Å, for a better observation of sonication power effects, results were presented in the zoomed pore width series of a typical 300- Å window of incremental pore volume.

The results showed incremental pore volume growth due to increasing ultrasound sonication power (shifting up of the pore distribution graphs by sonication power). This shows the positive effect of sonication power on cell wall damage. However, this effect was observed to be different for the four tested sonication periods (Fig. 3.5 and 3.6). The increase of incremental pore volume was more noticeable and distinguishable for samples treated for 20 minutes. This observation is interestingly indicating the importance of sonication time in cell wall damage. Although sonication power was observed to enhance cell damage (higher pore volume), it is the longer sonication period that allows higher powers to efficiently improve the treatment (greater cell wall damage). For example, as shown in Figure 3.6b, c, and d, a long sonication time (20 min.) led to a significant increase in incremental pore volume. Ultrasound treatment was strongly influenced by the power of sonication, mainly at long sonication times.

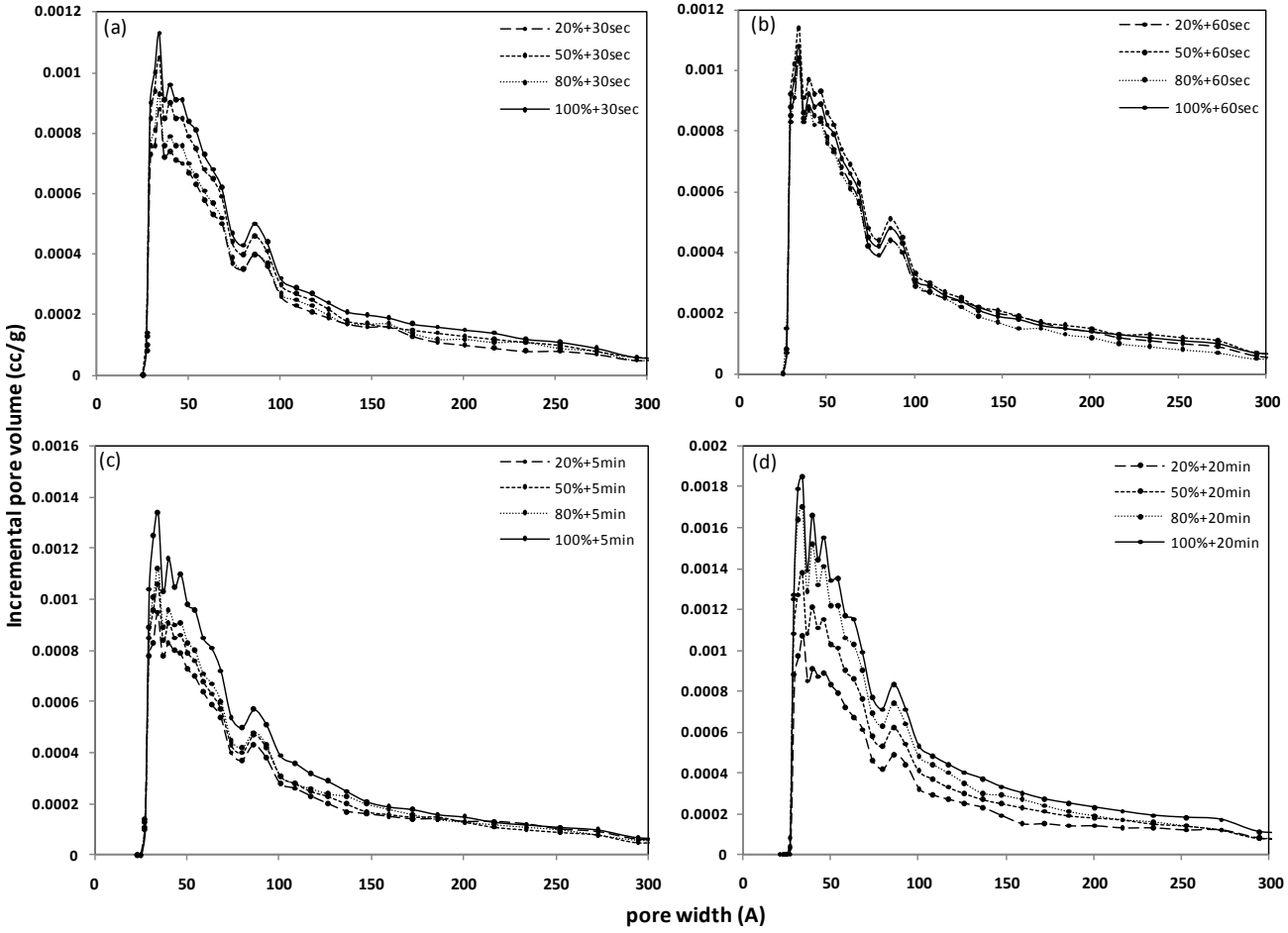

Figure 3.5. Pore size distribution of samples treated at four different sonication powers and the same sonication time of 30 sec. (5a), 60 sec. (5b), 5 min. (5c), and 20 min. (5d) for a typical pore width-window of 300 Å (measured by DFT).

Interestingly, all samples treated with different sonication powers showed similar pore size distribution patterns (Fig. 3.5). The pore size distribution patterns were similar to what was discussed earlier for the treated sample at 80% amplitude and 20 min. (see section 3.2). The cell wall pores produced by ultrasound in all tested conditions were in a specific range of pore size and the effect of sonication time and power was mainly on the quantity (volume) of pores.

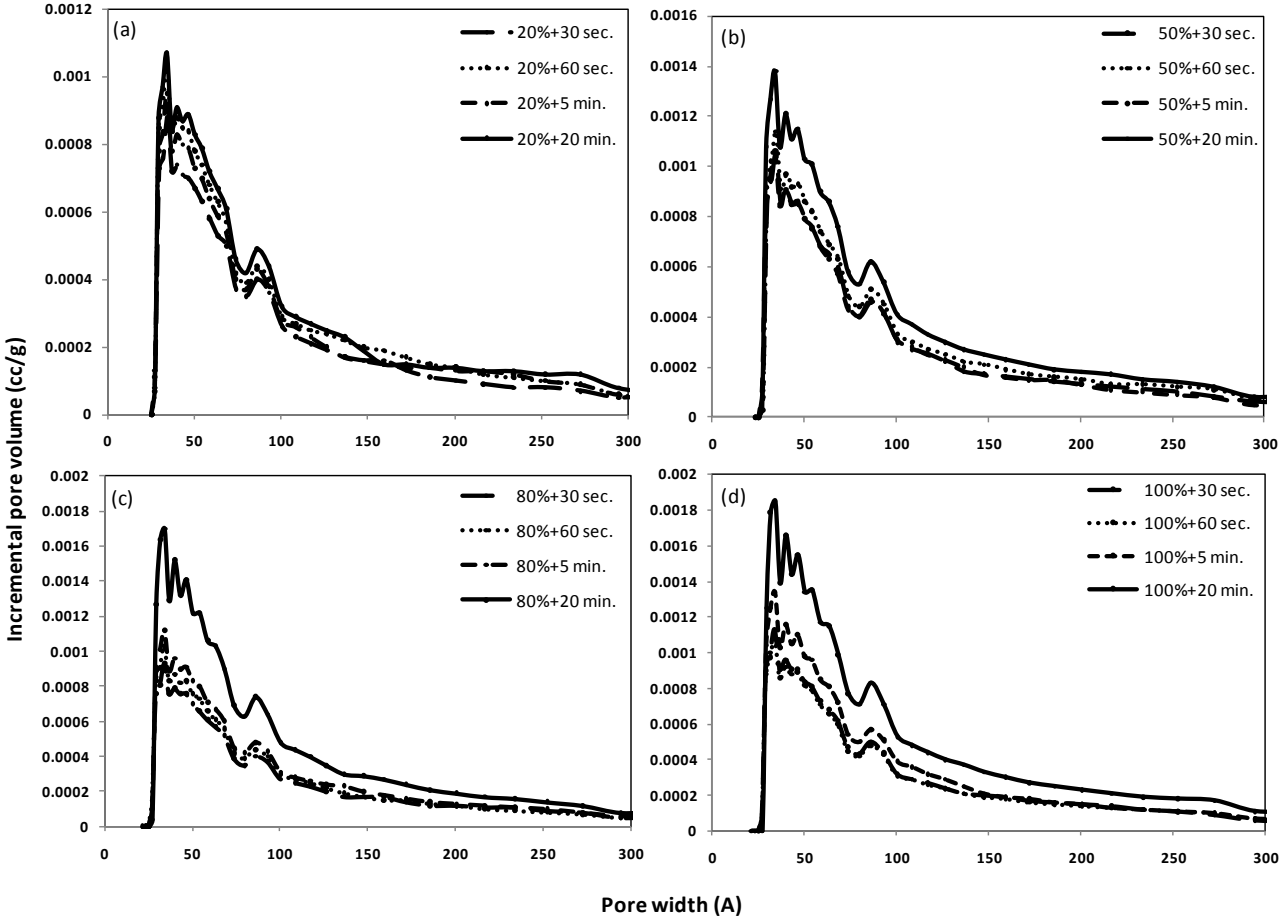

Figure 3.6. Pore size distribution of samples treated at four different sonication times and the same sonication power of 20% (5a), 50% (5b), 80% (5c), and 100% (5d) for a typical pore width-window of 300 Å (measured by DFT).

3.3.4. Effect of ultrasound on extraction yield and rate

The presence of more available surface area and pore volume should accelerate the release of phenolic compounds contained within the plant body due to cell wall disruption and easier access of the solvent to the cell contents. This hypothesis was investigated by performing a

series of extraction experiments for a wide range of different BET surface areas of treated samples. The effect of surface area on extraction rate and yield was investigated and subsequently the most efficient ultrasound condition for extraction of phenolic compounds was evaluated based on the extraction results.

Therefore, selective ultrasound conditions (sonication time and power) were chosen based on measured BET surface areas (Table 3.2) and consumed ultrasound energy (Table 3.3). A range of BET surface areas with good diversity (14.6, 17.05, 18.85, 22.25, 31.8 m^2/g) and efficiency of the treatment condition was also considered for this selection. A ultrasound treatment conditions that produced similar BET surface areas, the one with lower energy consumption was selected.

Fig. 3.7 illustrates the extraction of phenolic compounds from the untreated DDG and ultrasound pretreated DDG at five different conditions of ultrasound pretreatment (five different BET surface areas) at a particle moisture content of 1.02 % dry basis and an ethanol volumetric concentration of 30% at 30°C. This experimental condition in which the extraction yield of phenolic compounds from untreated DDG was minimum was chosen based on our previous study. At this extraction condition, the contribution of temperature, ethanol fraction of solvent and particle moisture content (extraction condition) to the extraction yield is minimized and consequently enables better investigation of the role (contribution) of BET surface area in extraction yield As presented in Fig. 3.7, the extraction rates and yields for all the tested levels of ultrasound (all the tested BET surface areas) were higher than those of the untreated sample. Among the tested BET surface areas, 18.85 and 22.25 m^2/g surface areas (100% + 30 sec. and 100% + 5 min. as ultrasound operating conditions) showed the highest extraction yields. At the early stages of extraction, the extraction rate associated with a surface area of 22.25 m^2/g was higher than that of 18.85 m^2/g: however, no difference was observed in the later stages of extraction. Fig. 3.8 shows the variations of yield versus surface area for six selective extraction times three initial stages (Fig. 3.8a, b, c) and three later stages of extraction (Fig. 3.8d, e, f). Extraction yield dropped when surface area increased to 31.80 m^2/g (associated with sonication condition of 100% + 20 min.). Acoustic cavitation provides interaction of energy and matter during sonication (Suslik, 1998). At 100% sonication power and 20 minutes sonication time, an irreversible damage of the phenolic compounds could be produced as a consequence of both the heat generated during the sonication process and the high ultrasound energy supplied to the

sample. This is in agreement with the study conducted by Roman et al. (2009) on the extraction of β-glucan from ultrasound pretreated barley. Therefore, 87 W ultrasound power (100% of the total power output) for sonication times of 30 sec. and 5 min. were seen to be suitable for the extraction. However, considering energy consumption (Table 3.6), a sonication time of 30 sec. seems to be more efficient. Disintegration of particles was observed at the sonication powers of 80% and 100%. The disintegrated particles were not too fine to cause any filtration problems. The extraction yield increased with a reduction of particle size because total surface area increases when the particle size decreases. Therefore, in addition to the mechanical effect of ultrasound on cell wall disruption, the positive effect of ultrasound pretreatment in reduction of particle size is speculated to shorten the extraction time and enhance the overall extraction yield.

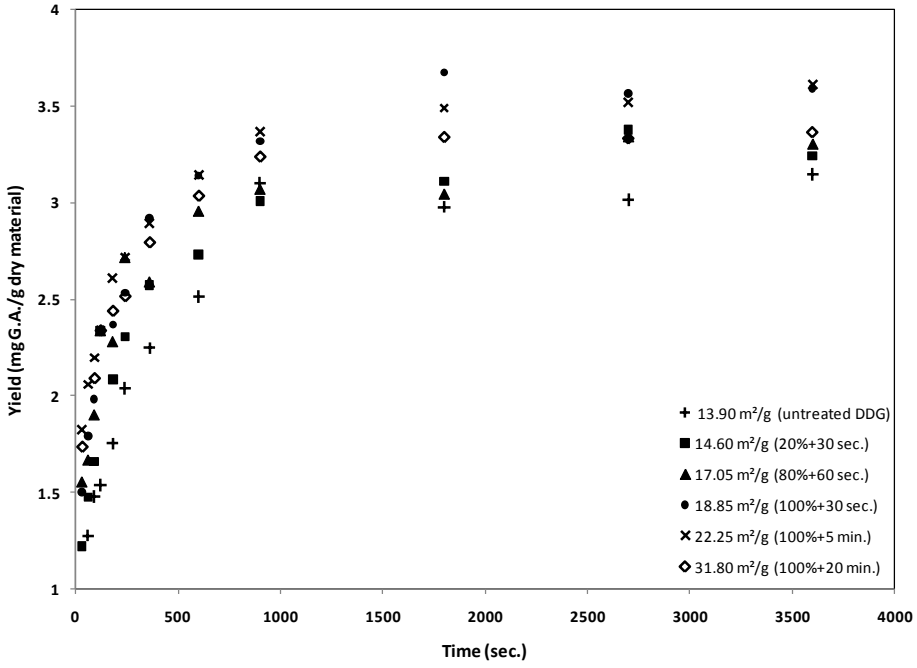

Figure 3.7. The effect of surface area of sample on the extraction of phenolic compounds at ethanol volumetric fraction of 30%, particle moisture content of 1.02% dry basis and 30°C.

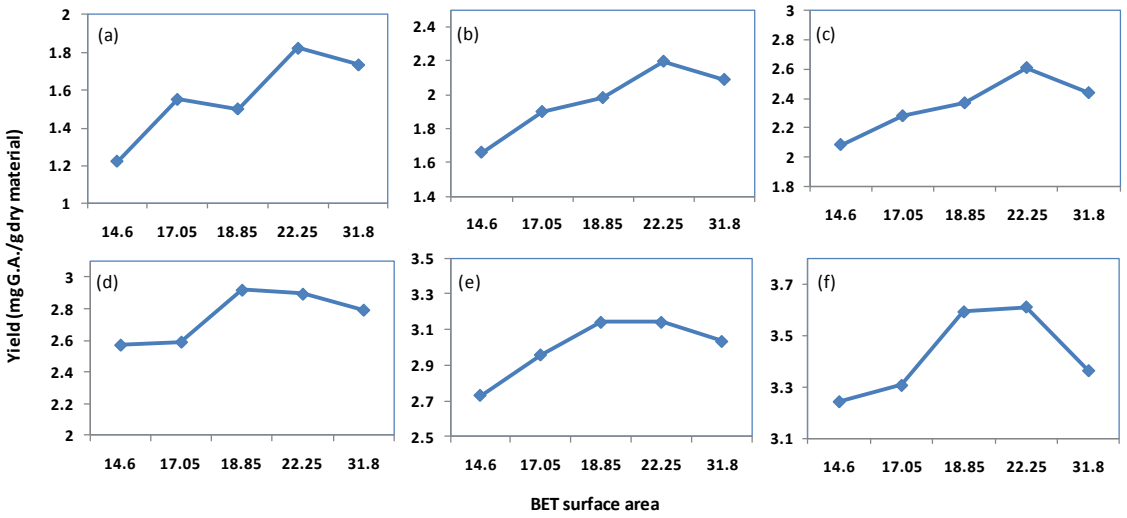

Figure 3.8. Variations of the yield with respect to BET surface area after (a) 30 sec. (b) 1 min 30 sec (c) 3 min. (d) 6 min. (e) 10 min. (f) 1 hour of extraction.

3.3.5. Effect of ultrasound on extraction rate constant

Using the second-order kinetics model, the extraction rate constant, k, was determined at a ethanol concentration of 30%, particle moisture content of 1.02% (dry basis) and 30°C. The data are shown in Table 3.6.

Table 3.6. Extraction rate constant and saturated concentration of phenolic compounds at ethanol volumetric fraction of 30%, particle moisture content of 1.02% dry basis and 30°C for different BET surface areas and associated energy consumption and treatment condition.

Treatment condition Sonication power%, sonication time	Consumed energy (J)	BET surface are (m^2/g)	K (L g^{-1} min^{-1})	Cs* (g L^{-1})
Untreated	0	13.90	0.057	0.151
20%, 30 sec.	750	14.60	3.622	0.160
80%, 60 sec.	3960	17.05	4.463	0.164
100%, 30 sec.	2610	18.85	3.933	0.178
100%, 5 min.	26100	22.25	4.530	0.179
100%, 20 min.	104400	31.80	7.156	0.166

* Saturated concentration of phenolic compounds.

As shown in Table 3.6, upon applying ultrasound, the second order extraction rate constant, *k*, rose from 0.057 to 7.156 which shows the positive effect of ultrasound pretreatment on extraction rate. Ultrasound pretreatment also increased the associated energy consumption, BET surface area and saturated extraction capacity.

3.4. Conclusion

Ultrasound pretreatment was found to be an effective operation for improving the extraction of phenolic compounds from DDG. Among the tested ultrasound conditions, 100% ultrasound power for 30 seconds was the best pretreatment condition. At this condition, a 14.29% increase in extraction yield was observed compared to the control. Our approach in characterizing the cell wall properties of samples by the gas adsorption method successfully allowed a mechanistic understanding of the mechanical effects of ultrasound on the cell wall structure at different levels of sonication time and power. Application of ultrasound increased the specific surface area and pore volume of samples, which showed the positive effect of ultrasound pretreatment on pore development and damaging cell walls. On the top of the increased pore volume, surface area and consequent enhancement of extraction yield and rate after the ultrasonic treatment confirmed the positive attributes of ultrasound pretreatment on the extraction of phenolic compounds from DDG.

References

Adamou Harouna-Oumarou H., Extraction solide-liquide aqueuse de l'aubier de tilleul en r´egimes discontinu et continu: caract´erisation, cin´etique, mod´elisation, d´eveloppement pilote, PhD thesis, Universit´e Pierre et Marie Curie, Paris, 31st Jan 2006.

ASABE standards 2009, ASAE S352.2; Moisture Measurement-Unground Grain and Seeds, St. Joseph, MI, USA, APR1988 (R2008).

Association of official Agricultural Chemists (AOAC), AOAC 930.15 Loss on Drying (Moisture) for Feeds. Official Methods of Analysis of AOAC International 17th edition. Washington, D.C: AOAC (2000a).

Azargohar R., 2009. Production Of Activated Carbon And Its Catalytic Application For Oxidation Of Hydrogen Sulphide. PhD Thesis, University of Saskatchewan, Saskatoon, SK, Canada.

Brunauer, S., P. H. Emmett, E. Teller, Adsorption of gases in multimolecular layers, Journal of the American Chemical Society, 60 (1938) 309-319.

BBOP (Barley bioproducts opportunities project), http://www.wbga.org/BBOP-April-08.pdf (2008) 1-12, accessed on January 2011.

Carpita N.; D. Sabularse; D. Montezinos; D. Delmer, Determination of the pore size of cell walls of living plant cells. Science, 225 (1979) 1144–1147.

Chemat S., A. Lagha, H. AitAmar, P.V. Bartels, F. Chemat, Comparison of conventional and ultrasound-assisted extraction of carvone and limonen from caraway seeds, J. flavour and fragrance, 19 (2004) 188-195.

Chesson A., P.T. Gardner, T.J. Wood, Cell wall porosity and available surface area of wheat straw and wheat grain fractions, J. Sci. Food Agric 75 (1997) 289-295.

Goto M., J.M. Smith, B.J. McCoy, Kinetics and mass transfer for supercritical fluid extraction of wood, Ind. Eng. Chem. Res. 29 (1990) 282.

Ho S. T., D. W. Hutmacher, A comparison of micro CT with other techniques used in the characterization of scaffolds, J. Biomaterials 27 (2006) 1362–1376.

Ho Y.-S., H. Adamou Harouna-Oumarou, H. Fauduet, C. Porte, Kinetics and model building of leaching of water-soluble compounds of Tilia sapwood, Sep. Purif. Technol. 45 (2005) 169.

Horvath, G., K. Kawazoe, Method for calculation of effective pore size distribution in molecularsieve carbon Y or. Chem. Eng. Japan, 16 (1983) 470.

Hoa S.T., D.W. Hutmacher, A comparison of micro CT with other techniques used in the characterization of scaffolds, Biomaterials 27 (2006) 1362–1376

Kojiro K.; T. Miki; H. Sugimoto; M. Nakajima; K. Kanayama, Micropores and esopores in the cell wall of dry wood. J. Wood Sci., 56 (2010) 107–111.

Lastoskie, C.; K. E. Gubbins; N.Quirke, Pore size distribution analysis of microporous carbons: a density functional theory approach, J. Phys. Chem. 97 (1993) 4786-4796.

Luque-Garcia J.L., M.D. Luque de Castro, Ultrasound: a powerful tool for leaching, Trends in Analytical Chemistry 22 (2003) 41-47.

McCann M.C.; B. Wells; K. Roberts, Direct visualization of cross-links in the primary plant cell wall, J. Cell Sci. 96 (1990) 323–334.

Meziane, S., H. Kadi and O. Lamrous, Kinetic study of oil extraction from olive foot cake. Grasasy Aceites, 57 (2006) 175-179. http://cat.inist.fr/?aModele=afficheN&cpsidt=18216571

Meziane, S. and H. Kadi, Kinetics and thermodynamics of oil extraction from olive cake. Am. Oil Chem. Soc., 85 (2008) 391-396. http://www.highbeam.com/doc/1P3-1461016971.html

Papadopoulos A. N.; C. A. S. Hill; A. Gkaraveli, Determination of surface area and pore volume of holocellulose and chemically modified wood flour using the nitrogen adsorption technique. Eur. J. Wood Wood Products 61 (2004) 453–456.

Roman O.B., S.L. Yague, E.A. Sanchez, Study of the effect of different pretreatments on the performance of the extraction of β-glucan from barley, Chemical Engineering Transactions 17 (2009) 927-932.

Rondeau-Mouro C.; D. Defer; E. Leboeuf; M. Lahaye, Assessment of cell wall porosity in Arabidopsis thaliana by NMR spectroscopy. Int. J. Biol. Macromol. 42 (2008) 83–92.

Singleton V.L., J.A. Rossi, Colorimetry of total phenolics with phosphomolibdic-phosphotungstic acid reagents, Am. J. Enology and Viticulture 16 (1965) 144-158.

So, G.C. and D.G. Macdonald, Kinetics of oil extraction from Canola (rapeseed). Can. J. Chem. Engin, 64 (1986) 80-86. http://72.14.235.132/search?q=cache:3AE7xdKJmdUJ:grasasyaceites.revistas.csic.es/index.php/grasasyaceites/article/download/34/33+Kinetics+of+oil+ extraction+from+Canola+(rapeseed&cd=1&hl=en &ct=clnk&gl=pkStone J.E.; M.A. Scallan, A structural model for the cell wall of water swollen wood pulps fibers on their accessibility to macromolecules, Cell. Chem. Technol. 2 (1968) 343–358.

Suslick, K. S., Sonochemistry, in Kirk-Othmer Encyclopedia of Chemical Technology, 4th Ed. J.Wiley & Sons, New York, vol. 26 (1998) 517-541.

Tarazona P., Free-energy density functional for hard spheres, Phys. Rev. A 31 (1985) 2672-2679.

Wang J., B. Sun, Y. Cao, Y. Tian, X. Li, Optimisation of ultrasound-assisted extraction of phenolic compounds from wheat bran, Food Chemistry, 106 (2008), 804-810

Wiese, K.L. and H.E. Snyder, Analysis of the oil extraction process in soybeans: A new continuous procedure. Am. Oil Chem. Soc., 64 (1987) 402-406. DOI: 10.1007/BF02549304 Wongkittipong R., L. Prat, S. Damronglerd, C. Gourdon, Solid–liquid extraction of andrographolide from plants—experimental study, kinetic reaction and model, Sep. Purif. Technol. 40 (2004) 147.

CHAPTER 4
Dielectric properties of a packed bed of wheat dried distillers grain (DDG) and ethanol/water for RF assisted extraction of phenolic compounds

Synopsis

To apply, design, simulate and optimize radio frequency assisted extraction of phenolic compounds from DDG, sufficient information about dielectric properties (dielectric constant and loss factor) of DDG particles is required for various conditions. In this chapter, the dielectric properties of DDG particles at different levels of temperature, frequency, particle moisture content and ethanol volumetric fraction of solvent are determined.

Abstract

The dielectric constant and dielectric loss factor of a packed bed of wheat DDG with ethanol/water solution were measured with three levels of initial moisture content of DDG particles (0.0373, 1.58 and 3.975 dry basis), four levels of temperature (25, 40, 55 and 70°C), and four levels of ethanol fraction of solvent (0%, 40%, 70% and 100%) over eight different frequencies (from 10 to 30 MHZ) in duplicate using a precision LCR (inductance, capacitance and resistance) meter and a liquid test fixture. The power penetration depth of the packed bed was measured for all applied experimental conditions at 13.56 and 27.12 MHz. The effect of temperature, ethanol volumetric fraction of solvent and particle moisture content on the dielectric constant, loss factor and power penetration depth were investigated. Both dielectric constant and loss factor of the packed bed decreased with frequency for all levels of ethanol fractions and temperatures. The dielectric constant and loss factor of the bed increased with temperature for all levels of particle moisture content and ethanol fraction; however, for the particle moisture content of 0.0373 d.b. with 100% and 70% ethanol, and also for the particle moisture content of 1.58 d.b. with 100% ethanol, the effect of temperature on dielectric constant was insignificant. The dielectric constant and loss factor of the packed bed were significantly decreased with ethanol volumetric fraction of solvent for all levels of temperature and particle moisture content. The dielectric constant and loss factor increased with moisture content for 40%, 70% and 100% ethanol; however, for 0% ethanol, the effect of moisture content was not significant. Power penetration depth decreased with temperature, and particle moisture content increased with ethanol fraction. Multiple regression equations for the dielectric constant and dielectric loss factor of the packed bed were developed at frequencies of 13.56 and 27.12 MHz.

Keywords: Dielectric properties; Dielectric constant; Dielectric loss factor; Radie frequency; Penetration depth; Dried distillers grain; Phenolic compounds;

Notation

A	surface area of each electrode, m^2
c	speed of light, m s^{-1}
E	volume fraction of ethanol in the solvent, m^3 [ethanol] m^{-3} [solvent]
C_p	capacitance, F
d_p	penetration depth, m
f	frequency, Hz
R_p	resistance, Ω
t	gap between the electrodes of the liquid test fixture, m
T	temperature, °C
M	particle moisture content, kg [H_2O] kg^{-1} [dry matter]
δ	loss angle
ε_0	permittivity of vacuum, F m^{-1}
ε_r	relative permittivity
ε_r'	dielectric constant
ε_r''	dielectric loss factor
τ	periodic time, s
$\omega_{\varepsilon_r'}$	uncertainty associated with dielectric constant
$\omega_{\varepsilon_r''}$	uncertainty associated with dielectric loss factor

4.1. Introduction

Natural pharmaceutical and nutraceutical products have been spotlighted by many researchers and related industries. Extraction from biological resources is economically more feasible compared to chemical synthesis of the products. Synthetic products might possess some side effects to human health. Phenolic compounds are among important bioactive compounds with interesting medicinal properties such as decreasing the risk of chronic diseases related to oxidative stress; oxidative stress based diseases such as: Parkinson diseases, multiple sclerosis, dementia, diabetes, several types of cancer, liver diseases, asthma, cystic fibroses, chronic obstructive pulmonary diseases (COPD), cardiovascular and digestive disease, kidney failure, and even common colds (BBOP, 2008). One of the biological resources which contain phenolic compounds is wheat dried distillers grain (DDG). DDG is a coproduct of bioethanol production process where ethanol is produced from wheat grains during a fermentation process. As DDG is easily available from ethanol production industries, it can be potentially considered as an alternative source of phenolic compounds. Considering continually growing demands for medicinal products like phenolic compounds, the development of more efficient extraction processes would be an urgent commercial demand. Currently solid-solvent extraction techniques (packed-bed solvent extraction) are commercially used for the extraction of medicinal natural products. For an efficient solid-solvent extraction, the solubility and effective diffusivity of target compound must be enhanced as they are the major parameters having strong effects on mass transfer rate. In the extraction, temperature is one of the important key factors affecting the solubility and effective diffusivity of extraction. To enhance the extraction process, the packed bed of DDG particles and solvent must be heated up uniformly to desired temperature and kept until the end of process. The process must avoid overheating the biological materials in the extraction unit due to degradation of bio-components. The use of microwave (MW) and radio frequency (RF) as fast and energy efficient heating sources can be considered for improving the extraction process. Without specific technical modifications, microwave is often unable to heat materials in a uniform manner, leaving overheated spots that may result in degradation of biological compounds and cold spots where the product is unheated (IMS, 2011). Another disadvantage of microwave heating method to deal with the small penetration depth of microwave for large scale applications (Kappe et al., 2009). Consequently, previous attempts to

use microwaves in commercial processes which require uniform heating have been unsuccessful and extremely costly (IMS, 2011). Compared with microwave (300 MHz-300 GHz), RF has lower frequency levels (3 KHz-300 MHz) which can provide a larger penetration depth and can make a uniform volumetric internal heat generation within a packed-bed solvent extraction unit of commercial size due to large penetration depth of RF. Studies have been conducted to employ RF heating in food processing, pasteurization, and sterilization (Moyer and Stotz, 1947; Kinn, 1947; Houben et al., 1991, 1990; Zhong et al., 2003), thawing frozen products (Jason and Sanders, 1962a, 1962b), post-back drying of cookies and snack foods (Anon, 1987, 1989), drying process (Mermelstein, 1997; Poulin et al., 1997; Balakrishran et al., 2004), thermal therapy (Maurizion et al., 2004) and RF-assisted extraction (Izadifar and Baik, 2008). However, use of RF heating in extraction is very recent trial and has not been fully investigated with further exploration. In RF heating the amount of heat generated inside the material depends on RF frequency, dielectric loss factor of the material (sample), and the strength of electric field. Dielectric properties including dielectric loss factor and dielectric constant play an important role in RF heating. Dielectric properties of the material and the solvent depend on frequency, moisture content and temperature.

4.1.1. Background of RF heating and dielectric properties

During RF heating, the product to be heated forms a "dielectric" between two metal capacitor plates. The RF generator makes an alternating electric field between two electrodes in the space that material or the packed- bed is placed. On one side, in the material polar molecules (i.e. H_2O) and ions (i.e. Na^+, Cl^-) try to be aligned with the polarity of the electric field and be displaced in the space, respectively. On the other side, polarity of the field alters million times per second (~27120000 cycles per second). So, flip-flop rotation of polar molecules and ion displacement induced inside the material. Dipole flip-flop rotation and the space charge displacement of ions cause friction which causes the material heat rapidly and uniformly throughout its mass (Kinn, 1947)

4.1.2. RF heating and background of dielectric properties

The dielectric properties are permeability, permittivity (capacitivity) and electrical conductivity of the heated material (Piyasena, 2003). Dielectric constant, dielectric loss factor and loss angle are determined by permittivity and all affect the RF heating. Permittivity is a

physical quantity which describes how an electric field affects, and is influenced by a dielectric medium and is measured by the ability of a material to polarize in response to the field which causes the reduction of the total electric field inside the material. So, permittivity relates to the ability of a material to transmit (or permit) an electric field. Dielectric properties significantly influence on penetration depth.

The real part of the complex permittivity, έ, is often named the dielectric constant or "capacitivity". The dielectric constant (έ) is the ability of the material to store electrical energy compared to the one in vacuum space. It is a constant for a material at a given frequency. The imaginary part of the complex permittivity is the dielectric loss factor (ε'') which means the ability of the material to dissipate the electrical energy and convert electrical energy into heat compare to the one in vacuum space. The material which has higher dielectric loss factor will absorb energy at a faster rate than a substance with the lower one. The loss tangent (tan δ) is an indicator of how well the material can be penetrated by an electrical field and how it dissipates electrical energy. The relationship between dielectric constant, dielectric loss factor and loss tangent is defined as:

$$\varepsilon'' = \acute{\varepsilon} \tan\delta \qquad (1)$$

The effect of permittivity on increase of temperature is defined as:

$$\Delta T = \frac{2\pi t f \varepsilon_0 \varepsilon_r' \tan\delta V^2}{C_p \rho} \qquad (2)$$

where ΔT represents the temperature increase (ºC); t is the time which temperature increase in that period (s); ε_o is the dielectric constant in vacuum space, 8.85419×10^{-12}F/m; f is frequency; ε_r' is relative dielectric constant or permittivity of the material; $\tan\delta$ is tangent of dielectric loss angle; V is electric field strength which is equal to voltage/distance between plates (V/cm); C_p is specific heat of the material which is heated (J/kgºC); and ρ is density of the material to be heated (kg/m^3) (Piyasena, 2003). So, dielectric heating rate increases with loss factor. Dielectric properties significantly influence on penetration depth.

Having an accurate knowledge of the dielectric properties of a packed bed of DDG particles filled with solvent at RF frequency is essential for optimization and design of the RF-assisted extraction process.

The objectives of the present study were (1) to measure the dielectric constant, dielectric loss factor and power penetration depth of a packed bed of DDG particles and solvent (water/ethanol) with various levels of temperature, particle moisture content, ethanol fraction of solvent, and frequency (2) to investigate the influences of temperature, particle moisture content, ethanol fraction of solvent, and frequency on dielectric properties and power penetration depth (3) to develop multiple regression models of dielectric constant and loss factor with temperature, particle moisture content, ethanol fraction of solvent, and frequency.

4.2. Materials and method

4.2.1. Sample preparation

The sample of wheat distillers grain that was collected for this study were originally wet, namely, wheat wet distillers grain (WDG) with the initial moisture content of 66.8% wet basis. It was supplied by Terra Grain Fuels, Inc., (Belle Plaine, SK, Canada) and was dried using an oven drying method in the lab to avoid industrial impurities that might be added to the sample during drying process in the industry. The WDG was put in an aluminum tray, placed in the oven, and dried at the temperature of 70°C for 1 day (24 hour). After drying the sample, dried distillers grain (DDG) was packaged and preserved in a cold room at 4°C until use. This prepared DDG was used throughout the experiments.

4.2.2. Particle size analysis

Based on the ASABE standard method, the particle size distribution of DDG particles was determined by sieving 500 g of DDG particles with a series of standard sieves with the standard sieve number of 6, 8, 12, 16, 20, 30, 40, 50, 60, 70, and 100 in duplicate (ASABE S352.2 APR1988, 2009).

4.2.3. Measurement of moisture content

The moisture content of the DDG particles was determined using the oven method (AOAC, 2000). Three aluminum dishes each dish containing 2 g of particles were covered and shake until

the contents were evenly distributed. Dishes were placed in an air oven as quickly as possible, covers removed and dried for 2 hours at 135°C. Particle moisture content was calculated on a dry basis and averaged for the triplicate measurements.

4.2.4. Measurement of porosity

The porosity of the base DDG sample (with particle moisture content of 3.73% dry basis) was calculated as follow:

$$Porosity = \left(1 - \frac{Bulk\ density}{Particle\ density}\right) \times 100\% \quad (3)$$

In this study, the particle density and bulk density of DDG particles were measured using a pycnometer, a large sample cell, and a single bulk weigh scale as shown in Fig. 4.1. DDG particles were loaded into the large sample cell up to about 2 cm below the holes of sample cell and then the loaded mass weighed. The volume of loaded mass into the cell was measured using a gas pycnometer. After conditioning and calibrating the pycnometer, the cell containing the particles was connected to the reference cell. The initial and final nitrogen gas pressure readings and the known reference and cell volumes were used to calculate the particles volume. The particle density was calculated as measured mass per unit particles volume.

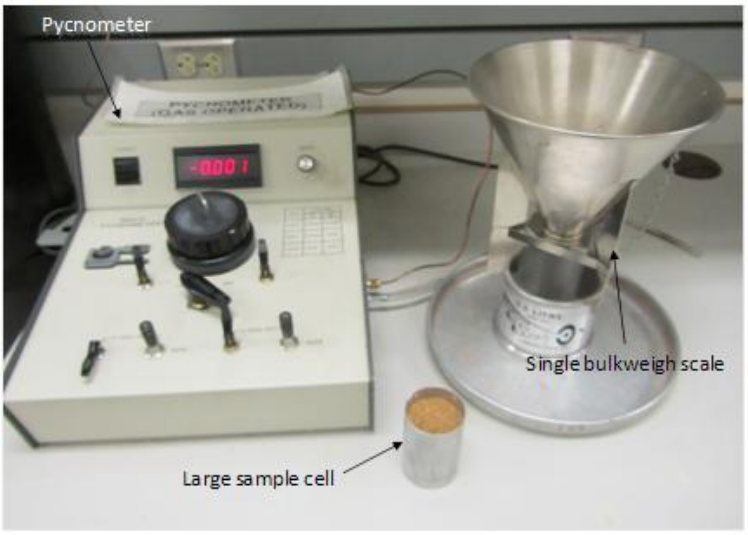

Figure 4.1. The porosity measurement system used in this study

To measure the bulk density, the volume of particles was obtained by pouring DDG particles into a 0.5 liter container using a Single bulkweigh scale (Fig. 4.2a), followed by rolling the top of container to fix the volume of particles at 0.5 liter (Fig. 4.2b and c). The particles inside the container were weighed and the bulk density was calculated. Triplicate measurements were averaged.

Figure 4.2. Procedure of measuring volume of particles in bulk density measurement

4.2.5. Preparation of different level of moisture content

Different levels of particle moisture content were prepared by spraying pre-determined amount of distilled water on the DDG particles, followed by periodic tumbling of the samples in sealed containers. Then the samples were kept for 4-5 days at room temperature to equilibrate and then stored at 4°C in a cold room before tests.

4.2.6. Experimental design

The influence of particle moisture content and ethanol concentration on dielectric properties of the bed was investigated for three levels of particle moisture content (3.73%, 158.0%, and 397.51% dry basis) and four levels of ethanol concentration (0%, 40%, 70%, and 100%). Ethanol fraction of solvent and moisture content were varied one at a time to investigate the interaction between particle moisture content and ethanol concentration. Different levels of ethanol fraction of solvent were prepared by using tap water and pure ethanol. The tap water with an electrical conductivity of 430 μSm^{-1} was used for the experiments. The minerals and ions typically found in tap water including sodium, potassium, calcium, and magnesium, can be effective to increase dielectric loss factor and consequently RF heating of a packed bed reactor of DDG particles. The capacitance and resistance were recorded over eight frequencies from 10 to 30 MHz (10, 13.5, 16, 18, 22, 25, 27.12, and 30) at four bed temperatures (25°C, 40°C, 55°C and 70°C). The

maximum temperature was chosen below the ethanol boiling point. All measurements were performed in duplicate.

4.2.7. Measurement of dielectric properties

- ***Dielectric property measurement equipments***

Measurement of capacitance (C_p) and resistance (R_p) of the bed in various experimental conditions was performed using a precision LCR meter (4285, Agilent Technologies, Palo Alto, CA) and a liquid test fixture (16452A, Agilent Technologies, Palo Alto, CA). The 16452A liquid test fixture employs the parallel plate method, in which the material under test is sandwiched between two electrodes and forms a capacitor. A 2mm spacer was used to provide the desired gap between electrodes. The LCR meter then measures the capacitance created from the fixture. The working frequency of liquid test fixture is in range of 20 Hz to 30 MHz. The values of capacitance (C_p) and resistance (R_p) were used to determine the dielectric constant and dielectric loss factor of a packed bed of the DDG particles with an ethanol/water solution. To provide the desired temperature for the materials in the liquid test fixture and keep the fixture and the packed bed temperature constant during measurement, a heating chamber (SH-641, ESPEC Corp., Japan) with an accuracy of ±0.1°C was used.

- ***Experimental description***

To begin with, the precision LCR meter was calibrated and set for eight working frequencies (10, 13.56, 16, 18, 22, 25, 27.12, and 30 MHz). Two frequencies of 13.56 and 27.12 MHz are attributed to industrial, scientific and medical applications by the European Radio Communications Committee and the US Federal Communication Commission (Izadifar and Baik, 2008). Before each test, the liquid test fixture was opened into two halves, washed all of its parts including two O-ring washers with distilled water and dried completely using pressurized air. The two O-ring washers were replaced and the liquid inlet and air outlet were plugged using two stoppers to avoid loss of the material from the fixture during the experiment (Fig. 4.3a). The liquid test fixture was placed horizontally on the bench, and DDG particles were loaded into the fixture up to just below the inlet/outlet holes, followed by a couple of gentle shakes of the fixture

to settle the particles uniformly in the fixture (Fig. 4.3b). Then, using a 1mL syringe, ethanol/water solution was gradually added to the bed from one side to the other side of the fixture (row by row) in order to direct air bubbles out of the particles (Fig. 4.3c). The solution was added to the bed until the packed bed of particles saturated by the solution and a thin layer of solution was on the particles. Next, the 2mm spacer was placed on the filled half fixture followed by fixing the second electrode on the top of the fixture (Fig. 4.3d). Then, the two stoppers were checked for any leaking of solution. If there was any leaking, the amount of sample or solution was changed. On one hand, since particles are swollen, the volume of solvent filling voids of the bed changes for particles with different moisture content. On the other hand, at high temperatures, thermal volume expansion of the sample results in leaking at the stoppers. The best ratio of particles and solution for each particle moisture content was obtained by trial and error. Afterwards, the fixture was transferred to the heating chamber without disturbing its horizontal posture and horizontally placed in the heating chamber to avoid phase separation. Then, the fixture in the heating chamber was connected to the LCR meter via the 1m test leads (16452-61601, Agilent Technologies, Palo Alto, CA) through a hole on the chamber wall. The hole was kept closed during experiment using a foam stopper. In preliminary experiments, the equilibrium time for the sample to reach the highest desired temperature was less than 45 min. After 45 min, the capacitance and resistance were read from LCR meter at a series of temperature over eight frequencies (see section 2.6.).

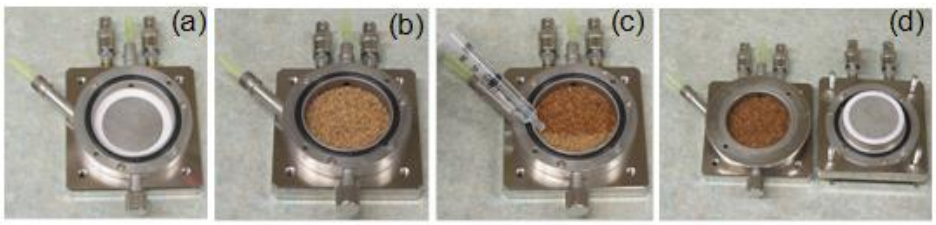

Figure 4.3. The procedure of preparing the packed bed of the DDG particles and ethanol/water solution in the 16452A liquid test fixture.

4.2.8. Calculation of dielectric properties

The obtained values of the capacitance and resistance were used to calculate the dielectric constant and loss factor using the following equations [20, 21], respectively:

$$\varepsilon_r' = \frac{t C_p}{A \varepsilon_0} \tag{4}$$

$$\varepsilon_r'' = \frac{t}{2\pi f R_p \varepsilon_0 A} \tag{5}$$

where t is the gap between the electrodes of the liquid test fixture (m), C_p is capacitance (F), f is frequency (Hz), A is the surface area of each electrode (m^2), and R_p is resistance (Ω).

4.2.9. Calculation of power penetration depth

The power penetration depth for each experiment was calculated using the dielectric constant and loss factor by the following relationship (Buffler, 1993):

$$d_p = \frac{c}{2\sqrt{2}\,\pi f \left\{ \varepsilon_r' \left[\sqrt{1 + \left(\frac{\varepsilon_r''}{\varepsilon_r'} \right)^2} - 1 \right] \right\}^{1/2}} \tag{6}$$

where d_p is the penetration depth (m) and c is the speed of light (3×10^8 m s^{-1}) in vacuum.

4.2.10. Determination of uncertainty associated with power penetration depth

The uncertainty of calculated power penetration depth was determined as follows (Huggins, 1983):

$$\omega_{d_p} = \left[\left(\frac{\partial d_p}{\partial \varepsilon_r'} \omega_{\varepsilon_r'} \right)^2 + \left(\frac{\partial d_p}{\partial \varepsilon_r''} \omega_{\varepsilon_r''} \right)^2 \right]^{1/2} \tag{7}$$

where $\omega_{\varepsilon_r'}$ and $\omega_{\varepsilon_r''}$ are the uncertainties associated with the dielectric constant and dielectric loss factor, respectively. Partial derivatives in Eq. (7) were obtained as (Izadifar and Baik, 2008):

$$\frac{\partial d_p}{\partial \varepsilon_r'} = \left(-\frac{c}{4\pi f \sqrt{2}} \right) \left[\frac{\gamma(\gamma-1) - \left(\frac{\varepsilon_r''}{\varepsilon_r'} \right)^2}{\varepsilon_r' \gamma(\gamma-1) \sqrt{\varepsilon_r'(\gamma-1)}} \right] \tag{8}$$

$$\frac{\partial d_p}{\partial \varepsilon_r''} = \left(-\frac{c}{4\pi f \sqrt{2}} \right) \left[\frac{\varepsilon_r''}{\varepsilon_r'^2 \gamma(\gamma-1) \sqrt{\varepsilon_r'(\gamma-1)}} \right] \tag{9}$$

where γ in Eqns. (8) and (9) is defined as (Izadifar and Baik, 2008):

$$\gamma = \sqrt{1 + \left(\frac{\varepsilon_r''}{\varepsilon_r'} \right)^2} \tag{10}$$

4.3. Results and discussions

The moisture content and porosity of the base sample (DDG) was 3.73% dry basis and 34.66%, respectively. The particle distribution of DDG particles is shown in Fig. 4.4. Among series of sieved DDG particles, the medium particle diameter of 0.84 mm (sieve number 20) was selected for experiments in this study. The appropriate size of the particle was for further study using packed bed extraction unit in radio frequency assisted extraction, and for the prevention of filtering problem of too small particles. The best ratio of particles and solution for each particle moisture content is presented in Table 4.1.

In this study the most of results are presented at frequencies of 13.56 and 27.12 MHz. The reason is that the RF heater (Strayfield FASTRAN SO1.5, Theale, UK) will be used for further investigations to improve the phenolic compounds extraction from DDG at 27.12 MHz. Furthermore, according to European Radio Communications Committee and the US Federal Communication Commission, these two frequencies are allocated to industrial, scientific and medical applications (Izadifar and Baik, 2008). Table 4.2 shows the mean values of dielectric constant and loss factor for all experimental conditions at two frequencies of 13.56 and 27.12 MHz. Uncertainties (twice the standard deviation) of the dielectric constant and loss factor were calculated from duplicate measurements at a 95% confidence.

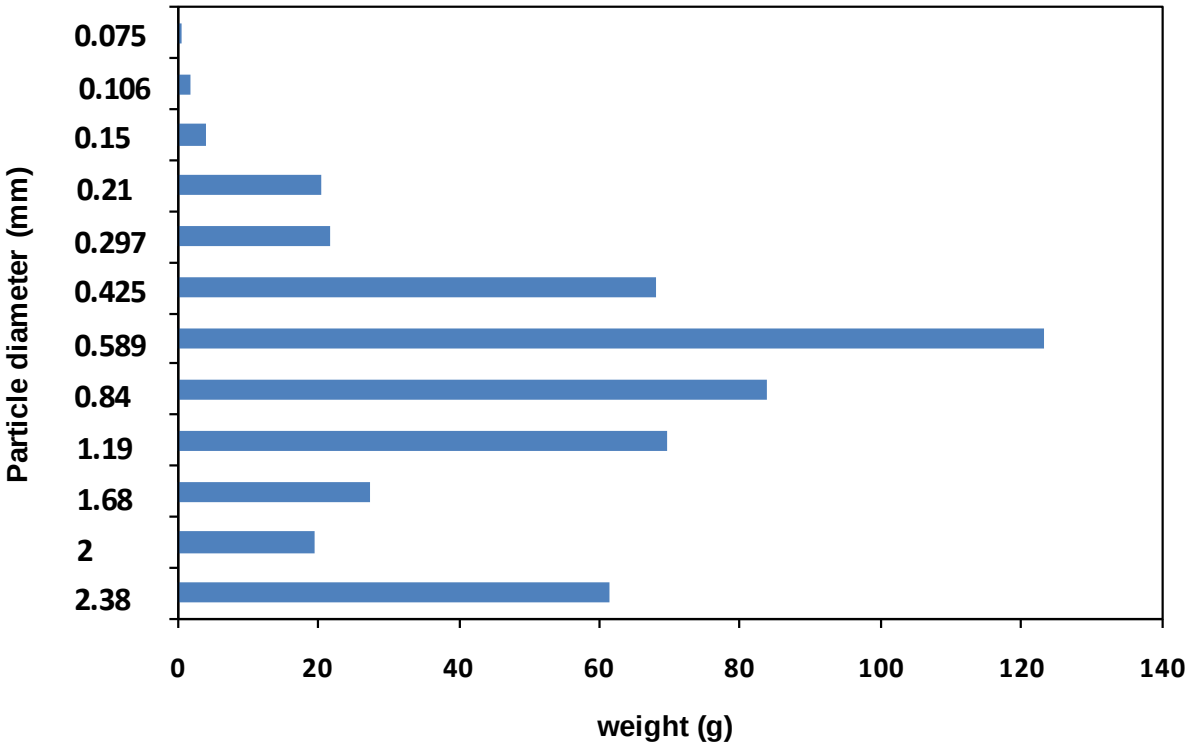

Figure 4.4. Particle size distribution of DDG particles.

Table 4.1. The amount of particles and solvent in the fixture for different particle moisture content.

Particle moisture content (dry basis)	Particle (g)	Solvent (ml)
3.73%	1.12	5.4
158.0%	1.98	4.5
397.51%	5.4	2.1

Table 4.2. Mean values, at 95% confidence, of dielectric constant and loss factor for four levels of ethanol concentration, three levels of particles moisture content, and four levels of temperature (T) at 13.56 and 27.12 MHz.

Moisture content (d.b.)	T	Frequency (MHz)			
		13.56		27.12	
		Dielectric constant (ε_r')	*Dielectric loss factor* (ε_r'')	*Dielectric constant* (ε_r')	*Dielectric loss factor* (ε_r'')
		100% tap water			
3.73%	25˚C	127.82±3.13	416.10±2.88	100.39±1.93	220.81±1.60
	40˚C	145.82±7.74	540.87±5.22	109.08±5.36	288.15±4.23
	55˚C	161.52±10.36	649.44±3.30	116.14±7.42	347.67±0.68
	70˚C	174.53±9.97	739.54±20.61	122.24±7.40	397.70±7.39

158.00%	25˚C	122.60±18.27	396.12±39.84	99.60±13.39	207.75±21.22
	40˚C	139.59±28.37	533.62±67.34	107.34±20.10	281.54±37.28
	55˚C	158.23±39.90	687.27±95.98	115.61±28.35	364.34±54.79
	70˚C	174.98±49.31	830.98±115.98	123.12±35.57	442.08±67.82
397.51%	25˚C	116.16±0.14	353.81±2.87	85.09±1.59	190.99±0.07
	40˚C	128.87±0.30	463.14±6.70	88.89±2.09	248.02±1.61
	55˚C	142.63±1.15	577.23±10.06	95.05±0.53	307.97±3.93
	70˚C	155.81±1.00	685.27±11.64	100.81±2.60	365.92±5.10
			40% ethanol and 60% tap water		
3.73%	25˚C	69.77±1.73	153.98±0.65	60.96±1.07	80.11±0.05
	40˚C	79.29±2.69	235.10±0.00	66.25±1.64	122.89±0.48
	55˚C	90.00±4.25	322.93±1.98	71.36±2.52	169.39±1.84
	70˚C	100.16±5.55	405.42±0.05	75.49±3.22	213.62±1.41
158.00%	25˚C	82.38±2.79	201.76±13.23	71.91±2.162	103.92±6.76
	40˚C	93.56±3.94	298.99±17.97	77.51±2.83	155.39±9.40
	55˚C	106.48±5.10	403.02±20.80	83.52±3.47	210.79±11.01
	70˚C	120.26±5.68	507.98±20.70	89.70±4.01	267.31±11.11
397.51%	25˚C	117.50±25.91	292.16±101.48	91.50±15.78	157.19±56.74
	40˚C	135.17±25.97	395.79±120.41	99.13±13.74	214.22±67.65
	55˚C	155.19±28.42	504.30±139.31	108.58±15.54	273.19±75.24
	70˚C	175.34±32.32	609.21±151.84	121.25±26.94	333.45±86.56
			70% ethanol and 30% tap water		
3.73%	25˚C	41.86±3.50	56.98±7.07	38.57±3.39	28.98±3.60
	40˚C	44.71±3.60	89.32±11.97	40.08±3.37	46.03±6.14
	55˚C	47.59±3.55	128.51±17.49	41.59±3.13	66.47±8.97
	70˚C	49.18±4.78	165.45±26.54	41.62±3.89	85.69±13.71
158.00%	25˚C	59.99±5.42	119.96±21.40	54.25±3.76	61.17±11.54
	40˚C	65.59±7.59	183.49±32.76	56.90±4.94	94.36±17.62
	55˚C	72.10±9.10	253.49±42.45	59.70±5.30	131.02±22.92
	70˚C	79.37±10.76	324.39±49.16	62.51±5.82	168.41±26.72
397.51%	25˚C	105.60±19.21	260.07±58.24	84.80±11.89	138.21±32.78
	40˚C	123.78±23.45	366.29±67.84	93.73±14.27	196.10±38.73
	55˚C	143.50±26.95	476.04±73.99	103.05±16.08	256.72±43.24
	70˚C	163.55±31.54	585.32±78.33	112.54±19.35	317.79±46.50
			100% ethanol concentration		
3.73%	25˚C	18.45±0.72	1.79±0.06	18.43±0.71	0.31±0.01
	40˚C	17.47±0.71	3.58±0.13	17.41±0.73	1.17±0.11
	55˚C	16.71±0.63	6.65±0.40	16.50±0.63	2.74±0.16
	70˚C	16.24±0.05	10.86±0.44	15.67±0.08	4.98±0.22
158.00%	25˚C	36.22±0.56	45.19±2.63	33.95±0.55	22.52±1.32
	40˚C	37.56±0.32	66.70±3.53	34.27±0.36	33.76±1.77
	55˚C	38.71±0.24	89.50±5.35	34.52±0.28	45.74±2.67

	70˚C	39.42±0.25	112.31±4.39	34.45±0.18	57.67±2.15
397.51%	25˚C	79.62±0.61	164.23±6.81	67.46±1.42	86.41±2.91
	40˚C	91.38±0.19	247.50±11.49	72.48±0.75	131.15±5.07
	55˚C	105.55±0.37	336.39±15.16	78.54±0.84	179.41±6.86
	70˚C	121.15±1.20	428.43±15.71	84.94±0.46	229.88±7.14

As it can be seen from Table 4.2, for some cases, the uncertainty based on duplicate measurements varies greatly from measurement to measurement. This can be attributed to one or more of the following reasons: (i) The difference between repeated measurements was significant when each of duplicate measurements were performed on separate days and the LCR meter was restarted and the cables were reconnected in between, which may have disturbed the calibration of LCR meter (systematic errors). (ii) The particle moisture content might have been changed in repeated measurements that can significantly affect dielectric loss factor and constant (iii) the air bubbles entrapment through sample might make error in dielectric property measurements.

Fig. 4.5 shows the variation of the dielectric loss factor with frequency for the packed bed of DDG particles (particle moisture content of 0.037 dry basis) with ethanol/water solution, for four temperatures and four volumetric concentrations of ethanol in water. The dielectric loss factor of the packed bed decreased with frequency for all levels of volumetric ethanol fraction of solvent and temperatures. This might be due to the fact that by increasing the frequency, molecules do not have enough time to follow the alternations of the applied field and align with the electric field. The curves in Fig. 4.5 illustrate that the dielectric loss factor increased with the temperature at a fixed ethanol concentration. The same results were observed for all applied particle moisture contents (Fig. 4.6). This can be attributed to the increase in thermal energy of ions and molecules with temperature. As thermal energy (kinetic energy) rises, the mobility of the ions and polar molecules enhances, causes more flip-flop rotation of polar molecules as well as oscillation of ions which results in more collision with neighboring molecules and more molecular frictions. However within the RF band, for biological materials the ionic loss component is dominant in dielectric loss factor (Ryyanen, 1995). As temperature increases, the viscosity of the solvent existing inside of particles decreases, so the conductivity of ionic compounds is enhanced and the dielectric loss factor increases (Tang et al., 2002). This observation that the dielectric loss

factor decreases with the frequency and increases with the temperature agrees with the observation reported by Guan et al. (2004) on the dielectric properties of mashed potatoes, Izadifar and Baik (2008) on dielectric properties of rhizome of *P.peltatum*, and Shrestha and Baik (2009) on dielectric properties of saponins. The highest dielectric loss factors were observed at 70°C.

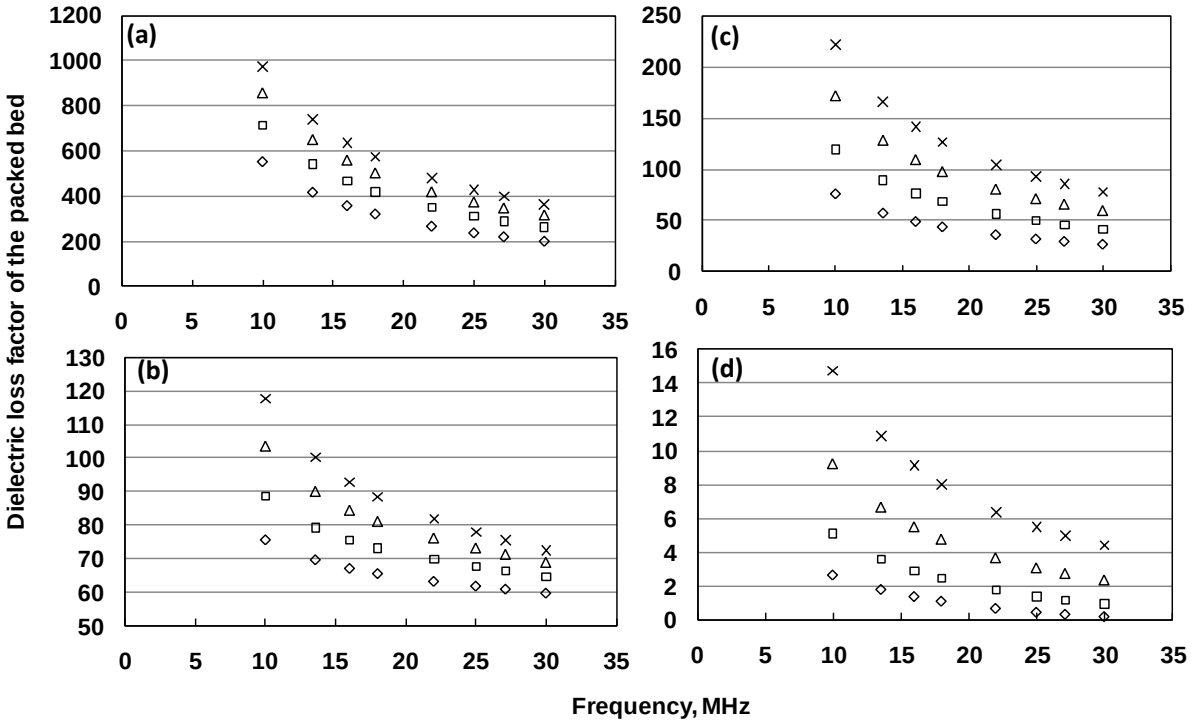

Figure 4.5. Variation of the dielectric loss factor of the packed bed with frequency for four levels of temperature and ethanol volumetric fraction of 0% (a), 40% (b), 70% (c), and 100% (d) at particle moisture content of 0.0373% d.b.: ◊, *25℃* □ *, 40℃; Δ, 55℃;* ✕ *, 70℃.*

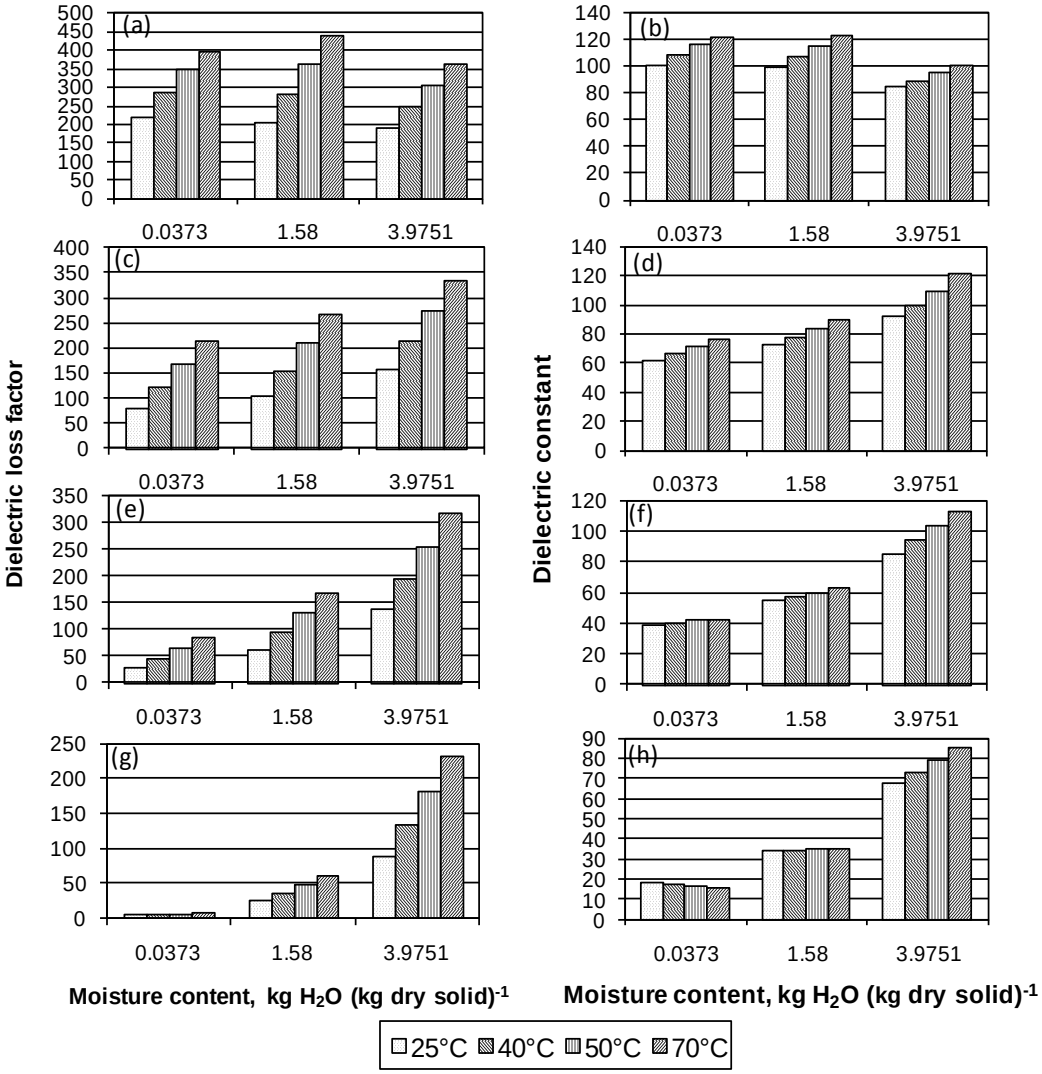

Figure 4.6. Variation of the dielectric loss factor (a, c, e, and g) and dielectric constant (b, d, f, and h) with particle moisture content for four levels of ethanol volumetric fraction of 0% (a and b), 40% (c and d), 70% (e and f) and 100% (g and h) at four levels of temperature at 27.12 MHz.

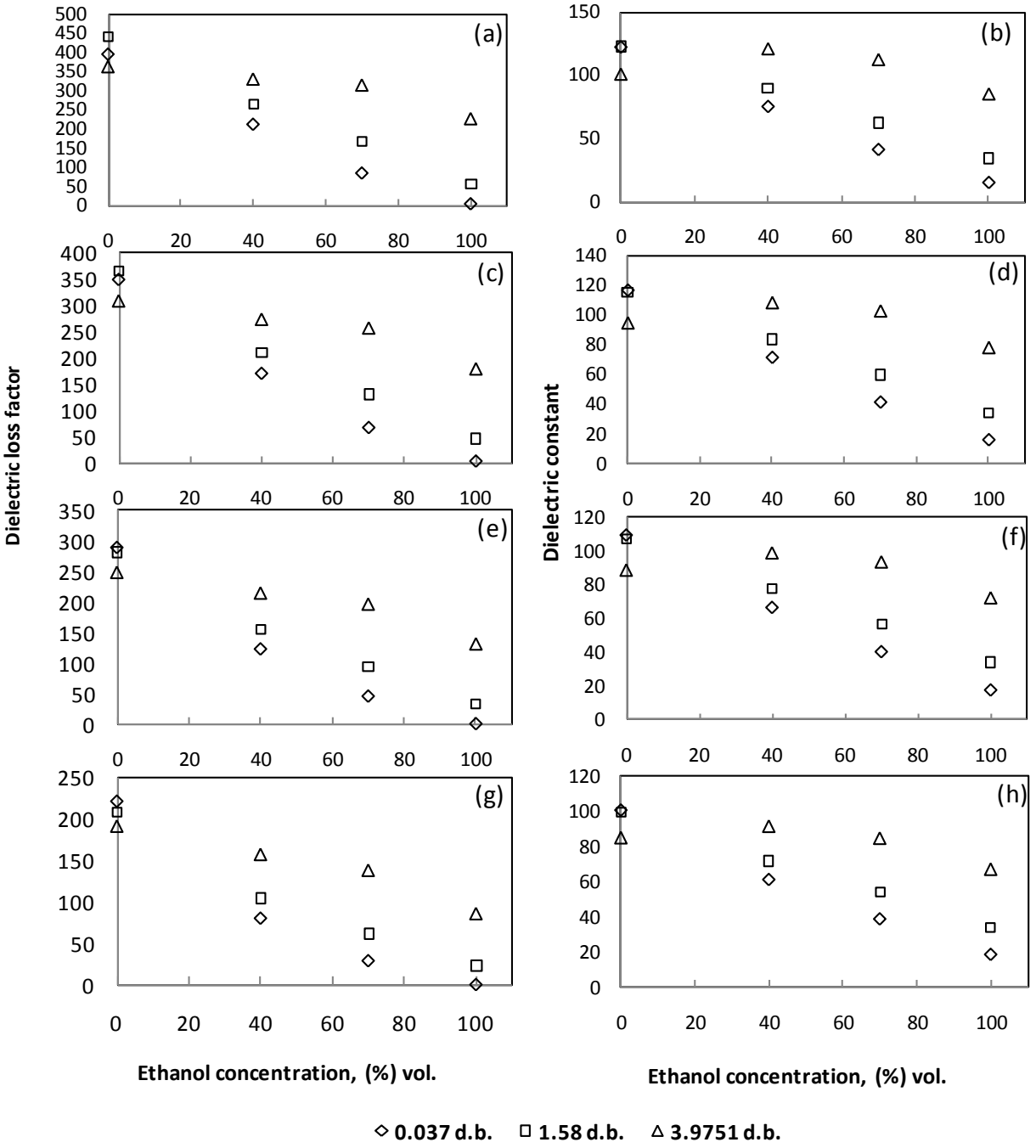

Figure 4.7. Variation of the dielectric loss factor (a, c, e, and g) and dielectric constant (b, d, f, and h) with volumetric ethanol concentration for three levels of particle moisture content at 27.12 MHz and four levels of temperature of 70°C (a and b), 55°C (c and d), 40°C (e and f), and 25°C (g and h).

Fig. 4.7 illustrates the variation of dielectric loss factor and constant of the packed bed with ethanol for four levels of temperature and three levels of particle moisture content at frequency

of 27.12 MHz. The dielectric constant and loss factor increased with particle moisture content and the effect of moisture content on dielectric constant and loss factor was more significant on particles with 3.98 dry basis moisture content compared with other levels of particles moisture content. At low levels of particle moisture content, the mobility of ions and solute molecules is restricted because they are bound to solid material (Izadifar and Baik, 2008). As the particle moisture content increases, the polarity of the packed bed enhances and also the mobility of water soluble ionic compounds and polar molecules is facilitated which results in the increase of dielectric loss factor (Fig 4.6) and constant. The dielectric constant and loss factor decreased with ethanol for all levels of particle moisture content and temperature.

In the interpretation of the correlation between ions and dipole polarization (which affects dielectric permittivity) of the packed bed and an alternating electric field at different experimental conditions, it is speculated that three factors have to be taken into account: (i) packed bed polarity (ii) solvent-solute molecular interaction (iii) molecular dynamics.

The dielectric permittivity of the packed bed is highly related to the polarity of the packed bed solution. Compare to water which is completely a polar solvent, ethanol (CH_3-CH_2-OH) has less polarity. Pure ethanol can be divided into two major classes, the polar side chain (OH) and nonpolar side chain (CH_3-CH_2). The polar nature of the hydroxyl group causes ethanol to dissolve many ionic compounds and the nonpolar end dissolve nonpolar substances, including most essential oils and medicinal agents (MICD). Polarity of the packed bed depends on the molecular interaction of solvent with dissolved compounds of DDG (polar or nonpolar compounds) at various ethanol volumetric fractions. If solvent-solute molecular interactions are strong, we may deal with either rigid polar associates that are able to reorient as a whole in a strong electric field or rigid nonpolar associates which result in low dielectric permittivity of the packed bed. Besides the polarity effect on reorientation, it is speculated that molecular dynamics have a large contribution to the reorientation. Molecular weight, size, chain length, and flexibility define the dynamics of molecules in the solvent environment of the packed bed in the presence of external electric field. Sengwa and Sankhla (2006) have studied the effect of chain length on dynamical structure of poly-polar solvent mixtures in dilute solution with microwave dielectric relaxation measurement. They showed that the increase in chain length and flexibility influence the molecular dynamics. In addition, the rate of motion in different compounds are

strongly depends on the size of compounds and the chemical bonds (hydrogen bonding, electron transfer, dipole association, etc.) they make with neighbouring compounds/solvent in the packed bed. Small size molecules have higher chance of movement compare with molecules with long chain length. Afflech et al. (1992) have shown the correlation between the rate of motion in the protein and the dielectric constant of the bulk solvent.

As Fig. 4.7, dielectric constant and loss factor with ethanol for 3.98 d.b. particle moisture content decreased suddenly around 70% ethanol. The reason for this is due to the fact that wheat DDG includes ash, acid ether extract, soluble NSP (non starch polysaccharides), insoluble NSP, crude protein (FOBI, 2011), and medicinal compounds such as beta-glucan and phenolic compounds. Crude protein is the component present in highest concentration in WWDG (wheat wet distillers grain) (FOBI, 2011). Cui et al. (1999) observed that treatment of a fraction of wheat bran with 70% ethanol at 70°C removed fat, free sugar, amino acids, and some phenolics. Also, it was found in our previous study (not shown here) that the optimum extraction condition of phenolic compounds from wheat DDG is at 70% ethanol, 70°C and 59% wet basis particle moisture content (which is close to WDG moisture content). At 70% ethanol, hydrogen bonding between ethanol and compounds like phenolic compounds, amino acids, and fat can decrease the polarity of the packed bed or might decrease the reorientation of molecules in the packed bed. Also bonds between ethanol and fat, phenolic compounds, and amino acids can produce long chain molecular structures, which make their molecular movement more difficult. Ethanol solution at higher than 70% led to the simultaneous extraction of some lipid components (Wang et al., 2008). Lipids are relatively non-polar molecules and they can be pulled out of sample using non-polar end of ethanol in the solvent. Lipids are long chain molecules and extraction of them makes the packed bed non-polar. However, by decreasing the ethanol volumetric fraction of solvent, the solubility of ions and polar compounds like soluble NSP (which are water soluble) increased which results in rise of polarity of the packed bed.

As can be seen from Fig. 4.7, 4.8, and 4.9 for all levels of temperature and particle moisture contents, both the dielectric loss factor and dielectric constant of the packed bed decreased as the volumetric fraction of ethanol in the solution increased from 0% (tap water) to 100% (pure ethanol). In addition to what discussed earlier, it has been previously shown by Izadifar and Baik (2008), and also Shresta and Baik (2009) that the dielectric loss factor of water is higher than that

of ethanol for frequencies of 13.56 and 27.12 MHz. The reason for this can be due to the polarity of tap water which is higher than ethanol (Izadifar and Baik, 2008). Therefore, higher ethanol concentration results in less polar molecules and ions, thus lower dielectric constant and loss factor of the packed bed. The dielectric constants and loss factors for different levels of frequency, ethanol volumetric fraction of solvent, and temperature for particle moisture content of 0.0373 d.b. are shown in Fig 4.8 and 4.9, respectively. The dielectric constant of the packed bed decreased with frequency and was more sensitive to frequency at lower ethanol concentration in the solvent. The dielectric constant and loss factor decreased rapidly with frequency at 0% ethanol concentration of solvent, while its variation with frequency was small for 40% ethanol and insignificant for 70% and 100% ethanol concentrations. This might be due to the fact that the movement of water molecules is easier than that of ethanol molecules because the molecular structure of water is symmetric while ethanol is not (Dr. Lee Wilson, personal communication, February 7, 2011). Also ethanol's hydroxyl group participates in hydrogen bonding, which makes the ethanol more viscous or forms a strong rigid associate causing difficult reorientation. The dielectric constant of the bed increased with temperature; however it was more significant when ethanol concentration decreased from 40% to 0%. The effect of temperature on dielectric constant was not significant when the ethanol volumetric fraction of solvent was high (70% and 100%). At 100% ethanol concentration, temperature had insignificant effect on the dielectric constant at 0.0373 and 1.58 d.b. particle moisture contents (Fig. 4.6 h). Since the effect of temperature on dielectric properties is more on thermal energy and agitations of ions and molecules, decrease of water content in the packed bed can significantly decrease the polarity of the packed bed which causes decreasing the temperature effect. As explain above, the effect of ethanol on decreasing the molecular dynamics of packed bed can also decrease the effect of temperature. These observations agree with the observation reported by Guan et al. (2004) and Izadifar and Baik (2008).

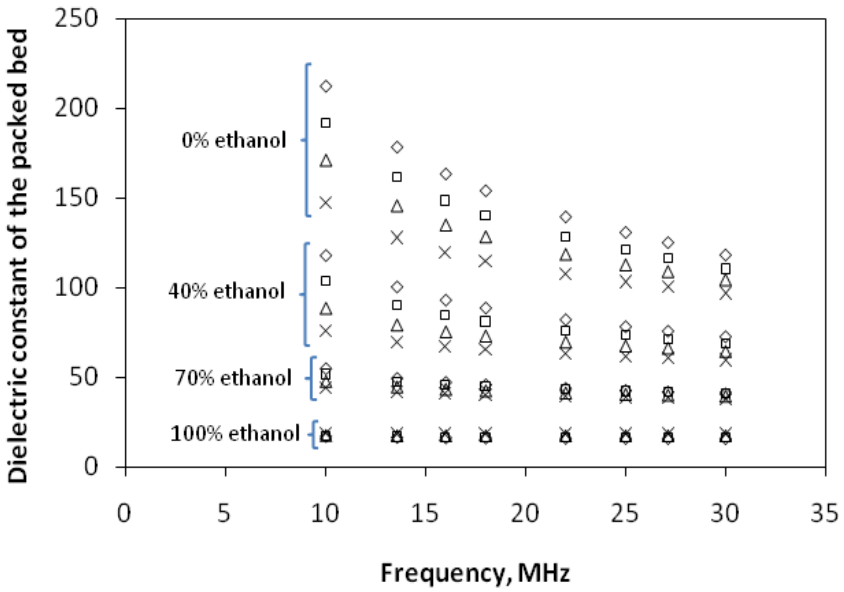

Figure 4.8. Variation of dielectric constant of the packed bed with frequency for four levels of ethanol volumetric fraction and four levels of temperature at particle moisture content of 0.0373 d.b: ✕, *25 ℃;* Δ , *40 ℃;* □, *55 ℃;* ◊ , *70 ℃.*

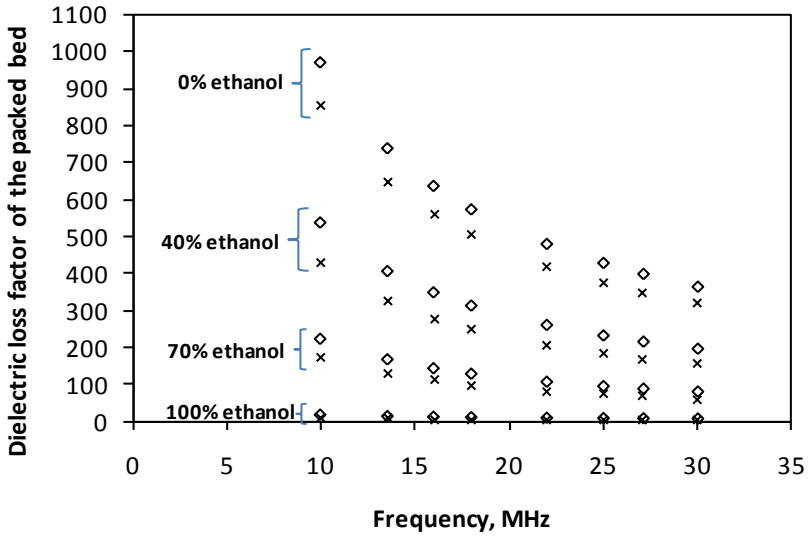

Figure 4.9. Variation of dielectric loss factor of the packed bed with frequency for four levels of ethanol volumetric fraction and two levels of temperature at particle moisture content of 0.0373 d.b.: ✕, *55 ℃;* ◊ , *70 ℃.*

A multiple regression analysis was performed using SPSS 14.0 for Windows Release 14.0.0 (5 Sep 2005) at frequencies of 13.56 and 27.12 MHz. Table 4.3 lists the regression equations with significant terms.

Table 4.3. Multiple regression equations for dielectric constant and dielectric loss factor of the packed bed at 27.12 MHz.

Frequency (MHz)	Regression equation	RMSE[a]	DF[b]	R^2
Dielectric constant				
13.56	$\acute{\varepsilon}'$=115.161-1.677E+0.037EM^2+0.812T-0.007TE+0.002MT^2-0.004ME^2+0.526EM+0.007E^2-8.660M	4.35	47	0.99
27.12	$\acute{\varepsilon}'$=95.751-1.247E+0.315EM+0.342T-0.003ME^2+0.005E^2-0.000037TE^2+0.001MT^2+0.038EM^2-1.719M^2	2.27	47	0.99
Dielectric loss factor				
13.56	ε''=161.754-3.455E+8.378T+0.895EM-0.055TE	43.21	47	0.96
27.12	ε''=83.858-1.858E+4.512T+0.488EM-0.03TE	23.87	47	0.96

[a] Root mean square error.
[b] Degree of freedom.

It was observed that the temperature, particle moisture content, and the ethanol volumetric fraction of solvent in the packed bed had significant effects on both the dielectric constant and loss factor of the packed bed. Using estimated regression equations, the effect of ethanol and temperature at 0.0373 d.b. particle moisture content and the influence of ethanol and particle moisture content at 70°C on dielectric constant and loss factor were investigated in Fig. 4.10 and 11, respectively.

Both dielectric constant and loss factor increase rapidly by decreasing the ethanol fraction of solvent (Fig 4.10 a and b). Although temperature has no significant effect on dielectric constant at high levels of ethanol fraction, dielectric constant increases slowly with temperature at low levels of ethanol volumetric fraction. As shown in fig. 4.10 b, the dielectric loss factor increases slowly with temperature at high levels of ethanol; however this variation becomes larger as the fraction of ethanol decreases.

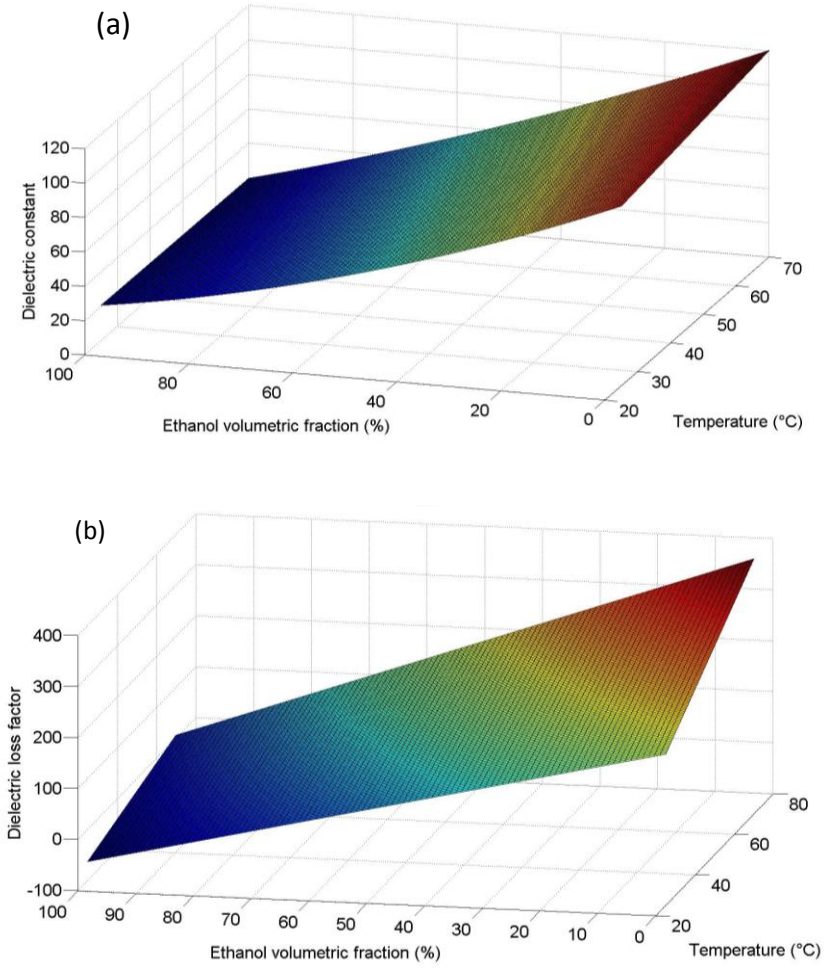

Figure 4.10. Variations of the dielectric constant (a) and loss factor (b) of packed-beds with ethanol volumetric fraction of solvent and temperature at 0.0373 dry basis particle moisture content.

As seen in Fig. 4.11 a and b, moisture content has nonlinear effects on dielectric constant, however for dielectric loss factor the moisture content turned out to have linear effects. Both dielectric constant and loss factor increase rapidly by decreasing ethanol fraction at a fixed moisture content, while an increase in moisture content at a fixed ethanol concentration also leads to a marked increase in both dielectric constant and loss factor.

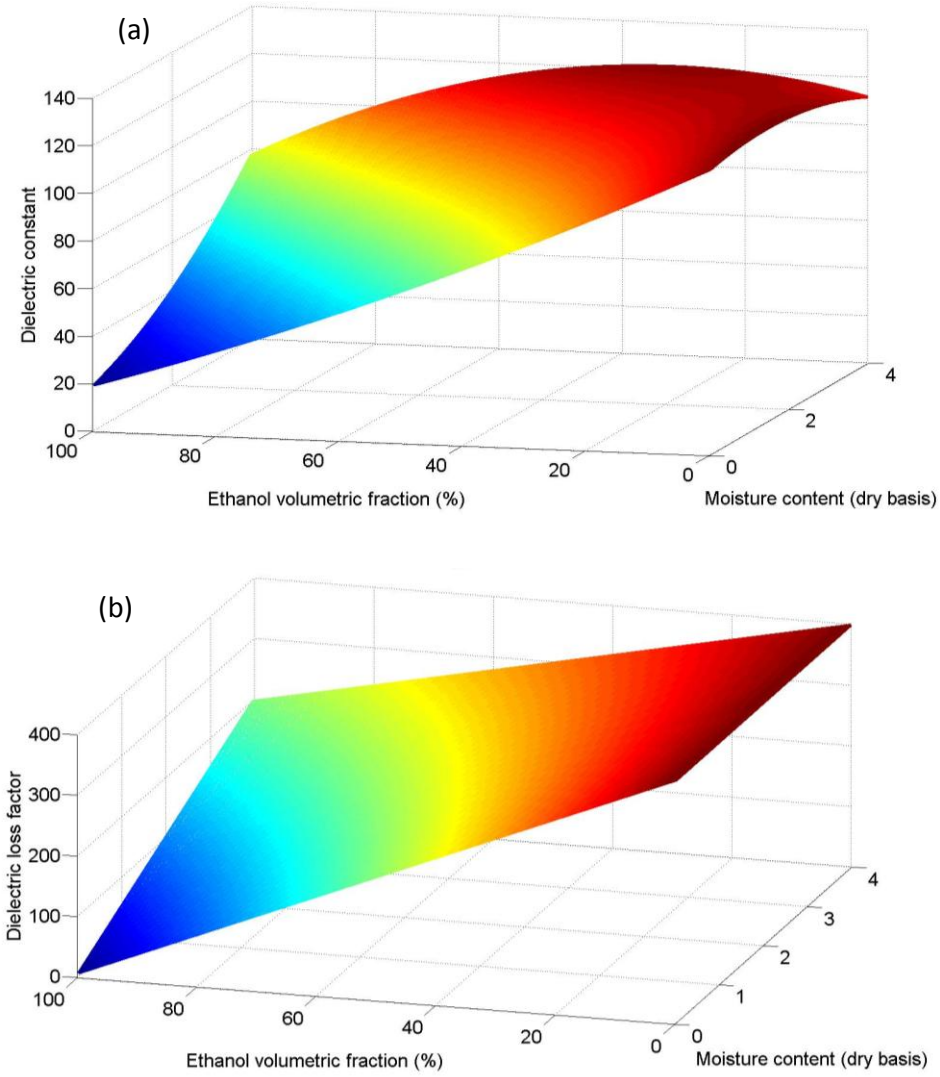

Figure 4.11. Variations of dielectric constant (a) and loss factor (b) of packed-beds with ethanol volumetric fraction of solvent and moisture content at temperature of 70°C.

The mean values and uncertainties associated with power penetration depth for various levels of ethanol, particle moisture content, and temperature in the packed bed at a 95% confidence level are shown in Table 4.4. The power penetration depth decreased with temperature for all levels of particle moisture content and ethanol volumetric fraction of solvent at 13.56 and 27.12 MHz. Similar observations were reported by Guan et al. (2004) for mashed potato at 27 MHz and Izadifar and Baik (2008) for rhizome of *P. peltatum* at 27.12 and 13.56 MHz.

Table 4.4. Mean values at a 95% confidence level of power penetration depth for four levels of ethanol concentration, three levels of particles moisture content, and four levels of temperature at 13.56 and 27.12 MHz.

Moisture content (d.b.)	T	Frequency (MHz)			
		13.56	27.12	13.56	27.12
		0% ethanol		40% ethanol	
3.73%	25˚C	0.14±0.00	0.10±0.00	0.25±0.00	0.20±0.00
	40˚C	0.12±0.00	0.08±0.00	0.19±0.00	0.14±0.00
	55˚C	0.11±0.00	0.08±0.00	0.16±0.00	0.12±0.00
	70˚C	0.10±0.00	0.07±0.00	0.14±0.00	0.10±0.00
158.00%	25˚C	0.14±0.01	0.11±0.01	0.22±0.01	0.17±0.01
	40˚C	0.12±0.01	0.09±0.01	0.17±0.01	0.13±0.00
	55˚C	0.10±0.01	0.07±0.01	0.14±0.00	0.10±0.00
	70˚C	0.09±0.01	0.07±0.01	0.12±0.00	0.09±0.00
397.51%	25˚C	0.15±0.00	0.11±0.00	0.16±0.04	0.12±0.03
	40˚C	0.13±0.00	0.09±0.00	0.14±0.03	0.10±0.02
	55˚C	0.12±0.00	0.08±0.00	0.12±0.02	0.09±0.02
	70˚C	0.11±0.00	0.07±0.00	0.11±0.02	0.08±0.01
		70% ethanol		100% ethanol	
3.73%	25˚C	0.45±0.05	0.39±0.05	8.43±0.34	24.92±1.06
	40˚C	0.33±0.03	0.26±0.03	4.22±0.17	6.56±0.62
	55˚C	0.26±0.02	0.20±0.02	2.17±0.13	2.58±0.16
	70˚C	0.22±0.02	0.16±.02	1.35±0.05	1.39±0.06
158.00%	25˚C	0.30±0.04	0.25±0.04	0.54±0.02	0.48±0.02
	40˚C	0.23±0.03	0.18±0.02	0.40±0.01	0.34±0.01
	55˚C	0.18±0.02	0.14±0.02	0.33±0.01	0.26±0.01
	70˚C	0.16±0.01	0.12±0.01	0.28±0.01	0.22±0.00
397.51%	25˚C	0.18±0.03	0.13±0.02	0.24±0.01	0.19±0.00
	40˚C	0.15±0.02	0.11±0.02	0.19±0.00	0.14±0.00
	55˚C	0.13±0.01	0.09±0.01	0.16±0.00	0.11±0.00
	70˚C	0.11±0.01	0.08±0.01	0.14±0.00	0.10±0.00

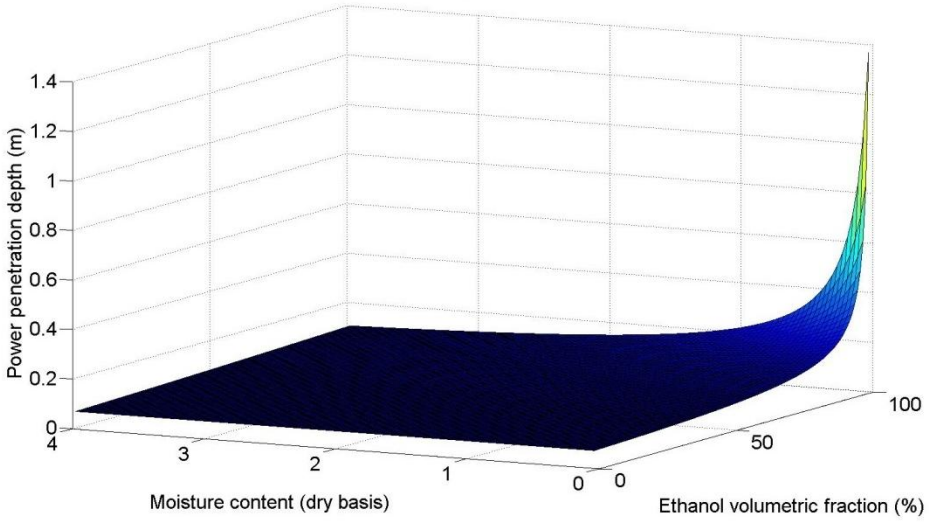

Figure 4.12. Variation of power penetration depth of the packed bed with particle moisture content and ethanol volumetric fraction of solvent at 70°C and 27.12 MHz.

As shown in Fig. 4.12, the power penetration depth does not show much variation at high moisture content and low ethanol fraction; however as moisture content and ethanol decreases and increases, respectively to their extreme values, a drastic increase is seen in power penetration depth.

Variation of penetration depth with temperature and ethanol is more significant for particles with higher moisture content compared with lower ones (Fig. 4.13a and b). As shown in Fig. 4.13 a, for particle moisture content of 1.58 d.b., the power penetration depth does not change significantly for high temperature and low ethanol concentration tested. As temperature decreases and ethanol increases to extreme values tested, power penetration depth increases dramatically. For particle moisture content of 3.98 d.b., the power penetration depth increases rapidly with the decrease of temperature and increase of ethanol fraction, and is led to a marked increase at the highest (100%) and lowest (25°C) ethanol fraction and temperature tested, respectively (fig. 4.13). Higher ethanol fraction of solvent, lower particle moisture content and lower temperature in the packed bed can significantly decrease the dielectric constant and loss factor of the packed bed. Thus, the dissipation of electromagnetic energy is decreased although electromagnetic field can penetrate more in the packed bed (Izadifar and Baik, 2008).

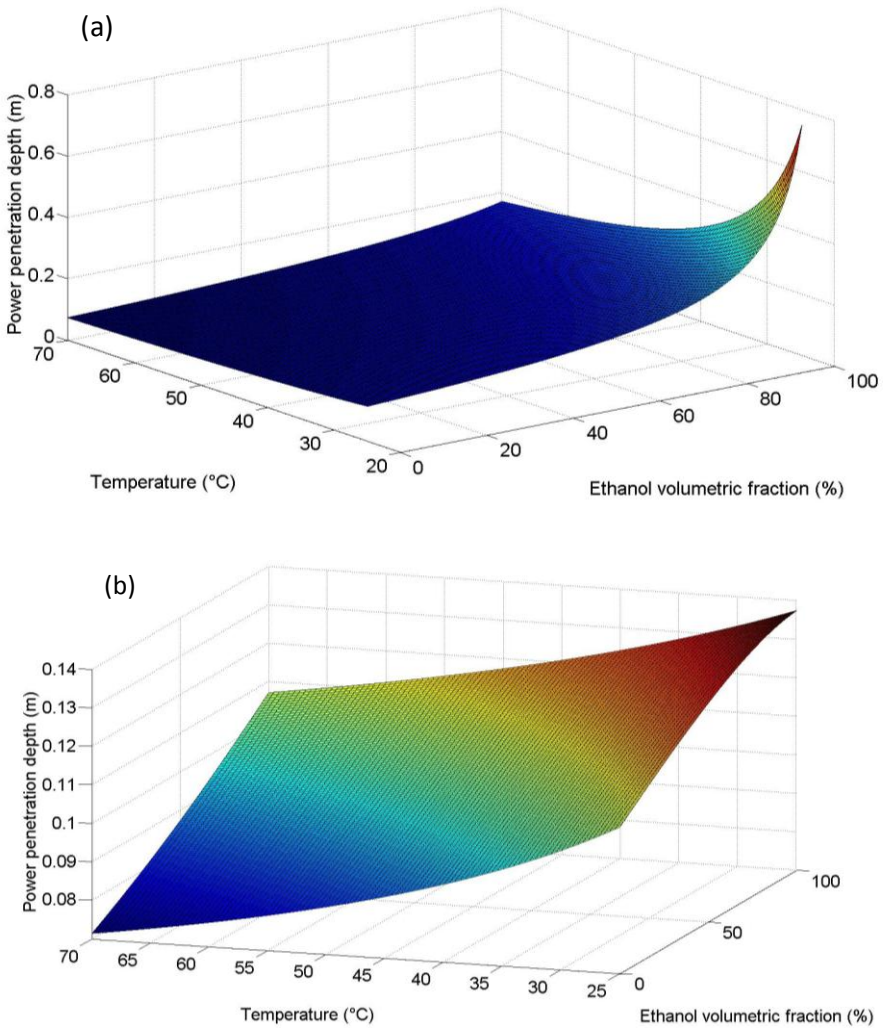

Figure 4.13. Variation of power penetration depth with temperature and ethanol volumetric fraction of solvent at particle moisture content of 1.5 (a) and 3.98 (b) dry basis at frequency of 12.57 MHz.

4.4. Summary and conclusion

Both dielectric constant and loss factor of a packed of DDG particles with ethanol/water solution decreased with frequency for all levels of ethanol fraction and temperature and were more sensitive to frequency at lower ethanol concentrations in the solvent. The dielectric constant and loss factor of the bed increased with temperature for all levels of particle moisture content and ethanol fraction; however, for 100% and 70% ethanol and particle moisture content of 0.0373 d.b., and also 100% ethanol and particle moisture content of 1.58 d.b., the effect of temperature on dielectric constant was insignificant. The dielectric constant and loss factor of the

packed bed decreased significantly with ethanol volumetric fraction of solvent for all levels of temperature and particle moisture content. The highest dielectric constant and loss factor were at 0% ethanol (100% tap water) and the lowest ones were at 100% ethanol fraction of solvent. The dielectric constant and loss factor increased with moisture content for 40%, 70%, and 100% ethanol; however, for 0% ethanol the effect of moisture content was not significant. The highest dielectric loss factor of the bed was observed at 0% ethanol fraction, 70°C, and particle moisture content of 3.98 d.b. Power penetration depth decreased with temperature and particle moisture content, and increased with ethanol fraction. The highest power penetration depth was observed at the lowest particles moisture content (0.0373 d.b.) tested and 100% ethanol at the lowest temperature tested (25°C).

References

Affleck R; Haynes C A; Clark D S. Solvent dielectric effects on protein dynamics, Biochemistry, 89 (1992), 5167-5170

Anon. An array of new applications are evolving for radio frequency drying. Food Engineering, 59(5) (1987), 180

Anon, RF improves industrial drying and baking processes. Process Engineering. 70 (1989), 33

AOAC (Association of official Agricultural Chemists) (2000). AOAC 930.15 Loss on Drying (Moisture) for Feeds. Official Methods of Analysis of AOAC International 17th edition. Washington, D.C: AOAC

ASABE (2009). ASAE standards. S352.2: Moisture Measurement-Unground Grain and Seeds, St. Joseph, MI, USA, APR1988 (R2008)

Balakrishnan P A; Vedaraman N; Sunder V J; Muralidharan C; Swaminathan G. Radiofrequency heating-a prospective leather drying system for future. Drying Technology, 22 (2004), 1969-1982

BBOP (Barley bioproducts opportunities project) (2008). http://www.wbga.org/BBOP-April-08.pdf 1-12 , accessed on January 2011.

Buffler C R (1993) Microwave cooking and processing, Van Nostrand Reinhold, New York.

Cui W; Wood P J; Weisz J; Beer M U, Nonstarch polysaccharides from preprocessed wheat bran: carbohydrate analysis and novel rheological properties. Cereal Chem, 76 (1) (1999), 129-133

FOBI (Feed Opportunities from Biofuels Industries) network, Chemical composition of WWDG-PC table in Monogastric nutrition presentation at FOBI Wind-up AGM Meeting, March 10, 2011, Saskatoon, Canada.

Guan D; Cheng M; Wang Y; Tang J, Dielectric properties of mashed potatoes relevant to microwave and radio-frequency pasteurization and sterilization processes, Journal of Food Science, 69(2004), 30-37

Halliday D; Resnick R; Walker J (2001). Fundamentals of physics, 6th edn. Wiley, New York.

Houben J; Schoenmakers L; Putten E; Roon P; Krol B, Radio frequency pasteurization of sausage emulsion as a continuous process. Journal of Microwave Power and Electromagnetic Energy, 26 (1991), 202-205

Huggins L F (1983) Analysis and Interpretation in: Instrumentation and Measurement for Environmental Sciences. ASAE, St. Joseph.

IMS (Industrial microwave systems) (2011). L.L.C., http://www.industrialmicrowave.com, accessed on January 2011.

Izadifar M; Baik O D. Dielectric properties of a packed bed of the rhizome of P. Peltatum with an ethanol/water solution for radio frequency-assisted extraction of podophyllotoxin. Biosystems Engineering, 100 (2008), 376-388

Jason, A C; Sanders H R, Dielectric thawing of fish. L. Experiments with frozen white fish. Food Technologies, 16(6) (1962b), 107-112

Jason, A C; Sanders H R, Dielectric thawing of fish. L. Experiments with frozen herrings. Food Technologies, 16(6) (1962a), 101-106

Kappe C O; Dallinger D; Murphree S. S. (2009). Practical Microwave Synthesis for Organic Chemists, WILEY-VCH Verlag GmbH & Co. KGaA, Weinheim, Germany

Kinn, TP, Basic theory and limitations of high frequency heating equipment. Food Technology, Food Tech. 1(2) (1947), 161-177

Lee D. Wilson, Department of Chemistry, 110 Science Place, Room 156, University of Saskatchewan, Saskatoon, SK, Canada

Maurizion B; Giovanni C; Mirko G; Giancarlo P; Giuseppe L; Riccardo O, Radio frequency (RF) ablation of renal tumours does not produce complete tumour destruction: results of a phase II study. European Urology Supplement, 3(2004), 14-17

Mermelstein N H, Interest in radiofrequency heating heats up. Food Technology, 51(1997), 94-95

MICD (Merck Index of Chemicals and Drugs), 9th ed.; monographs 6575 through 6669.

Moyer J C; Stotz E, The blanching of vegetables by electronics. Food Technology, 1(1947), 252-257

Piyasena P; Dussault C; Koutchma T; Ramaswamy H S; Awuah G, Radio Frequency heating of foods; principles, applications and related properties-A review. Critical Review in Food Science and Nutrition, 43(2003), 1-20

Poulin A; Dostin M; Proulx P; Kendalla J, Convective heat and mass transfer and evolution of moisture distribution combined convection and radio frequency drying. Drying Technology, 15(1997), 1893-1907

Ryynanen S, The electromagnetic properties of food materials. Journal of Food Engineering, 26(1995), 409-429

Sengwa R.J.; Sankhla S., Chain length effect on dynamical structure of poly(vinyl pyrrolidone){polar solvent mixtures in dilute solution of dioxane studied by microwave dielectric relaxation measurement, journal of physics, 67(2) (2006), 375-381

Shrestha B L; Baik O D (2009). Permittivity of Mixtures of Saponaria vaccaria and Ethanol-Water Solution for RF heating assisted extraction of Saponin, In press

SPSS for Windows, Rel. 14.0.0. 2005. Chicago: SPSS Inc.

Tang J; Feng H; Lau M (2002). Microwave heating in food processing. In: Advances in Agriculture Engineering (Young X; Tang J; Zhang C; Xin W, eds). Scientific Press, New York

Wang J. B; Sun Y; Cao Y; Tian X; Li, Optimisation of ultrasound-assisted extraction of phenolic compound from wheat bran, J. Food chem. 106 (2008) 804-810

Wang S; Monzon M; Gazit Y; Tang J; Mitcham E J; Armstrong J W, Temperature dependent dielectric properties of selected subtropical and tropical fruits and associated insect pests, Transactions of ASABE, 48 (2005), 1873-1881

Zhong Q; Sandeep K P; Swartzel K R, Continuous flow radio frequency heating of water and carboxymethylcellulose solution. Journal of Food Science, 68 (2003), 217-223

CHAPTER 5
Overall Summary and conclusion

Synopsis

This chapter incorporates achievements from the preceding chapters to suggest an effective extraction method that could be used in future studies of ultrasound-RF assisted extraction system. This chapter also contains study limitations and some recommendations for further studies.

Currently, solid-liquid extraction techniques are commercially used for the extraction of natural medicinal products. These techniques need lengthy extraction time as well as large volume of polluting solvent (Jianyong et al., 2001). These conventional methods of extraction suffer some weak points such as solvent preheating and temperature gradient within the bed during extraction (Izadifar and Baik, 2009). The solvent must be pre-heated before it is used for the extraction. It takes some times until the whole solvent warms up to the target operating temperature. In the extraction, cell wall of the wheat grain is an important barrier for mass transfer of phenolic compounds from inside to outside the cell. Diffusion of phenolic compounds through cell wall needs lengthy time. In this study it was tried to develop an innovative extraction technology to extract phenolic compounds from DDG with ultrasound (US) and potential radio frequency (RF) application to increase product yield and decrease extraction time and energy consumption.

Pre-treating fermented wheat wastes by ultra sound (US) waves can damage cell walls and also develop the pores of the cell walls, which results in improved extraction rate and yield of bioactive compounds (i.e. phenolic compounds). And also, RF heating assisted extraction can potentially provide uniform volumetric internal heat generation within a packed-bed solvent extraction unit at commercial scales. To develop an efficient extraction method with ultrasound pretreatment and potentially RF heating, first the effect of ultrasound on the cell wall and extraction rate constant should be investigated. Furthermore, on the top of the determination of the optimum ultrasound pretreatment condition, mechanism and kinetics of the extraction

operation of phenolic compounds from DDG, thermal and physical properties of the materials involved must be characterized. For further investigation of using RF heating during the packed bed solvent extraction, dielectric properties of the bed must be characterized. The objective of this chapter is to integrate achievements from the preceding chapters to suggest an effective extraction method that could be used in ultrasound-RF assisted extraction system.

5.1. Extraction kinetics of phenolic compounds

Temperature, ethanol fraction of the aqueous ethanol solvent, and moisture content of DDG particles are important parameters which can significantly influence the kinetics of solid-liquid extraction of phenolic compounds. The extraction yield can be improved if the effective diffusivity of phenolic compounds is increased by modifying the extraction parameters.

5.1.1. Effect of temperature on the extraction of phenolic compounds

The extraction temperature had a direct influence on saturated concentration of phenolic compounds (Cs) and the extraction rate constant (k). Cs and k both increased with temperature from 30 to 70˚C. The rate of mass transfer within initial minutes of extraction is greater at higher temperature so that the fastest extraction rate was observed at 70˚C. This is due to the thermal kinetics of mass transfer and the thermodynamic effect on solubilization of phenolic compounds inside the solid. In addition, by increasing the temperature, the viscosity of DDG extracts and surface tension of the solvent inside the solid matrix is decreased which results in accelerating the whole extraction (Izadifar and Baik, 2008).

5.1.2. Effect of ethanol volumetric fraction on phenolic compounds extraction

As ethanol concentration increased from 30% to 70%, a significant improvement in the yield was observed; however, the amount of extracted phenolic compounds decreased considerably by increasing the ethanol concentration of solvent from 70% to 90%. The total extracted phenolic compounds nearly reached a peak at around 70% ethanol.

5.1.3. Effect of particle moisture content on phenolic compounds extraction

The particle moisture content had significant effect on the kinetics of phenolic compounds extraction. When particle moisture content increased from 3.75% to 59% wet basis,

the extraction yield increased considerably. The increase in particle moisture content exhibited the increase in effective diffusivity values at a fixed ethanol concentration and temperature. Considering these results, it would be more efficient to extract phenolic compounds from wet distillers grains (WDG) without drying rather than from DDG with lower moisture content. In this case, even time and energy for drying can be saved as well.

5.1.4. Kinetic model of extraction process

Solid-liquid extraction process of phenolic compounds from DDG was found to be the most appropriately fitted by a second-order model. The activation energy for all extraction conditions was lower than 20 kJ/mol, which indicates phenolic compounds extraction from DDG was controlled by diffusion.

5.1.5. Effective diffusivity of phenolic compounds

The effective diffusivity of phenolic compounds varied from 6.34×10^{-10} to 3.37×10^{-9} $m^2\ min^{-1}$ with extraction conditions, and the highest effective diffusivity was obtained when using 55% ethanol volumetric fraction of solvent at 50°C and particle moisture content of 59% wet basis. The effective diffusivity of phenolic compounds rose as the extraction temperature increased from 30°C to 70°C at a fixed ethanol concentration and particle moisture content. The increasing effect of temperature on mass diffusivity is attributed to the lower fluid viscosity and higher solubility and thermal kinetics of mass transfer of phenolic compounds at higher temperature (Izadifar and Baik, 2008).

5.2. Dielectric properties of the packed bed of the DDG particles

Generated RF heating in a packed bed of DDG particles and water-ethanol solution is highly related to the packed bed dielectric loss factor and dielectric constant. The dielectric constant and loss factor of bed are dependent on the packed bed conditions.

5.2.1. Effect of ethanol volumetric fraction on dielectric properties of the bed

At 27.12 MHz, which is an industrially allocated frequency, for all levels of temperature and particle moisture contents, both the dielectric loss factor and dielectric constant of the packed bed decreased rapidly as the volumetric fraction of ethanol in the solution increased from 0% (tap water) to 100% (pure ethanol). The polarity of tap water is higher than ethanol and

dielectric loss factor of water is higher than that of ethanol (Izadifar and Baik, 2008). Therefore, higher ethanol concentration results in less polar molecules and ions, thus lower dielectric constant and loss factor of the packed bed. In the interpretation of the correlation between ions and dipole polarization of the packed bed not only the packed bed polarity of solvent should be considered, the solvent-solute molecular interaction and molecular dynamics can be taken into account. Polarity of the packed bed depends on the molecular interaction of solvent with dissolved compounds of DDG (polar or nonpolar compounds) at various ethanol volumetric fractions. Beside the polarity effect on reorientation, it is speculated that molecular dynamics have a large contribution to the reorientation. Molecular weight, size, chain length, and flexibility define the dynamics of molecules in the solvent environment of the packed bed in the presence of external electric field.

5.2.2. Effect of temperature on dielectric properties of the bed

The dielectric loss factor of the packed bed of DDG particles and ethanol-water solution increased with the temperature at all levels of ethanol concentration and particle moisture content. This can be due to the increase in thermal energy of ions and molecules with temperature. As thermal energy (kinetic energy) rises, the mobility of the ions and polar molecules enhances, causes more flip-flop rotation of polar molecules as well as oscillation of ions which results in more collision with neighboring molecules and more molecular frictions. In addition dielectric loss factor is more dependent on ionic conductivity rather than dipole polarization (Ryynanen, 1995). Since ionic conductivity highly depends on temperature and also biological materials like DDG has considerable amount of ionic compounds, temperature rise causes increase in dielectric constant. Considering solvent in the bed, tap water contains various dissolved ions, as ethanol concentration of the solvent decreased, the increase in dielectric loss factor of the bed with temperature was more considerable. The highest dielectric loss factors were observed at 70°C.

The dielectric constant of the bed increased with temperature; however it was more significant when ethanol concentration decreased from 40% to 0%. The effect of temperature on dielectric constant was not significant when the ethanol volumetric fraction of solvent was high (70% and 100%). At 100% ethanol concentration, temperature had insignificant effect on the dielectric constant at 0.0373 and 1.58 d.b. particle moisture contents. The effect of temperature

on dielectric properties is more on thermal energy and agitation of ions and molecules. Increase of ethanol content in the packed bed decrease the polarity and molecular dynamics of the packed bed which results in decrease of temperature effect on the dielectric properties of the bed.

5.2.3. Effect of particle moisture content on dielectric properties of the bed

The particle moisture content has a significant contribution to the dielectric properties of the bed. Ionic compound and polar molecules which have a great contribution in electromagnetic energy dissipation and polarization of the bed are water soluble. The dielectric constant and loss factor increased with particle moisture content. The dielectric loss factor of the packed bed is low at low levels of particle moisture content because the mobility of ions and solute molecules is restricted as they are bound to solid material (Izadifar and Baik, 2008). As the particle moisture content rises, the polarity of the packed bed enhances and also the mobility of water soluble ionic compounds and polar molecules is facilitated which results in the increase of dielectric loss factor and constant. At frequency of 27.12 MHz, the highest dielectric loss factor was observed at particles with 3.98 dry basis moisture content.

5.2.4. Effect of frequency on dielectric properties of the bed

The dielectric loss factor of the packed bed decreased with frequency for all levels of volumetric ethanol fraction of solvent and temperatures. This can be attributed to the fact that by increasing the frequency, molecules do not have enough time to follow the alternations of the applied field and align with the electric field. The dielectric constant of the packed bed decreased with frequency and was more sensitive to frequency at lower ethanol concentration in the solvent. The dielectric constant and loss factor decreased rapidly with frequency at 0% ethanol concentration of solvent, while its variation with frequency was small for 40% ethanol and insignificant for 70% and 100% ethanol concentrations. This might be due to the fact that the movement of water molecules is easier than that of ethanol molecules because the molecular structure of water which is symmetric while ethanol is not (Dr. Lee Wilson, personal communication, February 7, 2011) and also the ethanol hydroxyl group participation in hydrogen bonding which causes difficult reorientation.

5.2.5. Power penetration depth of RF in the packed bed

The power penetration depth decreased with temperature for all levels of particle moisture content and ethanol volumetric fraction of solvent at 13.56 and 27.12 MHz. the power

penetration depth does not show much variation at high moisture content and low ethanol fraction; however as moisture content and ethanol decreases and increases, respectively to their extreme values, a drastic increase is seen in power penetration depth. As temperature decreases and ethanol increases to extreme values tested, power penetration depth increases dramatically. For particle moisture content of 3.98 d.b., the power penetration depth increased rapidly and led to a marked increase at the highest (100%) and lowest (25°C) ethanol fraction and temperature tested, respectively. Higher ethanol fraction of solvent, lower particle moisture content and lower temperature in the packed bed significantly decrease the dielectric constant and loss factor of the packed bed although electromagnetic field can penetrate more in the packed bed (Izadifar and Baik, 2008).

The maximum and minimum values of power penetration depth of RF in the packed bed were 24.92 m and 0.07 m, respectively. The maximum penetration depth was resulted at 27.12 MHz, 100% ethanol, 25˚C, and 3.73% d.b. particle moisture content. Penetration depth was minimum at all tested particle moisture contents at 27.12 MHz, 0% ethanol, and 70˚C. The same minimum penetration depth of the bed was also observed at 27.12 MHz, 100% ethanol, 55˚C, and 158.00% d.b. particle moisture content. For the extraction condition of 70% ethanol, 70°C, and high particle moisture content of 397.51% d.b., in which high extraction yield and rate of phenolic compounds from DDG are expected, the dielectric loss factors are 585.3 and 317.8 at the frequencies of 13.56 and 27.12 MHz, respectively. For the condition RF heating should be done in packed beds not taller than 0.11 m and 0.08 m for maximum uniformity at 13.56 and 27.12 MHz, respectively. The dielectric properties of the matter observed in this study was good enough to verify the possibility of RF assisted extraction.

The multiple regression equations of the dielectric loss factor and dielectric constant for 27.12 MHz can be used in further study in simulation of RF-assisted packed bed extraction of phenolic compounds from DDG.

5.3. Ultrasound assisted extraction

Mechanical fragmentation of biological solids is usually used to destroy cell membranes and to facilitate solute release during extraction. Pre-treating DDG particles using ultrasound waves can potentially damage more cell walls and also develop the pores of the cell wall, making

the cell wall permeable to the solute, which results in improved extraction yield and rate of bioactive compounds (i.e., phenolic compounds).

5.3.1. Effect of sonication power and duration on physical properties of DDG

The N_2 gas adsorption method revealed the presence of mesopores and macropores but not micropores for untreated DDG. Measurements indicated that untreated DDG was mainly composed of 2.45% of macropores and 97.55% of mesopores. The surface area and total pore volume for untreated DDG were 13.905 m^2/g and 0.012 cm^3/g respectively. It was observed that the ultrasound pretreatment increases BET surface area and pore volume of sample and the BET surface area was increased with sonication time and power. The obtained BET surface areas at low powers (e.g. 20%) and long sonication times (e.g. 20 min.) were similar to those of high powers (e.g. 100%) and short sonication times (e.g. 30 sec). In addition, consumed energy by the ultrasound processor was less in high powers and short sonication times (e.g. 100% at 30 sec.) compared to that of low powers and long sonication times (e.g. 20% at 20 min.). Therefore, using higher sonication power at shorter sonication time would be more efficient in terms of resultant BET surface area as well as energy consumption.

The total pore volume of sample was increased with sonication power and it was more noticeable at longer sonication time. No micropores were detected by both HK and DFT methods, and DFT method detected pores with the pore width of 20 to 500 Å (mesopores) and 500 to 1400 Å (macropores) in treated samples. However, measurements indicated that the mechanical effect of ultrasound on the sample mainly appears as greater volume of pores in the range of mesopore size. In addition, detected macropores only form a limited fraction of measured pore volume in the sample. The incremental pore volume growth by increasing sonication power mainly at long sonication times which shows the positive effect of sonication power and time on cell wall damage. The cell wall pores that were already presented and also produced more and developed by ultrasound in all tested conditions were in a specific range of pore size and the effect of sonication time and power was mainly on the quantity (volume) of pores.

5.3.2. Effect of sonication power and duration on extraction rate and yield

The extraction rates and yields for the treated samples with all the tested levels of ultrasound (all the tested BET surface areas) were higher than those of the untreated sample. The extraction rate increased when the BET surface area rose from 13.90 to 14.60 and 17.05 m^2/g.

Among the tested BET surface areas, 18.85 and 22.25 m^2/g surface areas (100% + 30 sec and 100% + 5 min; ultrasound power level and time) showed the highest extraction yields. Extraction yield dropped when surface area increased to 31.80 m^2/g (100% + 20 min). An irreversible damage of the phenolic compounds could be produced as a consequence of both the heat generated during the sonication process and the high ultrasound energy supplied to the sample at this treatment condition. At 80% and 100% sonication power, disintegration of particles was observed and the resultant particle size was not too fine to make any filtration problem. The disintegration of particles results in an increase in extraction yield because of the increase in total surface area of the particles. Therefore, in addition to the mechanical effect of ultrasound on cell wall disruption and pore development, the positive effect of ultrasound pretreatment in reduction of particle size is speculated to shorten the extraction time and enhance the overall extraction yield. Among the tested BET surface areas, the extraction rate increased with BET surface area. At highest BET surface area which is related to 100% sonication power and 20 min. sonication time, the saturated concentration of phenolic compounds decreased. Taking the extraction rate constant, saturated concentration, and consumed ultrasound energy into account, the 100% ultrasound power (equivalent to 87 W ultrasound power) for 30 seconds was the best ultrasound pretreatment condition.

5.3.3. Effect of sonication power and duration on pH

The pH of ultrasound treated samples varied from 5.05 to 5.10 and there was no significant difference among different sonication conditions.

5.4. General conclusions

The extraction mechanism and kinetics of phenolic compounds as well as the best ethanol fraction of ethanol-water solution, the extraction temperature, and particle moisture content for extraction of phenolic compounds from DDG were determined in this study. The kinetics of the extraction of phenolic compounds from DDG followed second-order trend suggesting that the phenolic compounds extraction comes in two successive stages: a fast dissolution of phenolic compounds followed by a slow molecular diffusion of phenolic compounds from DDG particles to the solvent. The activation energy for all the extraction conditions was lower than 20 kJ/mol, which indicates that phenolic compounds extraction from DDG is controlled by diffusion. The

maximum extraction rate and yield were obtained with 70% ethanol concentration, 70°C extraction temperature, and 59% particle moisture content (w.b.). The findings from this stage of study suggest the use of high moisture content particles (i.e. WDG) for extraction of phenolic compounds.

Also, the effect of high-power ultrasound pretreatment on developing cell wall pores, destruction of DDG cell walls and the extraction yield and rate was investigated. The ultrasound pretreatment of DDG particles was found to be an effective operation for improving the extraction rate and yield of phenolic compounds from DDG. The method of nitrogen (N_2) adsorption at 77 K successfully enabled a mechanistic understanding of the mechanical effects of ultrasound on the cell wall structure at different levels of sonication time and power. The increasing surface area, pore volume and pore size as well as increasing extraction yield and rate after the ultrasonic treatment, showed the positive effect of ultrasound pretreatment on developing present pores and breaking down cell walls. The ultrasound pretreatmnet condition of 100% sonication power (87 W ultrasound power) for 30 seconds was determined as the best pretreatment condition in which the surface area and extraction rate constant increased from 13.90 to 18.87 m^2/g and from 0.057 to 3.933 L g^{-1} min^{-1}, respectively. At this condition, 14.29% increase in extraction yield was observed compared to the control. On the top of the increased pore volume, surface area, and consequent enhancement of extraction yield and rate after the ultrasonic treatment confirmed the positive attribute of ultrasound pretreatment on the extraction of phenolic compounds from DDG.

In addition, dielectric properties of the packed bed of DDG particles and ethanol/water solution were characterized. A packed bed of DDG particles at 0% ethanol fraction, 70°C, and particle moisture content of 3.98 d.b resulted in the highest dielectric loss factor of the bed. Overall, dielectric constant and loss factor of packed bed decreased with frequency and ethanol volumetric fraction of solvent, and increased with temperature and particle moisture content. Power penetration depth decreased with temperature and particle moisture content, and increased with ethanol fraction. The highest power penetration depth was observed at the lowest particles moisture content (0.0373 d.b.) tested and 100% ethanol at the lowest temperature tested (25°C). The information from this stage of study can be used for further study in application of RF heating for extraction of phenolic compounds from DDG. In general, the results of this study are

useful for design of phenolic compounds extraction process with ultrasonic pretreatment and RF assisted extraction process equipment as well.

5.5. Recommendations for future studies

Some of the possible extensions to the current research study are as follows:

- The conventional solid-liquid extraction of phenolic compounds from DDG was conducted at 500 rpm stirring speed (chapter 2 and 3). The flow rate of solvent in the Erlenmeyer at this mixing speed can be determined by a magnetic flowmeter (the most common velocity device used for flow rate measurement) which can easily measure velocity of liquids with solids in suspension or an orifice plates or a venture tube (Chemical Engineering Tools and Information, 2011). Then ultrasound pre-treated biomaterials can be loaded to a RF packed bed solvent extraction unit and subjected to radio frequency heating. Since a solvent reservoir can supply solvent at different flow rate, a flow rate close to the determined solvent flow rate can be chosen. During extraction in RF packed bed extraction unit, temperature and concentration of solutes can be measured with location and time. The extraction rate constant and saturated concentration of phenolic compounds can be calculated from taken samples at different locations of packed bed with time. Results from this experiment can be compared with the results in chapter 3 to investigate the efficiency of RF assisted packed bed extraction method with conventional solid-liquid extraction method.

- Izadifar and Baik (2009) demonstrated that RF assisted packed bed extraction can be successfully used for extraction of podophilotoxin. Potentially RF assisted extraction can be applied for the extraction of phenolic compounds from DDG. Designing, simulation, and optimization of such process demands sufficient information about dielectric properties (dielectric constant and loss factor) of DDG particles at different levels of temperature, frequency, particle moisture content, and ethanol volumetric fraction. The proposed multiple regression equations (Table 4.3), which describe the

variation of dielectric constant and dielectric loss factor of DDG particles with respect to temperature, particle moisture content, and ethanol fraction of the solvent, can be employed for simulation and optimization of RF assisted extraction of phenolic compounds. Based on the findings in this research, the yield of extraction of phenolic compounds can be maximized at 70% ethanol, 70°C, and 59% particle moisture content (chapter 2). This proposed condition can be applied to the RF assisted packed bed extraction of phenolic compounds from DDG particles.

- Adding an ionic component like KCl or NaCl can improve RF heating rate in the packed bed. The type and the concentration of the ionic components in the solvent are important. The ionic components should be cheap, chemically inert, soluble in the solvent, and can satisfactorily provide high dielectric loss factor in the packed bed. So, the dielectric loss factor of different types of ionic components like NaCl and KCl in the packed bed of ethanol-water solution for different ethanol volumetric fraction of solvent and temperatures with and without particles should be measured using liquid test fixture as described in chapter 4. The best ionic compound considering properties and economic features can be selected.

- The quality of ultrasound performance on damaging the particles' cell wall can be a function of chamber geometry and the probe shape of ultrasound apparatus. The particles can be treated by ultrasound at various combinations of probe shape and chamber geometry and the effect of their interactions on the destruction of the cell wall can be investigated by N_2 adsorption method at 77 K.

- It was observed that the applied sonotrode with a flat tip diameter of 7 mm covers small area of the chamber. Therefore particles are less likely to be subjected to sound waves uniformely. To have more effective ultrasonic treatment so that all particles are treated uniformly, designing and using a convex plate sonotrode (Fig.5.1a) or a radial sphere sonotrode (Fig.5.1b) attached to an ultrasonic processor can increase the sound

wave propagation area in the chamber which results in more uniform ultrasound treatment of particles.

-

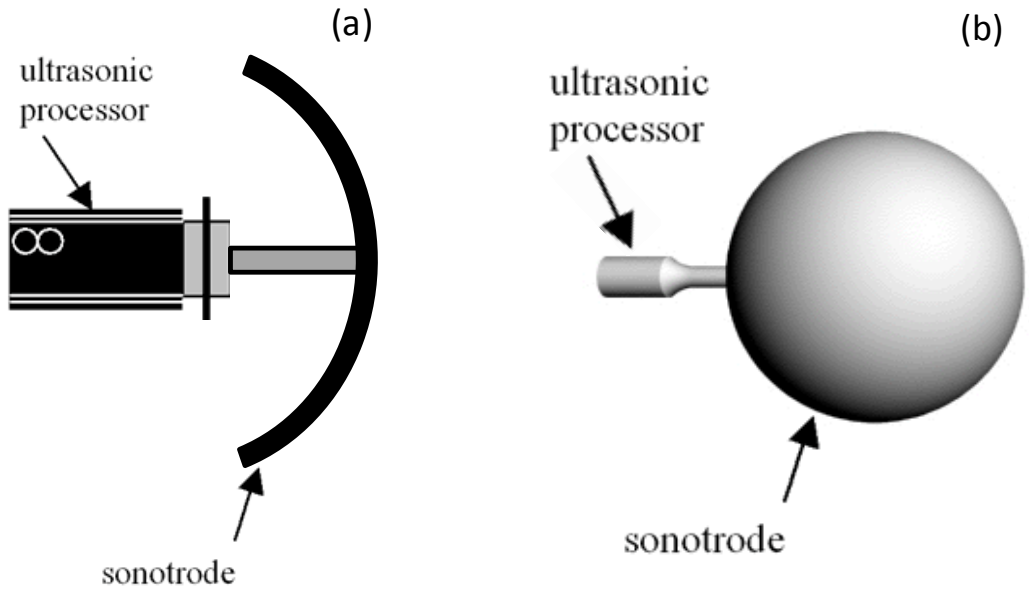

Figure 5.1. Schematic diagram of convex sonotrode plate (a) and radial sphere sonotrode (b)

To minimize the thermal effect of ultrasound inside the chamber, some reusable freezable ice cubes or some completely sealed freezable plastic containers containing distilled water or liquid nitrogen can be used inside the chamber. The freezable plastic ice cubes or small sealed containers holding water can be frozen in advance and put inside the chamber during ultrasonic treatment. The small containers filled with liquid nitrogen can be used as well. In preliminary experiments this idea was applied using small pre frozen water containers. The temperatures at different locations of the chamber were recorded with time during treatment using a data logger. It was observed that the thermal effect of ultrasound was decreased significantly after applying small reusable freezing ice containers inside the treating chamber. To apply this method for decreasing the thermal effect of ultrasound, the influence of ice containers presence in the chamber on the effectiveness of ultrasound treatment should be investigated. Two sets of ultrasound treatment experiments can be performed in the exactly same sonication condition as described in section 3.2.2. but one chamber with just particles and distilled water, and the other

with particles, distilled water, and ice containers (or liquid nitrogen containers). The effect of ultarasound on physical properties of the cell wall in these two series of treated particles can be compared using N2 adsorption method at 77 K as described in section 3.2.6. In case the amount of water in the treating chamber is not important ice cubes can be replaced by ice containers in the chamber.

5.6. Study limitations

Some of the limitations involved with this study are as follows:

- Since mechanical waves like sound waves rely on a medium to move, it looses energy as it travels. So by getting distance from the source of sound wave the energy of waves is decreased or vanished. In this study, small amount of particles was placed in short distance to the sonotrode and it was assumed that all particles were affected by ultrasound uniformly.

- Kinetic parameters were calculated from only 3 levels of temperatures. It is better to calculate the kinetics parameters for wider range of temperature to reach a firm conclusion.

- To minimize thermal effect of sonication during treatment just surface temperature of the sample (surface of the chamber) was kept at 0°C.

- The optimum condition of extraction was calculated experimentally while a better way of calculation can be based on numerical modeling.

- It was considered that the geometry of all DDG particles is flat slab and for simplicity particles are considered as a one-dimensional slab.

References

Chemical Engineering Tools and Information, website, http://www.cheresources.com/flowmeas.shtml, Accessed on Nov. 2011.

Izadifar M., O.D. Baik, Radio frequency-assisted extraction of podophyllotoxin: Prototyping of packed bed extraction reactors and experimental observations, Chemical Engineering and Processing 48 (2009) 1437-1444.

Jianyong W, Lidong L and Foo-tim C, Ultrasound assisted extraction of ginseng saponins from ginseng roots and cultured ginseng cells. Ultrasonics Sonochemistry, (2001) 347-352.